THE INFLUENCE OF FETAL GROWTH RESTRICTION AND INFECTION ON THE CEREBRAL METABOLIC RESPONSE TO ACUTE HYPOXIA.

James Charles Dixon, M.B. Ch.B.

Thesis submitted for the Degree of
Doctor of Medicine (M.D.)
of the University of London.

September, 2004

ProQuest LLC
789 East Eisenhower Parkway
P.O. Box 1346
Ann Arbor, MI 48106-1346

Acknowledgements.

I am indebted to Professor Charles Rodeck (Head of Department) and Dr Donald Peebles MD (Senior Lecturer) for their encouragement and supervision, and for giving me the opportunity to undertake research as a Clinical Research Fellow within the Department of Obstetrics and Gynaecology at University College London.

I am especially grateful for the advice, assistance and technical support of Dr Ern Cady Ph.D., Dr John Thornton Ph.D., Dr Andrew Priest Ph.D., Dr Alan Bainbridge Ph.D. and Professor Roger Ordidge Ph.D. in the Department of Medical Physics and Bioengineering, University College London. In addition, I wish to express my appreciation of the work of Dr Suzie Miller PhD, who performed early experiments to assess the feasibility of cerebral MRS in chick embryos.

I wish to thank Dr Gena Raivich MD, DSc and Dr Matthias Galiano MD for their assistance in the development of the histology techniques used in this research.

Abstract.

Intrauterine growth restriction and infection are significant risk factors for neonatal hypoxic ischaemic encephalopathy in term neonates. It was hypothesised that these two factors increase the susceptibility of the fetal brain to hypoxic ischaemic damage by their influence on cerebral metabolism and development.

Cerebral energy and structural metabolites in a late gestation *in-ovo* chick embryo model of acute hypoxia and fetal growth restriction were measured non-invasively using proton and phosphorus Magnetic Resonance Spectroscopy. The influence of fetal growth restriction and acute hypoxia on cerebral metabolites was assessed. In addition, the individual and combined effects of growth restriction, acute hypoxia and systemic infection on morphological markers of neuronal injury were assessed.

Acute hypoxia increased mean cerebral lactate/creatine (Cr) (0.58 to 1.56) and alanine/Cr (0.14 to 0.29) that gradually returned to normal after restoration of normoxia. Growth restriction was associated with an attenuated lactate/Cr response to acute hypoxia (0.32 to 0.92), and significantly increased cerebral β-hydroxybutyrate/Cr (0.57 vs. 0.25) and reduced cerebral intracellular energy reserves, inositol/Cr (1.15 vs. 1.61) and N-acetylaspartate/Cr (0.74 vs. 0.89) under normoxic conditions.

The cerebral energy and structural metabolite concentration changes associated with fetal growth restriction were consistent with impaired oxidative phosphorylation, ketosis, and altered brain development. However, despite the significantly different lactate response to hypoxia, there was no histological

evidence that growth restriction affected markers of neuronal injury or exacerbated the effects of acute hypoxia.

The scientific and medical literature was reviewed to January 2004.

TABLE OF CONTENTS

GLOSSARY. 9
LIST OF FIGURES 10
LIST OF TABLES. 12

1 INTRODUCTION 13

1.1 FETAL GROWTH RESTRICTION. 16
1.1.1 Aetiology. *16*
1.1.2 Evidence of an association with brain injury. *17*
1.1.3 Influence of fetal growth restriction on cerebral metabolism. *20*
1.1.4 Influence of fetal growth restriction on cerebral development. *22*
1.2 INTRAUTERINE INFECTION 25
1.2.1 Evidence of an association with brain injury. *26*
1.2.2 Interaction with hypoxia. *28*
1.3 FETAL CEREBRAL METABOLISM. 31
1.3.1 Energy substrates. *31*
1.3.1.1 Glucose. 31
1.3.1.2 Ketone bodies 32
1.3.1.3 Lactate. 32
1.3.2 Principal energy substrate. *33*
1.3.3 Response to hypoxia. *34*
1.4 FETAL CEREBRAL PERFUSION. 36
1.4.1 Normoxia. *36*
1.4.2 Acute hypoxia. *37*
1.4.3 Chronic hypoxia. *38*
1.5 MECHANISMS OF BRAIN INJURY. 41
1.5.1 Hypoxic-ischaemia. *41*
1.5.2 Fetal growth restriction. *42*
1.5.3 Infection. *43*
1.6 CURRENT METHODS OF ANTENATAL FETAL ASSESSMENT 44
1.6.1 Ultrasound. *44*
1.6.2 Cardiotocography *46*
1.7 SUMMARY 48

2 MAGNETIC RESONANCE AND PERINATAL CEREBRAL METABOLISM 50

2.1 HISTORICAL BACKGROUND. 50
2.2 NUCLEAR MAGNETIC RESONANCE 50
2.2.1 Physics principles *50*
2.2.2 Factors affecting MRS spectral quality *54*
2.2.2.1 Water suppression 54
2.2.2.2 Fat suppression 55
2.2.3 Computer based methods of analysing MR spectra *55*
2.2.4 Diffusion Weighted Imaging (DWI) *56*
2.3 MAGNETIC RESONANCE AND THE PERINATAL BRAIN. 56
2.3.1 Magnetic Resonance Spectroscopy (MRS) *56*
2.3.2 Perinatal Diffusion Weighted Imaging (DWI) *58*
2.3.3 Human fetal magnetic resonance spectroscopy (MRS) *61*

3 THE CHICK EMBRYO..... 63

3.1 PHYSIOLOGY AND DEVELOPMENT..... 63
3.2 NEURODEVELOPMENT..... 65
3.3 CARDIOVASCULAR RESPONSE TO HYPOXIA..... 66
3.4 ABSENCE OF MATERNAL INFLUENCES..... 67
3.5 MODEL OF FETAL HYPOXIA..... 67
3.5.1 Preparation for acute hypoxia..... 67
3.5.2 Control of acute hypoxia..... 68
3.5.3 Susceptibility to hypoxia..... 69
3.6 CHICK EMBRYO MODEL OF FETAL GROWTH RESTRICTION..... 69
3.7 SUMMARY..... 70

4 METHODS AND MATERIALS..... 71

4.1 CHICK EMBRYO PREPARATION..... 71
4.1.1 Normal day 19 chick embryos..... 71
4.1.2 Growth restricted day 19 chick embryos..... 72
4.1.3 Inoculation of day 18 chick embryos with lipopolysaccharide.... 73
4.2 MAGNETIC RESONANCE SPECTROSCOPY (MRS) METHODS..... 73
4.2.1 Sedation of chick embryo..... 73
4.2.2 Chick embryo brain location..... 74
4.2.3 Proton (^1H) spectroscopy (relative signal amplitudes)..... 75
4.2.4 Diffusion Weighted Magnetic Resonance Imaging..... 76
4.2.5 Phosphorus (^{31}P) spectroscopy (relative amplitudes)..... 77
4.2.6 Proton MRS cerebral metabolite quantitation method..... 79
4.2.6.1 Basic Physics:..... 79
4.2.6.2 Quantifying spectra..... 80
4.2.6.3 Proton (^1H) spectroscopy (absolute concentrations)..... 82
4.3 CHICK EMBRYO BRAIN HISTOLOGY..... 88
4.3.1 Fixation protocol..... 88
4.3.2 Cryostat cutting protocol..... 90
4.3.2.1 Cerebral hemispheres (Anterior brain)..... 90
4.3.2.2 Optic tecti, cerebellum and brain stem (Posterior brain)..... 91
4.3.3 Fixation and dehydration of tissue sections..... 91
4.3.4 Staining protocol..... 91
4.4 NISSL STAINED CHICK EMBRYO BRAIN CELL COUNTING PROTOCOL..... 92
4.4.1 Cerebral hemispheres..... 93
4.4.2 Optic tectum and cerebellum..... 94
4.4.3 Sample size..... 95

5 A COMPARISON OF THE ABSOLUTE AND RELATIVE CONCENTRATIONS OF CEREBRAL METABOLITES OF DAY 19 NORMALLY GROWN AND GROWTH RESTRICTED CHICK EMBRYOS *IN-OVO* INVESTIGATED BY PROTON AND PHOSPHORUS MAGNETIC RESONANCE SPECTROSCOPY..... 97

5.1 INTRODUCTION..... 97
5.2 MATERIALS AND METHODS..... 98
5.3 RESULTS..... 101
5.4 DISCUSSION..... 101
5.5 CONCLUSIONS..... 105

6 THE CEREBRAL METABOLIC RESPONSE TO ACUTE HYPOXIA OF THE DAY 19 CHICK EMBRYO *IN-OVO* MEASURED BY PROTON MAGNETIC RESONANCE SPECTROSCOPY 111

6.1 INTRODUCTION. 111
6.2 MATERIALS AND METHODS. 112
6.2.1 MRS 112
6.2.2 Histology 113
6.3 RESULTS. 114
6.3.1 MRS 114
6.3.2 Histology 115
6.3.2.1 Hyperstriatum ventralis, hippocampus and optic tectum 115
6.3.2.2 Cerebellum. 116
6.4 DISCUSSION. 116
6.5 CONCLUSIONS. 120

7 A COMPARISON OF THE CEREBRAL METABOLIC RESPONSE TO ACUTE HYPOXIA OF DAY 19 NORMALLY GROWN AND GROWTH RESTRICTED CHICK EMBRYOS *IN-OVO* MEASURED BY PROTON MAGNETIC RESONANCE SPECTROSCOPY. 126

7.1 INTRODUCTION. 126
7.2 MATERIALS AND METHODS. 128
7.2.1 MRS 128
7.2.2 Histology 129
7.3 RESULTS. 130
7.3.1 MRS 130
7.3.2 Histology 131
7.3.2.1 Hyperstriatum ventralis, hippocampus and optic tectum 131
7.3.2.2 Cerebellum. 132
7.4 DISCUSSION. 133
7.5 CONCLUSIONS. 136

8 THE EFFECT OF GROWTH RESTRICTION ON CEREBRAL INTRACELLULAR ENERGY RESERVES IN THE CHICK EMBRYO *IN-OVO* DURING ACUTE HYPOXIA MEASURED BY PHOSPHORUS MAGNETIC RESONANCE SPECTROSCOPY 146

8.1 INTRODUCTION. 146
8.2 MATERIALS AND METHODS. 148
8.3 RESULTS. 150
8.4 DISCUSSION. 150
8.5 CONCLUSIONS. 152

9 A DIFFUSION WEIGHTED MAGNETIC RESONANCE IMAGING STUDY OF THE EFFECT OF ACUTE HYPOXIA AND GROWTH RESTRICTION ON CEREBRAL METABOLISM IN THE CHICK EMBRYO *IN-OVO*. 158

9.1 INTRODUCTION. 158
9.2 MATERIALS AND METHODS. 159
9.3 RESULTS. 161
9.4 DISCUSSION. 162
9.5 CONCLUSIONS. 163

10 AN EXPERIMENT TO DETERMINE THE REQUIRED DOSE OF SALMONELLA TYPHI LIPOPOLYSACCHARIDE ADMINISTERED ON DAY 18 OF INCUBATION TO CAUSE 50% MORTALITY (LD50) IN CHICK EMBRYOS BY DAY 22 167

10.1 INTRODUCTION. 167
10.2 MATERIALS AND METHODS. 169
10.3 RESULTS. 170
10.4 CONCLUSIONS. 170

11 AN INVESTIGATION OF THE EFFECT OF SYSTEMIC SALMONELLA TYPHI LIPOPOLYSACCHARIDE AND ACUTE HYPOXIA ON DAY 21 CHICK EMBRYO CEREBRAL HISTOLOGY. 174

11.1 INTRODUCTION. 174
MATERIALS AND METHODS. 176
11.2 176
11.3 RESULTS. 177
11.3.1 Hyperstriatum ventralis, hippocampus and optic tectum. 177
11.3.2 Cerebellum. 178
11.4 DISCUSSION. 178
11.5 CONCLUSIONS. 179

12 FURTHER WORK. 181

13 OVERVIEW 183

APPENDIX 1 186
REFERENCE LIST 188

GLOSSARY.

ADC	Apparent Diffusion Coefficient
ADP	Adenosine diphosphate
ATP	Adenosine triphosphate
βHB	β-hydroxybutyrate
CAM	Chorioallantoic Membrane
CI	Confidence Interval
Cr	Creatine
CTG	Cardiotocograph
DWI	Diffusion Weighted Imaging
FID	Free Induction Decay
Hi	Hippocampus
HIE	Hypoxic Ischaemic Encephalopathy
HV	Hyperstriatum ventralis
GR	Growth Restriction
IL	Interleukin
IQ	Intelligence Quotient
IUGR	Intrauterine growth restriction
LPS	Lipopolysaccharide
MRS	Magnetic Resonance Spectroscopy
NAA	N-acetylaspartate
NMR	Nuclear Magnetic Resonance
NS	Number of Summed echoes
OR	Odds Ratio
OT	Optic Tectum
pCO_2	Partial pressure of carbon dioxide
PCr	Phosphocreatine
Pi	Inorganic phosphate
pO_2	Partial pressure of oxygen
SD	Standard Deviation
SGA	Small for Gestational Age
T1	Spin-lattice or longitudinal relaxation time
T2	Spin-spin or transverse relaxation time
TE	Echo Time
TR	Repetition Time
TNF-α	Tissue Necrosis Factor α
VOI	Volume of interest

LIST OF FIGURES

Figure 2.1 Free induction decay signal showing a decaying ($e^{-t/T2}$) sinusoid with a frequency ω_o, where T2 is the spin-spin relaxation time 53
Figure 3.1 A chick embryo and internal egg structures 64
Figure 4.1 Sagittal MRI of day 19 chick embryo *in-ovo* showing spine and brain. 84
Figure 4.2 Components required for chick embryo cerebral MRS: chick embryo *in-ovo*, a 2.5 cm diameter circular surface coil, neonatal sphygmomanometer cuff (attached to opaque white tubing), fluoroptic thermistor (black wire) and 150ml plastic bag (attached to transparent green tubing). 85
Figure 4.3 Assembled components required for chick embryo cerebral MRS, with the chick embryo brain was fixed over the centre of the circular surface coil 86
Figure 4.4 MRI of chick embryo brain with superimposed 6mm x 6mm x 6.6mm sampling voxel. 87
Figure 4.5 Clamped cannula in heart during brain perfusion and fixation. A 17G cannula was inserted through the apex of the heart into the left ventricle, with its opening beneath the major cardiac outlet vessels causing them to dilate with perfusate. 89
Figure 5.1 Cerebral proton MR spectrum of a day 19 growth restricted chick embryo in air. 106
Figure 6.1 Cerebral proton MR spectra from the brain of a day 19 normally grown chick embryo before, after 40 minutes of acute hypoxia and at the end of a 2 hour recovery period in air. Spectral peaks corresponding to choline, creatine, N-acetylaspartate (NAA) and lactate are identified. 121
Figure 7.1 Cerebral proton MR spectra from the brain of a day 19 growth restricted chick embryo before, after 40 minutes of acute hypoxia and at the end of a 2 hour recovery period in air. Spectral peaks corresponding to choline, creatine, N-acetylaspartate (NAA), lactate and β–hydroxybutyrate (βHB) are identified. 137
Figure 7.2 Mean cerebral lactate/Cr (±SD) in normally grown chick embryos exposed to hypoxia (black bars) and normoxia (grey bars). 138
Figure 7.3 Mean cerebral lactate/Cr (±SD) in growth restricted chick embryos exposed to hypoxia (black bars) and normoxia (grey bars). 139
Figure 7.4 Mean cerebral lactate/Cr (±SD) of normally grown (black bars) and growth restricted (grey bars) chick embryos exposed to hypoxia. 140
Figure 7.5 Mean cerebral alanine/Cr (±SD) in normally grown chick embryos exposed to hypoxia (black bars) and normoxia (grey bars). 141
Figure 7.6 Mean cerebral alanine/Cr (±SD) in growth restricted chick embryos exposed to hypoxia (black bars) and normoxia (grey bars). 142
Figure 7.7 Mean cerebral β–hydroxybutyrate/Cr (±SD) in normally grown (black bars) and growth restricted (grey bars) chick embryos exposed to hypoxia. 143
Figure 8.1 Cerebral phosphorus MR spectrum of a day 19 growth restricted chick embryo in air. The spectral peaks corresponding to phosphocreatine (PCr), inorganic phosphate (Pi), phosphomonoesters (PME), phosphodiesters (PDE), α,β and γ phosphates of ATP are identified. 155

Figure 8.2 Mean cerebral PCr/Pi (±SD) in normally grown (black bars) and growth restricted (grey bars) day 19 chick embryos during acute hypoxia (4% oxygen concentration for 60 minutes)..... 156
Figure 8.3 Mean cerebral ΔPCr/Pi (±SD) in normally grown (black bars) and growth restricted (grey bars) day 19 chick embryos during acute hypoxia (4% oxygen concentration for 60 minutes). * signifies p=0.04..... 157
Figure 9.1. Mean cerebral ADC (x100) (black bars) and lactate/Cr (x10) (grey bars) (±SD) of day 19 normally grown chick embryos in response to 4% oxygen for 110 minutes followed by 2.5% oxygen for 44 minutes (n=4). 165
Figure 9.2 Mean cerebral choline/Cr (black bars) and N-acetylaspartate/Cr (grey bars) (±SD) of day 19 normally grown chick embryos in response to 4% oxygen for 110 minutes followed by 2.5% oxygen for 44 minutes (n=4). 166
Figure 10.1 Diagram of chick embryo and internal egg structures..... 172
Figure 10.2 Chick embryo cumulative mortality (%) on day 22 of incubation in response to different lipopolysaccharide (LPS) doses on day 18. 3mg LPS was associated with 44% cumulative mortality..... 173

LIST OF TABLES.

Table 3-1 Gas partial pressures and pH in the mammalian fetus and chick embryo at day 14 – 15 of incubation. 67
Table 4-1 Microtome protocol for 20micron tissue sections to sample 8 and 7 tissue planes in the anterior and posterior brain specimens respectively..... 90
Table 4-2 20 micron tissue section cresyl violet staining protocol..... 92
Table 4-3 Brain areas and cell types counted in day 21 chick embryo brain. 96
Table 5-1 Mean cerebral metabolite concentrations (mmols/Kg ww) and standard deviation (SD) of day 19 normally grown (NG) and growth restricted (GR) chick embryos measured by proton MRS. 107
Table 5-2 T_2-weighted mean cerebral metabolite/Cr and standard deviation (SD) of day 19 normally grown (NG) and growth restricted (GR) chick embryos measured by proton MRS. 108
Table 5-3 Mean cerebral phosphocreatine/inorganic phosphate (PCr/Pi) and mean chemical shift between PCr and Pi and standard deviations (SD) of day 19 normally grown (NG) and growth restricted (GR) chick embryos measured by phosphorus MRS. 109
Table 5-4 Cerebral metabolite concentrations (mmols/Kg ww) in the chick embryo and human..... 110
Table 6-1 Gas mixture and duration of supply in two groups of day 19 chick embryos..... 122
Table 6-2 Cerebral mean lactate/Cr T_2-weighted signal amplitudes and standard deviation (SD) of chick embryos at Day 19 of incubation, before, during and after hypoxia (H) and in embryos that remained in air (N). 123
Table 6-3. Cerebral mean alanine/Cr T_2-weighted signal amplitudes and standard deviation (SD) of chick embryos at Day 19 of incubation, before, during and after hypoxia (H) and in embryos that remained in air (N). 124
Table 6-4 Cerebral cell densities (cells/ unit area) in the hyperstriatum ventralis, hippocampus and optic tectum of day 21 chick embryos exposed to air (N) and acute hypoxia (H) on day 19 of incubation..... 125
Table 7-1 Gas mixture and duration of supply in four groups of day 19 chick embryos..... 144
Table 7-2 Mean cerebral lactate/Cr T_2-weighted signal amplitudes (±SD) of normally grown (NG) and growth-restricted (GR) chick embryos during acute hypoxia and recovery in air (H), and during continuous normoxia (N). 145
Table 8-1 Mean PCr/Pi (±SD) in normally grown (NG) and growth restricted (GR) day 19 chick embryos before and at the end of acute hypoxia (4% oxygen concentration for 60 minutes). 153
Table 8-2 Mean chemical shift between PCr and Pi (ppm) (±SD) in normally grown (NG) and growth restricted (GR) day 19 chick embryos before and at the end of acute hypoxia (4% oxygen concentration for 60 minutes). .. 154
Table 9-1 Mean cerebral ADC (± SD) in day 19 normally grown (NG) and growth restricted (GR) chick embryos during acute hypoxia and recovery in air (H) and during continuous normoxia (N). 164
Table 10-1 Lipopolysaccharide (LPS) dose and cumulative mortality between day 18 and 23 of incubation after LPS inoculation on day 18..... 171
Table 11-1 Gas mixture and duration of supply in four groups of day 19 chick embryos..... 180

1 INTRODUCTION.

The principle concern of many parents when a baby is conceived is that it is healthy. Perinatal and infant mortality have gradually reduced over the past 70 years (Registrar General's Statistical Reviews for England and Wales) through the introduction of asepsis, antibiotics, rhesus immunisation prevention and improved standards of living and health. However, one of the common fears of parents-to-be is that their baby will be "brain-damaged". This term embraces a wide variety of clinical conditions and causal factors associated with cerebral injury. The care of affected individuals exacts huge emotional and financial costs and hence the causes and mechanisms of cerebral injury are important areas of research.

Perinatal brain injury can reveal itself in several ways. Neonatal encephalopathy is one of the earliest manifestations and is characterised by seizures or abnormal consciousness, feeding or respiratory difficulties of presumed central origin, and abnormal reflexes and muscle tone (Sarnat and Sarnat, 1976). The prevalence of neonatal encephalopathy ranges from 1.8 to 7.7:1000 live births at term (Adamson et al., 1995;Badawi et al., 1998a;Ergander et al., 1983;Finer et al., 1981;Hull and Dodd, 1992;Levene et al., 1985;Nelson and Leviton, 1991;Thornberg et al., 1995).

Cerebral palsy is the most profound form of brain injury in infants that survive. The condition encompasses a group of non-progressive motor disorders that present before two years of age, and originate in the brain rather than the spinal cord or muscles. (Badawi et al., 1998c). Although the individual risk of cerebral palsy at term is approximately 1:1000 live births and 1:20 in very premature infants, term deliveries account for about half the cases of cerebral

palsy because they are more numerous than premature deliveries. Gestational age and neuro-radiological abnormalities are important predictors of cerebral palsy in premature neonates, whereas the presence and severity of encephalopathy are the most relevant factors in neonates born at term. Perinatal brain injury can also have more subtle consequences such as neurodevelopmental delay and reduced IQ (Hagberg and Kyllerman, 1983).

Although antenatal and intrapartum care have improved considerably in the past decades with a significant reduction in the incidence of birth asphyxia as indicated by a reduced incidence of low Apgar scores, the incidence of cerebral palsy has remained stable (Guyer et al., 1997). Indeed, randomised control trials of electronic fetal monitoring with or without fetal blood sampling have failed to show a significant reduction in perinatal mortality, low Apgar score and admission to neonatal intensive care (Thacker, 2004). In fact, no obstetric intervention introduced for the purpose of preventing or alleviating the effects of perinatal hypoxic-ischaemia has so far demonstrated any affect of the rate of cerebral palsy.

Impaired gas exchange in the fetal brain can arise because of reduced oxygen (hypoxia) or blood flow (ischaemia) and is an important contributory factor to brain injury that affects about 6 births in 1000 in the UK (Wyatt, 1996). Those neonates that survive are at high risk of cerebral palsy. However, intrapartum hypoxia alone is responsible for only a minority of cerebral palsy cases in babies born at term (6 – 21%), and about half of cases in babies born prematurely (Hagberg, 1993;Naeye et al., 1989;Nelson, 2002). If the sources of physiological stress in labour arising from the transient impairment of uterine and placental perfusion due to contractions are similar in premature and term

labours, then the reduced contribution of intrapartum hypoxia to CP in normally grown neonates born at term, suggests they are less susceptible to hypoxia and may employ compensatory mechanisms to protect themselves.

In the last decade, the emphasis has shifted from isolated perinatal asphyxia as the predominant cause of perinatal brain injury in term babies, to recognise that specific antenatal factors show a significant association with perinatal brain injury. For example, maternal mental retardation, fetal malformation, maternal seizures, metabolic anomalies, infection, autoimmune disease and thrombophilias, growth restriction, death of a twin and maternal hyperthyroidism are antenatal features associated with cerebral palsy (Blair and Stanley, 1990;Grether and Nelson, 1997;Nelson et al., 1998;Nelson and Ellenberg, 1985;Nelson and Ellenberg, 1986) (Pharoah and Cooke, 1997;Volpe J.J, 1995). These factors may act alone or in combination with one another or fetal hypoxia. It is not surprising that similar risk factors such as a family history of neurological disorder or seizures, maternal thyroid disease, severe pre-eclampsia, moderate to severe bleeding and intrauterine growth retardation have been identified as risk factors for neonatal encephalopathy (Adamson et al., 1995). It is unclear whether antenatal risk factors initiate cerebral injury by means of altered neuron energy metabolism or other means.

Two common antenatal risk factors for neonatal encephalopathy and cerebral palsy are fetal growth restriction and infection. Impaired fetal growth affects between 3-15% of pregnancies, while histological evidence of chorio-amnionitis occurs in up to 20% of term and 60% of pre-term pregnancies, and clinical chorioamnionitis presents in 5-10% of pregnancies (Shalak and Perlman, 2002).

1.1 Fetal growth restriction.

The terms "intrauterine growth restriction" and "small for gestational age" are frequently used imprecisely and synonymously. The definitions of fetal growth impairment are usually expressed relative to a population weight centile or standard deviations below the mean fetal weight at a given gestational age. The conventional definition of small for gestational age in the United Kingdom is an estimated fetal weight or birthweight less than the 10th centile for gestational age (Clausson et al., 2001), although there is an argument for the threshold to be set at the 15th centile as fetal mortality is increased in infants below this level (Myers and Ferguson, 1989). The term "intrauterine growth restriction" is reserved for fetuses and neonates weighing below the 3rd centile or more than 2 standard deviations below the mean weight for a gestational age.

Centile thresholds derived from large population studies for the definition of growth impairment fail to take account of the maternal, paternal, and obstetric factors that affect an individual pregnancy and about 20% of fetuses identified as small for gestational age by such means will be constitutionally small without growth impairment (Mamelle et al., 2001). Therefore individualised growth charts have been proposed but have not entered into regular clinical use in the United Kingdom (Gardosi, 1998).

1.1.1 Aetiology.

Fetal growth restriction may be classified according to its origin. Viral infection and aneuploidy in the fetus are often associated with symmetrical growth restriction because anabolism is compromised or intrinsically flawed.

Most small for gestational age fetuses are the result of impaired nutrient and gaseous exchange between the mother and fetus, as a consequence of placental dysfunction or uterine abnormalities. Potential underlying causes may be failed trophoblastic invasion of spiral arteries as found in pre-eclampsia (Naicker et al., 2003) (Matijevic and Johnston, 1999) (Gerretsen et al., 1981) or accumulative placental infarction secondary to maternal thrombophilia (Heilmann et al., 2003) (Brenner and Kupferminc, 2003) or sickle cell disease (Sun et al., 2001). "Asymmetrical" growth restriction develops because of redistribution of cardiac output in favour of essential organs such as the heart, brain and adrenal glands, at the expense of non-essential organs such as the gut, liver and kidneys and is characterised by normal or reduced head growth with significantly impaired abdominal and limb growth. The imbalance between fetal demand and supply tends to increase with gestational age and asymmetrical growth impairment usually presents in the late second or third trimester.

1.1.2 Evidence of an association with brain injury.

Intrauterine growth restriction (IUGR) is associated with increased perinatal morbidity and mortality (Koops et al., 1982;Smith-Bindman et al., 2003;Taylor and Howie, 1989). In particular, there is evidence from several studies of an association between growth restriction and an increased risk of neonatal encephalopathy and seizures in the newborn (Adamson et al., 1995;Badawi et al., 1998a;Bukowski et al., 2003).

The evidence of a link between growth restriction and cerebral palsy is however, more contentious. Several retrospective studies have reported an association between IUGR and cerebral palsy in both babies born at term (Blair

and Stanley, 1990) (Williams and O'Brien, 1997) and those born extremely prematurely (Gray et al., 2001;Uvebrant and Hagberg, 1992). By contrast, others have failed to show an increased risk of cerebral palsy with IUGR in very premature babies (Amin et al., 1997;Topp et al., 1996), and fetuses less than 32 weeks gestation or less than 1500g and classified as small for gestational age (Kok et al., 1998;Murphy et al., 1995). However these studies are open to criticism as Amin (1997), Topp (1996) and Murphy (1995) studied very pre-term infants, in whom the incidence of growth restriction is very low. An apparent association between IUGR and reduced risk of cerebral palsy in very premature fetuses may arise because the distribution of IUGR with gestational age is skewed towards later gestations, so that the majority of cases of IUGR occur after 28 weeks gestational age. When account is taken of the skewed distribution, there is no evidence of a reduced risk of bilateral spastic cerebral palsy in very low birthweight infants (Dammann et al., 2001).

There is also substantial evidence showing an association between intrauterine growth restriction and neurodevelopmental delay in children and young adults. One prospective study of a cohort of infants exposed to IUGR showed a significant reduction in neurodevelopmental score at 3 years of age (Fattal-Valevski et al., 1999) and specific difficulties in co-ordination, lateralisation, spatial and graphomotor skills at age 6-7 years (Leitner et al., 2000). Another prospective study of children born prematurely between 27-33 weeks gestation who had ultrasound evidence of cardiovascular output redistribution in response to intrauterine growth restriction ("brain sparing"), found that they had significantly lower mean IQ scores at 5 years of age and delayed reduction of visual evoked potential latency at 1 year of age compared to

IUGR fetuses without brain sparing (Scherjon et al., 2000). Subtle neurodevelopmental problems such as lower full-scale IQ scores and behavioural problems of inattention and anxiety at ages 9 –11 years are also associated with IUGR (Low et al., 1992).

The neurodevelopmental consequences of IUGR remain in puberty. In a small prospective study, 33 growth restricted neonates born at term had significantly reduced IQ and increased special education requirements at age 12–14 years compared to 13 appropriately grown neonates (Hill et al., 1984). Two large prospective studies of over 12,000 and 13,000 children showed associations between reduced IQ test and school marks at age 13 (Lagerstrom et al., 1991) and lower intelligence test scores at 17 years (Paz et al., 2001) with fetal growth restriction.

However, the adverse effect of IUGR on neurodevelopment may be less influential than social and economic factors. A case-control study of 673 children that compared the verbal and performance IQ of term small for gestational age children and their appropriately grown peers at five years of age showed impaired intrauterine growth accounted for only 1-2% of the variance in IQ compared to 20-30% for parental factors (Sommerfelt et al., 2000). These findings are supported by an ambitious prospective study of term neonates whose weight, length and IQ were compared at birth and at 7 years of age (Strauss and Dietz, 1998). Although a significant association was shown between IUGR and lower IQ and Bender-Gestalt motor development scores at 7 years of age in the overall population, the association was absent in similar sex sibling pairs in which only one had IUGR. This suggests that IUGR may be a confounding factor, with little direct impact on neurodevelopment compared to socio-

economic and parental factors. The association between growth restriction and premature delivery may also enable it to act as a confounding factor rather than a determinant of neurodevelopment (Zeitlin et al., 2000).

1.1.3 Influence of fetal growth restriction on cerebral metabolism.

Several studies suggest important metabolic changes affecting cerebral vulnerability to hypoxic-ischaemic injury are associated with intrauterine growth restriction. Fetal rat model studies have demonstrated that growth restriction is associated with hypoglycaemia, acidosis, hypercapnia and hypoxia (Jansson and Persson, 1990) (Ogata et al., 1985;Ogata et al., 1986). These animal model findings are supported by human cordocentesis studies that found small for gestational age (SGA) fetuses were relatively hypercapnic, hypoxic, hyperlacticaemic, acidotic and hypoglycaemic (Economides and Nicolaides, 1989;Nicolaides et al., 1989;Soothill et al., 1986) and had lower umbilical arterial pH and greater mean base deficits at birth compared to appropriately grown fetuses (Andres et al., 1999). The effect of systemic hypoglycaemia on cerebral glucose metabolism is unclear as early studies of IUGR rat fetuses reported brain glucose and glycogen concentrations were maintained in normal limits (Brown and Vannucci, 1978) however, recent studies have shown significantly reduced cerebral glucose and adenosine triphosphate (ATP) (Lin et al., 1998). Human studies in healthy normal and SGA infants using non-invasive phosphorus (^{31}P) magnetic resonance spectroscopy (MRS) found no difference in phosphocreatine (PCr), ATP, and intracellular pH, which suggests cerebral intracellular energy reserves and the ratio of oxidative phosphorylation to

anaerobic glycolysis are undisturbed by moderate growth impairment, however these findings may not reflect the intrauterine state (Azzopardi et al., 1989b).

Fetal ultrasound studies show redistribution of cardiac output in favour of essential organs such as the brain, heart and adrenal glands in response to growth restriction (van den Wijngaard et al., 1989;Dubiel et al., 2002). This compensatory haemodynamic response may enable cerebral oxidative metabolism to be maintained initially by increased cerebral blood flow (thus protecting the 'oxygen margin of safety') despite the utero-placental insufficiency and impaired blood gas exchange. In addition, if this initial response becomes inadequate, further protection is provided by increased cerebral oxygen extraction (Flecknell et al., 1983;Richardson et al., 1996). These compensatory responses partly account for the relatively unimpaired head growth ("brain sparing") found in asymmetrical IUGR fetuses. Use of alternative energy substrates and reduced metabolic demand are further adaptive mechanisms that may also minimise the effect of utero-placental insufficiency. Essential metabolic functions could expect to be maintained by these adaptive responses and they would appear to be cerebro-protective. However, it has been speculated that the cerebral metabolic margin of safety may be critically reduced by severe intrauterine growth restriction, to the extent that normal physiological hypoxic stresses of birth may exceed the cerebral metabolic adaptive capabilities and cause cell damage.

1.1.4 Influence of fetal growth restriction on cerebral development.

The putative clinical effects of growth restriction on neurodevelopmental delay may also be a mediated by changes in cerebral structural and molecular development. Such an association was found in a study of brain volume and grey/ white matter ratio which were both independently associated with the degree of growth restriction in a group of 28 neonates and infants (at 32-80 weeks post-menstrual age) (Toft et al., 1995) and a 40% reduction in birthweight was associated with a 16-23% reduction in brain volume that affected the volume of grey matter more than white matter. Other histological studies of growth restricted animal models have shown abnormal development of the visual cortex (Rees et al., 1998), hippocampus and cerebral cortex (Mallard et al., 1998) and cerebellum. The cerebellum appears to particularly susceptible to growth restriction and displays reduced granule cell dendrite numbers and Purkinje cell dendrite tree branching (Mallard et al., 1998), cell density, deletion and ectopia (Lee et al., 2001).

Intrauterine growth restriction may also influence neurodevelopment via the postnatal process of myelination and brain maturation. Myelin quantity is significantly reduced in growth restricted infants up to 60 days of age (Bourre et al., 1981), and studies in hypoxaemic growth restricted sheep fetuses have shown significantly reduced myelin basic protein staining in cortical white matter with shortened and fragmented fibres and disproportionately thinner myelination (Mallard et al., 1998). Similar detrimental effects on myelination were reported in other fetal sheep and guinea pig studies (Nitsos and Rees, 1990;Rees et al., 1990).

Although the majority of histological and functional studies confirm that intrauterine growth restriction is detrimental to cerebral development, one study reported an unexpected shortening of visual evoked potentials in severely growth restricted infants at 6 months of age compared to normally grown neonates. It was initially suggested that neuro-physiological maturation was accelerated and might be a beneficial adaptive process in growth restricted fetuses (Scherjon et al., 1996). However, this speculation was refuted by a follow up study at 5 years of age, that showed growth restricted children had significantly poorer cognitive outcomes (Scherjon et al., 2000).

The effect of IUGR on cerebral development may also be mediated by reduced free thyroxine and free tri-iodothyronine (Kilby et al., 1998) and reduced thyroid receptor expression in the cerebral cortex and cerebellum of growth restricted fetuses (Kilby et al., 2000). This proposal is supported by findings that the cerebral changes associated with isolated thyroid hormone deficiency are similar to those of growth restriction (Ferreiro et al., 1987).

There is considerable evidence of altered brain composition and development as a result of intrauterine growth restriction; these changes are partly due to altered cerebral metabolism in response to the chronic oxygen and nutrient deprivation of utero-placental insufficiency. I proposed to investigate the following hypotheses regarding the influence of growth restriction on cerebral metabolism and structure:

1. Chronic hypoxia and substrate deprivation will lead to changes of cerebral energy substrate concentrations and composition, and decreased intracellular energy reserves.

2. Therefore, growth restriction will be associated with an altered metabolic response to acute hypoxia as intracellular energy reserves will decline more rapidly and lactate generation will be impaired because of constrained substrate availability.

3. Growth restriction will be associated with increased susceptibility to brain injury in response to acute hypoxia.

1.2 Intrauterine infection.

Fetal and intrauterine infection is associated with perinatal brain injury. Viral infections such as rubella, cytomegalovirus and herpes, and toxoplasmosis are acknowledged causes of brain injury. However, intrauterine bacterial infections are more prevalent and are an insidious cause of perinatal morbidity and mortality as a result of premature delivery and damage to the central nervous system.

Bacterial infection is associated with pre-term labour and premature rupture of membranes, and indirectly to premature delivery with its consequent morbidity and mortality. Pre-term labour is associated with amnionitis in up to 70% of cases and infection plays an important role in premature rupture of membranes. It has been speculated that bacteria such as bacteroides species, anaerobic streptococci and Gardenerella vaginalis, which produce the enzyme phospholipase A_2 that activates prostaglandin precursors, may have a role in initiating uterine contractions and pre-term labour. Other organisms including bacteroides species, Group B Streptococcus and Escherichia coli have the potential to disrupt the integrity of the amniotic membranes and cause premature rupture, and bacterial vaginosis has been implicated as the cause of up to 50% of idiopathic pre-term labour (Hay et al., 1994).

Chorioamnionitis is another process by which bacterial infection can cause perinatal morbidity and mortality. Clinical chorio-amnionitis, diagnosed with an accuracy of about 80% (Dashe et al., 1999) by the presence of pyrexia (> 38°C) in addition to two of the following; maternal or fetal tachycardia, uterine tenderness, offensive amniotic liquor, elevated markers of acute infection (e.g.

leucocytosis, C reactive protein), is an infection of the chorionic and amniotic membranes and their contents and has an incidence of 5-10% (Shalak and Perlman, 2002). However, histological chorio-amnionitis, characterised by polymorphonuclear infiltrates in the placenta and membranes is more prevalent and complicates about 20% of term and 80% of pre-term pregnancies (Shalak and Perlman, 2002).

1.2.1 Evidence of an association with brain injury.

Recent studies that show the risk of spastic cerebral palsy in near term and term infants is increased nine times in the presence of markers of infection (Dashe et al., 1999;Grether and Nelson, 1997) and doubled with chorio-amnionitis in pre-term infants (Schendel et al., 2002) demonstrate the association between perinatal infection and perinatal brain injury. Risk factors and markers of materno-fetal infection, such as intra-amniotic cytokines, prolonged rupture of membranes at term or intrapartum maternal pyrexia are strongly associated with neonatal cerebral dysfunction ranging from neonatal encephalopathy to cerebral palsy (Badawi et al., 1998b;Grether and Nelson, 1997;Lieberman et al., 2000;Nelson et al., 1998). A recent meta-analysis found a positive correlation between clinical chorio-amnionitis and cerebral palsy in full-term infants (relative risk 4.7; 95% Confidence intervals (CI) 1.3 – 16.2) (Wu and Colford, Jr., 2000), while another study reported a four-fold increase in risk in term infants (Schendel et al., 2002).

Inflammatory mediators are also associated with cerebral palsy. Cytokines interleukin (IL) 1, IL-8, IL-9, TNF-α and RANTES were significantly increased in children who later developed cerebral palsy compared to unaffected

children (Nelson et al., 1998), while IL-6 is significantly linked with periventricular leukomalacia (Martinez et al., 1998) and chorio-amnionitis in premature and term neonates (Chaiworapongsa et al., 2002) (Yanowitz et al., 2002). Mays et al's (1995) finding that periventricular leukomalacia is associated with maternal appendicitis suggests systemic inflammatory mediators have an important role (Mays et al., 1995).

Several mechanisms by which cytokines may cause brain injury have been proposed. Two processes that might exacerbate the effect of a hypoxic-ischaemic challenge are systemic hypotension (Dinarello, 1996) and/or blood brain barrier disruption (de Vries et al., 1996) leading to cerebral oedema (Young, 1995) which can impair cerebral blood flow still further. Systemic hypotension and cerebral oedema can significantly reduce cerebral oxygen delivery and injure areas of the brain with a compromised oxygen supply. An interaction between cytokines and blood pressure was demonstrated by an inverse correlation between umbilical cord blood IL-6 concentration of premature neonates exposed to chorio-amnionitis and systolic, mean and diastolic blood pressure (Yanowitz et al., 2002). However, relative cerebral vascular resistance measured by middle cerebral artery Doppler ultrasound was independent of cord IL-6 concentration, which suggests cytokines act systemically via their affect on cardiac function or peripheral vascular resistance. Other studies have demonstrated an association between elevated cord levels of TNF-α in cases of severe chorio-amnionitis and neonates who subsequently develop perinatal asphyxia, respiratory distress or infection (Dollner et al., 2002).

1.2.2 Interaction with hypoxia.

In clinical practice there is often poor correlation between the severity of maternal infection or chorio-amnionitis and subsequent neonatal encephalopathy or permanent brain injury, which suggests other factors may be implicated. Reports that 25% of neonatal encephalopathy cases are associated with a combination of antenatal and intrapartum risk factors (Badawi et al., 1998b), and non-infectious maternal pyrexia is linked with perinatal brain injury (Lieberman et al., 2000) support the suggestion that interactions between adverse risk factors may have a role in the initiation of perinatal brain injury. Certainly, the combination of infection and intrapartum hypoxia-ischaemia dramatically increases the risk of cerebral palsy (OR: 78.0, 95% CI: 4.8-406) (Nelson and Grether, 1998). These clinical findings are corroborated by experiments that showed lipopolysaccharide (LPS) administered to neonatal rat pups four hours before unilateral hypoxia-ischaemia led to a significantly larger brain lesion than with either LPS or hypoxia alone (Eklind et al., 2001). Surprisingly, when LPS was administered several days before cerebral ischaemia in adult rats, it appeared to have a preconditioning effect and the severity of brain injury was reduced (Ahmed et al., 2000). Possible explanations for these contrary findings are that the physiological response to LPS may change with age or the interval between LPS and hypoxia is critical.

Several mechanisms have been proposed for the apparent synergy between intrauterine infection and hypoxia. These include up-regulation of the innate immune system and early initiation of inflammatory processes by hypoxia with glial activation (Eklind et al., 2001), increased nitric oxide production by activated astrocytes leading to mitochondrial dysfunction and failure of oxidative

phosphorylation (Bal-Price and Brown, 2001), and endotoxin induced hypoglycaemia and impaired metabolic response to hypoxia with decreased glycolysis and a smaller lactate response (Young et al., 1983). Further evidence of synergy between infection and hypoxia to cause perinatal brain injury is shown by a significant reduction in the incidence of periventricular leukomalacia (OR 0.15 95% confidence interval 0.04 - 0.57) in very premature fetuses diagnosed with chorio-amnionitis who are delivered by Caesarean section (Baud et al., 1998). This suggests avoiding vaginal delivery and its associated intrapartum hypoxia may be protective when infection is present.

Several studies in the fetus and adult have found evidence that increased brain temperature alone, even if non-infectious in origin, can cause neuronal dysfunction especially when combined with hypoxia-ischaemia (Dietrich et al., 1990;Lieberman et al., 2000;Reith et al., 1996). These findings that suggest susceptibility to hypoxic cerebral injury may be influenced by the basal metabolic rate, are consistent with other studies which show the long term histological outcome of perinatal hypoxia-ischaemia is significantly improved by systemic hypothermia for several hours after the hypoxic insult (Bona et al., 1998).

On the basis these data, I intend to investigate the proposal that systemic bacterial endotoxin causes neuronal injury via effects on cerebral energy metabolism that are exacerbated by acute hypoxia. The hypotheses to be tested are:

1. Systemic bacterial endotoxin will alter cerebral energy substrate concentrations and decrease intracellular energy reserves.

2.The cerebral metabolic response to acute hypoxia will change as a consequence of systemic bacterial endotoxin and intracellular energy reserves will decline more rapidly.

3. Systemic bacterial endotoxin will be associated with increased susceptibility to acute hypoxic brain injury.

A common theme of several studies is the potential for cerebral metabolism to be affected adversely by hypoxic-ischaemia and the secondary effects of infection such as hypotension, hypoglycaemia and pyrexia. The interaction of hypoxia and infection may be additive or synergistic. Infective systemic hypotension and cerebral oedema may compromise cerebral oxygen delivery, and hypoglycaemia and pyrexia due of infection may adversely affect cerebral energy substrates availability and metabolic demands during acute hypoxia. To determine the relative significance of hypoxia and infection in the origin of perinatal brain injury, it would be beneficial to isolate the effects of hypoxia and infection on cerebral metabolism and histology, and to compare them with the result of both factors acting in unison.

1.3 Fetal Cerebral Metabolism.

Energy is essential for maintaining neuronal homeostasis, cell synthesis, neurotransmitter release and uptake, and nerve impulse conduction. Adenosine tri-phosphate (ATP) possesses labile high energy phosphate bonds (equivalent to 12,000 calories per mole of ATP) that provide energy rapidly in response to demand by splitting a phosphoric acid radical away to leave adenosine diphosphate (ADP). ATP is renewed by the combination of ADP and inorganic phosphate when energy from an energy substrate is available. ATP production occurs in the cytosol and mitochondria and is most efficient when energy substrates are converted to ATP by oxidative phosphorylation. ATP production by anaerobic glycolysis can continue in the absence of oxygen but is considerably less efficient. Although ATP is buffered by the high energy phosphate bond (equivalent to 13,000 calories per mole) of phosphocreatine (PCr) that acts a cellular energy store, cerebral energy reserves are limited and the margin between maximum energy requirements and generation is narrow. Therefore, a continuous supply of energy substrates and oxygen delivered by the cardiovascular system is essential. The majority of cerebral energy is used for signalling purposes, especially cell membrane bound sodium transport channels, while very little is used for vegetative processes (Ames, III, 2000).

1.3.1 Energy substrates.

1.3.1.1 Glucose.

Glucose is the principle cerebral energy substrate in the human fetus from mid gestation onwards. Glucose supplied to the fetal brain comes directly from

the mother by facilitated diffusion across the placenta or from gluconeogenesis in the fetal liver and enters the brain across the blood brain barrier by facilitative glucose transporter proteins. 38 ATP per glucose molecule can be generated by glycolysis and oxidative phosphorylation, but only 2 ATP per glucose molecule under anaerobic conditions when only glycolysis occurs.

1.3.1.2 Ketone bodies.

Ketone bodies (acetoacetate and β-hydroxybutyrate) derived from fatty acids are important energy substrates in fetal and adult human cerebral metabolism. The fetal uptake of ketone bodies is 1.5 times higher than glucose between 12 – 21 weeks gestational age (Adam et al., 1975) and the adult human brain can adapt and function normally when ketone bodies account for two-thirds of cerebral energy needs, even though glucose is usually the preferred substrate (Owen et al., 1967). Neonatal rats also utilise β-hydroxybutyrate and acetoacetate for cerebral energy generation (Cremer and Heath, 1974;Vicario et al., 1991). Ketone bodies are metabolised immediately in the brain (Miller, 1986) and cerebral uptake is proportional to the arterial concentration.

1.3.1.3 Lactate.

The role of lactate in mammalian cerebral energy metabolism is controversial. By convention, lactate is considered an end-product of anaerobic glycolysis that diffuses readily into the extracellular space and allows glycolysis to continue for several minutes rather than seconds, as would be the case if pyruvate and NADH+ were not removed from the site of glycolysis. Cerebral lactate was considered a sign of anaerobic metabolism, however it has recently been suggested that it is also the primary energy substrate for some cerebral cell populations. It is speculated that a significant proportion of cerebral energy

comes from the conversion of glucose to lactate at one cell location (to yield 2 ATP/ glucose molecule), and from the oxidation of lactate to water and carbon dioxide (via pyruvate and the Kreb cycle) at another cell location (to yield 36 ATP/ glucose molecule) (Magistretti and Pellerin, 1999). Lactate has been shown to be an alternative cerebral energy substrate under normoxic conditions in neonatal murine, adult human and fetal rabbit studies (King et al., 1997;Lapidot and Haber, 2000;Thurston et al., 1983).

1.3.2 Principal energy substrate.

The principal fetal cerebral energy substrate differs by species, and can alter with developmental age and adapt according to physiological circumstances. For example, although lactate and β-hydroxybutyrate provide 70% and 20% of cerebral energy requirements respectively in 6 day old rat pups, by day 15, lactate is replaced by glucose as the principle cerebral substrate, whilst the contribution of β-hydroxybutyrate is unchanged (Dombrowski, Jr. et al., 1989). In-vitro studies of day 10 neonatal rat brain slices also show that although β-hydroxybutyrate attenuates the fall in phosphocreatine in response to aglycaemic hypoxia and aids phosphocreatine recovery once normoxia is restored, yet the effect is lost in the adult rat brain (Brooks et al., 1998). Mouse cerebral monocarboxylate transporter mRNA expression peaks at postnatal day 15 and persists in adult parenchymal cells but disappears from endothelial cells, which suggests monocarboxylates (β-hydroxybutyrate, acetoacetate and lactate) are important brain energy substrates in the murine neonate and intercellular exchange of lactate is present in the adult (Pellerin et al., 1998).

The preferred energy substrate may also be influenced by location within the brain, as the oxygen tension varies from about 90microM adjacent to a capillary to as low as 2microM in areas relatively distant from capillaries where oxidative metabolism is limited by oxygen availability. However, glycolysis can proceed because the glucose concentration of 4mM varies little through out the brain. Lactate produced in one cerebral location may be oxidised in a better vascularised areas nearby. The negative correlation between lactate dehydrogenase and cytochrome oxidase, and positive correlation between cytochrome oxidase and capillary density (Borowsky and Collins, 1989), is evidence of a heterogeneous distribution of oxidative and glycolytic metabolism that is influenced by the local oxygen concentration.

1.3.3 Response to hypoxia.

The initial response to acute fetal hypoxia is an increase of cerebral oxygen extraction that can variably maintain cerebral oxygen consumption until oxygen delivery falls by about 50%. If oxidative phosphorylation declines beyond the ability of anaerobic glycolysis to compensate, then intracellular stores of PCr and ATP decline and the cell membrane becomes depolarized. Consequently, voltage-dependent calcium channels open and large quantities of calcium ions enter the cell to activate proteases, lipases and endonucleases, and initiate cell damage. When normoxia is restored, protein biosynthesis is restored in undamaged regions of the brain, but remains inhibited in more vulnerable areas. Intracellular PCr and ATP stores are rebuilt and lactate is cleared by conversion to pyruvate and subsequent oxidative phosphorylation or elution from the brain to the liver.

The initial metabolic response to chronic hypoxia is similar to acute hypoxia with increased oxygen extraction and activation of anaerobic glycolysis if necessary. However, if hypoxia is sustained for more than a week, oxygen consumption adapts to match oxygen delivery, and the energy demand from processes such as growth and movement activity are substantially reduced (Anderson et al., 1986;Hooper et al., 1990). Fetal serum glucose concentration is reduced and lactate is increased in response to prolonged hypoxemia (Owens et al., 1987) and cordocentesis studies have confirmed relative hypercapnia, hypoxia, hyperlacticaemia, acidosis and hypoglycaemia in the small-for-gestational-age (SGA) human fetus (Economides and Nicolaides, 1989;Nicolaides et al., 1989;Soothill et al., 1987). These conditions may constrain the ability of anaerobic glycolysis to compensate for a superimposed acute hypoxic event, thereby making growth restricted fetuses vulnerable to cerebral injury.

Under normal circumstances, third trimester human fetal cerebral energy metabolism relies principally on glucose, oxygen and oxidative phosphorylation. Cerebral cells can use alternative energy substrates and metabolic strategies to compensate for deficiencies in glucose or oxygen, but energy production for cell growth, function and maintenance can fail if these adaptive processes are over-extended. Vulnerable fetuses could be identified if adaptations of cerebral metabolism and development in response to chronic hypoxia and intrauterine growth restriction could be characterised.

1.4 Fetal cerebral perfusion.

The fetal cardiovascular system is responsible for acquiring oxygen and nutrients from the mother via the placenta, and then distributing them throughout the body. It has a complementary role of collecting many of the end products of metabolism and cell catabolism and transferring them to the maternal circulation for disposal. It can also adapt to changes in the fetal condition and intra-uterine environment, and these adaptations are the basis of current techniques for non-invasive assessment of fetal well-being by ultrasound and cardiotocography. An assessment of the capabilities and limitations of the techniques currently used relies upon an understanding of the fetal cardiovascular responses to acute and chronic hypoxia, which can occur during labour and growth restriction respectively.

1.4.1 Normoxia.

Under conditions of normal fetal oxygenation, studies in the near term fetal lamb show the cerebral blood flow is auto regulated and kept constant despite variations in blood pressure over a 45-80mmHg range. Cerebral blood flow is inversely related to the partial pressure of oxygen and proportionate to the partial pressure of carbon dioxide in the carotid artery (Jones, Jr. et al., 1978;Lucas et al., 1966). The fetal heart rate is determined by the slow intrinsic electrical impulse originating in the sino-atrial node which is modified by the effect of the autonomic nervous system via the sympathetic and vagus nerves (Hanson, 1988), and blood-borne catecholamines released from the adrenal medulla.

1.4.2 Acute hypoxia.

During acute hypoxia in the late gestation sheep fetus, there is an initial bradycardia mediated by chemo-receptors, followed by a gradual increase in heart rate mediated by increased noradrenaline and adrenaline concentrations that remain elevated for 24 hours and less than 12 hours respectively and act on β-adrenergic receptors in the sino-atrial node. There is also a short-term increase in fetal heart rate variability in response to acute hypoxia, which steadily decreases with the onset of acidaemia (Dalton et al., 1977). If severe hypoxia ensues, the late decelerations that develop are not reflex responses but are likely to be due to the direct hypoxic effect on the sino-atrial node or conducting pathways or a depressant humoral effect (Caldeyro-Barcia r. et al., 1966).

The vascular response to reduced partial pressure of oxygen in vessels supplying the brain and heart is to dilate, whereas the opposite is observed in vessels supplying other vascular beds such as the carcass and gastrointestinal tract (Gilbert et al., 1990;Reuss et al., 1982;Lampe et al., 1988). In addition, catecholamines, vasopressin and angiotensin concentrations are increased in response to acute hypoxia and their vaso-constrictive effect causes arterial blood pressure to increase which enhances oxygen delivery and blood flow to the brain, heart, placenta and adrenal glands. However, the cerebral vasculature fails to auto-regulate during hypoxia and cerebral perfusion is dependent on and proportional to arterial blood pressure in the blood pressure range where auto-regulation would normally occur (Tweed et al., 1983).

During hypoxia, the blood flow is greatest to the brain stem, which may have survival advantages as important autonomic centres (including the vasomotor centre) in the brainstem are preserved. Chemoreceptor and

baroreceptor mediated reflexes also ensure the blood flow to the cerebrum, midbrain, medulla and pons cerebellum are increased during isocapnic hypoxia (Jansen et al., 1989). Even if severe hypoxaemia with acidaemia ensues, preferential perfusion of the brain, heart, adrenal gland, and placenta continues until the terminal bradycardia that precedes fetal death (Block et al., 1990).

There are some circumstances, such as an interruption of uterine blood supply, when cerebral perfusion is not maintained despite an increase in arterial blood pressure, which suggests there is an equivalent increase in cerebral vascular resistance mediated by catecholamine activated chemo-receptors (Jensen A et al., 1985). Fetal haemorrhage and the resultant ischaemia can cause similar problems. Near term arterial blood pressure in the fetal lamb is usually at the lower end of the 45 – 80 mm Hg cerebral blood flow auto-regulation range, so cerebral perfusion is significantly reduced if a fetal blood volume loss of greater than 15% occurs, such as with abruption or feto-maternal haemorrhage. In such circumstances, prostanoids are important modulators of cerebral blood flow, and have been shown to increase and help to maintain cerebral blood flow during hypotensive haemorrhage.

1.4.3 Chronic hypoxia.

By contrast, fetal sheep studies show insignificant changes in heart rate in response to chronic hypoxia with progressive acidaemia, whilst only a small rise in heart rate is observed in chronically hypoxic growth restricted fetal sheep compared to appropriately grown counterparts (Robinson et al., 1983). During prolonged hypoxaemia, bradycardias tend to normalise because of increased activity of the neuro- and medullary sympathetic nervous system.

As in acute hypoxia, blood is preferentially directed towards the heart, brain, placenta, adrenal glands and spleen, at the expense of other parts of the body but the redistribution is less pronounced than in acute hypoxia because of diminished hormonal changes, underlying metabolic alterations, and partial normalization of fetal blood gases (Abuhamad et al., 1995;Baschat et al., 1997;Campbell et al., 1991;Richardson and Bocking, 1998;Cohn et al., 1974;Mari et al., 1996;Wladimiroff et al., 1986). This redistribution is accomplished by increased catecholamine release from the adrenal medulla and sympathetic nerve endings that centralise circulation in favour of the brain, adrenals and heart. Although blood flow is increased to the brain during prolonged hypoxia, the magnitude of the increase is insufficient to maintain normal cerebral oxygenation, and oxygen delivery is progressively compromised as the duration of hypoxia extends (Rurak et al., 1990). It has been speculated that the observed reduction in cerebral oxygen consumption in response to severe hypoxia is a protective adaptation (Richardson et al., 1989). If a chronic hypoxic insult is not too severe, then the initial pCO2 rise and fall in pH revert to normal after 24-48 hours hypoxia despite a persistently reduced pO2.

Decreased resistance in the middle cerebral artery flow velocity waveform and increased umbilical artery resistance are clinical evidence of redistribution in a fetus. The fetal growth pattern is altered and characterised by normal head growth because blood is diverted towards it by redistribution, but with reduced abdominal girth because of decreased hepatic glycogen deposition, and reduced limb growth. Renal perfusion is also reduced by redistribution (Kamitomo et al., 1993) so urine output and liquor volume decrease.

Cardiac output falls if chronic hypoxia is severe. The left sided cardiac output is usually lower than the right with a left to right cardiac output ratio of 0.77 (De Smedt et al., 1987). As redistribution progresses, the afterload in the left ventricle which primarily supplies the brain via the ascending aorta is reduced and the afterload in the right ventricle which supplies the lower body and placenta via the ductus arteriosus) is increased and the cardiac output ratio tends towards unity (Rizzo and Arduini, 1991). Right atrial pressure will increase as the right side of the heart starts to fail, and cause significantly reduced flow velocities in the ductus venosus ("a wave" deceleration) during atrial contraction and increased reverse flow components in the inferior vena cava (Hecher et al., 1995;Reed et al., 1990).

The fetal responses to acute and chronic hypoxia act to preserve blood and oxygen delivery to the heart, brain and adrenal glands by cardiovascular redistribution through the action of the sympathetic nervous system and humoral factors on the heart and arterial vessels. Ultrasound offers a non-invasive method of identifying chronically hypoxic fetuses by fetal biometry and flow velocity waveform studies of cerebral and umbilical vessels. Fetal blood sampling from the umbilical vein (cordocentesis) enables more information to be obtained about pH, lactate, and gas partial pressures but entails a risk of premature delivery and intrauterine death. Despite the information that may be gathered by these invasive and non-invasive techniques, it is not possible to measure the cellular metabolic status of the brain and other organs and assess whether the cardiovascular compensatory mechanisms are intact or failing. If such crucial information could be obtained non-invasively, it might prove extremely valuable for planning the premature delivery of a compromised fetus.

1.5 Mechanisms of brain injury.

The manner of a cerebral pathological insult influences the combination of several metabolic, cytological, chemical, and haemodynamic processes that may be invoked to cause neuronal cell injury and death.

1.5.1 Hypoxic-ischaemia.

A significant disruption of cellular energy generation secondary to hypoxic ischaemia (HI) can impair the function of ATP dependent cell membrane ion channels, alter the cell membrane potential and cause excitatory amino acid release. When HI impairs oxidative phosphorylation, anaerobic glycolysis is usually invoked to meet cellular energy demands and maintain cell homeostasis. However, if HI is severe and ATP requirements are not met, then ATP dependent ion channels pumps fail, potassium efflux and sodium influx occurs, and the cell membrane becomes depolarised. Cell membrane depolarisation triggers voltage-dependent calcium channels to open, with an influx of calcium into the cell as a result (al Mohanna et al., 1994;Deshpande et al., 1987). Calcium also enters through agonist dependent channels such as those controlled by the N-Methyl-D-Aspartate (NMDA) receptor, whose affinity and basal activity is increased by hypoxia (Mishra and Delivoria-Papadopoulos, 1992). Cytosolic calcium is also increased by calcium efflux from the mitochondria and the sarcoplasmic reticulum. Mitochondria are an important buffer of intracellular calcium and their function is impaired by hypoxia (Beal, 1996;Herrington et al., 1996).

The combination of high cytosolic calcium and excitatory amino acids release (especially glutamate), can overwhelm suppressant neurotransmitters and

cause seizures and increased cerebral metabolism that further aggravates the deficiency of ATP (Espinoza and Parer, 1991). Raised cytosolic calcium activates other deleterious calcium-mediated events. Firstly, intracellular calcium dependent membrane phospholipase A and C are activated to hydrolyse phosphoglycerides or glycerophosphatidates such as lecithin, to form fatty acid and lysophospholipid products. These contribute to membrane breakdown, while the subsequent conversion of fatty acids to leukotrienes and prostaglandins, such as arachidonic acid and cyclo-oxygenase contribute to the inflammatory response when they are released from cell membranes (Scott DL et al., 1990).

1.5.2 Fetal growth restriction.

It is plausible that the association between growth restriction and cerebral injury may be due to chronic hypoxaemia reducing the margin of safety of oxidative phosphorylation, and hypoglycaemia and lactic acidaemia constraining the anaerobic glycolysis response to acute hypoxia. Under these circumstances, it is speculated that the likelihood of cellular energy failure, membrane depolarisation, excitotoxic neurotransmitter release and receptor activation in response to acute hypoxia is increased by intrauterine growth restriction.

Growth restriction is also associated with altered cerebral structure and delayed development (Bourre et al., 1981;Mallard et al., 1998;Nitsos and Rees, 1990;Rees et al., 1990). These features suggest two further mechanisms that may make growth restricted brains susceptible to hypoxic injury. Immature nervous systems are relatively plentiful in iron that catalyses the conversion of H_2O_2 to the hydroxyl (OH) radical, which is a potent cause of cell membrane peroxidation and DNA oxidation (Ferriero, 2001;Bracci et al., 2001;Dorrepaal et

al., 1996;Palmer et al., 1994;Palmer et al., 1999) and may cause increased HI neuronal damage. In addition, chronic hypoxia studies in 7 day rat pups show immature oligodendrocytes are far fewer than in control animals, which suggests the subsequent development of pre-oligodendrocytes and immature oligodendrocytes may be adversely affected by growth restriction and its associated chronic hypoxia.

1.5.3 Infection.

Fetal infection can affect the cerebral response to hypoxic-ischaemia by inducing hypotension, hypoglycaemia and impaired cerebral perfusion secondary to oedema. Another mode of action may be through the inflammatory response. Acute brain injury evoked by cerebral hypoxia-ischaemia results in a transient but substantial increase in expression of IL-1β, and TNF-α mRNA in brain regions susceptible to irreversible injury, and there is evidence that pharmacological antagonism of IL-1 receptors can attenuate injury in the perinatal rat model (Silverstein et al., 1997). Several studies have shown cytokines are synthesized and secreted by CNS cells such as microglia, astrocytes and neurons in response to injury (Saliba and Henrot, 2001) (Maeda et al., 1994;Hedtjarn et al., 2002;Ivacko et al., 1997). Injury not only enhances cytokine expression locally, but also systemically, as demonstrated by increased IL-1, IL-6, and TNF-alpha in the peripheral blood of infants who suffered perinatal asphyxia and later died or were affected by cerebral palsy. It is speculated that local and systemic infection around the time of HI may exaggerate the inflammatory response and exacerbate brain injury.

1.6 Current methods of antenatal fetal assessment.

One of the aims of clinical surveillance of the fetus is to reduce the incidence of perinatal brain injury. However, the ability of current clinical tools to identify these fetuses is limited. Past obstetric history, antenatal risk factors and clinical examination are used to distinguish "high risk" pregnancies for increased fetal and maternal surveillance. However, to identify a compromised fetus and decide the timing of intervention, current non-invasive techniques of fetal assessment are limited to ultrasound biometry and biophysical profile, Doppler blood flow waveform velocity assessment and cardiotocography. Fetal biometry is the principle method of detecting growth restriction, flow velocity waveforms and fetal biophysical profile are used primarily to judge the timing of delivery and cardiotocography (CTG) is used to screen for fetal hypoxia and "fetal distress".

1.6.1 Ultrasound.

Ultrasound can identify anatomical anomalies, abnormal growth patterns and vascular flow rates. Head, abdominal and femur measurements are plotted on population standardised growth charts (Altman and Chitty, 1997) to identify fetuses with abnormal growth patterns. Measuring the liquor volume or deepest pool is an indirect assessment of fetal renal perfusion secondary to compensatory fetal cardiac output redistribution and chronic hypoxia. Umbilical and middle cerebral artery flow waveform velocities and pulsitility or resistance indices provide direct indications of cardiac output redistribution away from non-essential vascular beds to the brain and heart. Impaired placental gaseous exchange is associated with increased umbilical artery flow pulsitility because of

an increase in placental resistance and alterations in umbilical artery vascular tone. When the cardiac output is diverted towards the brain, the pulsitility indices in the carotid and middle cerebral artery are reduced. A fetus is not at risk of acidaemia or abnormal neurodevelopment during the early stage of compensated redistribution. However, a stepwise sequence of changes in Doppler parameters will occur if the fetal condition deteriorates. Firstly, the thoracic aorta pulsitility index is increased or flow is absent at the end of diastole, which is significant as it denotes an increased risk of neonatal enterocolitis (Hackett et al., 1987) and delayed neurodevelopment at 4 years (Fouron et al., 2001). Secondly, myocardial dysfunction will ensue and cause umbilical vein notching or pulsations that reflect increased pressure in the right atrium (DeVore G.R. and Horenstein J., 1993) and reduced or reversed ductus venosus flow during atrial contraction (Kiserud T. et al., 1994), when the compensatory mechanisms are over-extended. Abnormal ductus venosus velocity waveforms signify that metabolic acidaemia has supervened and the risk of neurodevelopmental delay (Low et al., 1995;Soothill et al., 1992), multi-organ failure and intrauterine death are significantly increased.

It is important to be wary of being falsely reassured by a normal middle cerebral artery flow velocity waveform, because cardiac dysfunction can cause the flow velocities to revert to normal. In such circumstances, abnormal venous Doppler flow velocity waveforms will reveal the true situation. The full sequence of Doppler changes associated with progressive deterioration of the fetal condition as described above is unusual beyond 32-34 weeks gestation, when it is of limited use. Multi-vessel Doppler analysis is not 100% specific and sensitive and further information is required to adequately assess the status of the fetus.

The Biophysical Profile is a composite scoring system of fetal movement, tone, breathing movements, amniotic fluid volume and cardiotocograph for assessing fetal well-being (Manning, 1999). A score lower than 8 out of 10 is highly suggestive of fetal compromise. Comparison of the ability of flow velocity waveforms and the Biophysical Profile to identify a compromised fetus is difficult. However, in severe growth restriction, fetal vascular changes occur 24 hours before there is a significant deterioration in biophysical profile score in about 70% of cases (Baschat et al., 2001).

It is difficult for the clinician to balance the risks of prematurity against those of fetal cardiovascular decompensation and to the judge the optimum time of delivery to avoid cerebral damage, and minimise morbidity and mortality secondary to prematurity. Doppler waveform velocities primarily reflect cardiac function and myocardial oxygenation, which is an indirect and imprecise indication of cerebral metabolism and compromise. The fetal tone, breathing, gross movement and cardiotocogram components of the biophysical profile reflect central nervous system function, but are influenced by gestational age and fail to reflect the function of higher cerebral centres, which is a principal concern.

1.6.2 Cardiotocography

Cardiotocography was introduced into British clinical practice about two decades ago without the benefit of randomised control trials or evidence of its effectiveness, as a tool for identifying fetal hypoxia and acidaemia. There is no strong evidence of its beneficial use in labour for the avoidance of neonatal encephalopathy (Spencer et al., 1997) or cerebral palsy, as it has a high false

positive rate and the incidence of both conditions is relative low (less than 7:1000 births). Therefore it should not be used by itself outside the setting of a clinical trail. Its use for assessing fetal well-being is limited by its subjective and inconsistent evaluation and considerable intra- and inter-observer variation. Agreement has not been reached regarding which aspects of the CTG are most significant in relation to fetal blood gases and pH values. More critically, a recent review of four randomised trials performed in the 1980's of antepartum cardiotocography in intermediate and high-risk pregnancies did not show a significant benefit on perinatal morbidity or mortality (Pattison and McCowan, 2000).

CTG scoring techniques have proved problematic. The false negative rate is low, but estimates of false positive rates range from 50 – 80% (Schifrin B.S. and Clement D., 1991). In a large review of 155,636 children, of whom 95 had cerebral palsy and 78 were monitored, there was a false positive rate of 99.8 % (Nelson et al., 1996). Clearly, maternal morbidity and mortality are increased if caesarean sections are performed in response to abnormal CTG findings. It would be helpful if studies of fetuses with abnormal CTG findings could improve the specificity of the CTG.

An attempt was made to overcome the problem of inconsistent CTG interpretation by the use of computer based advanced neural networks to analyse the cardiotocogram and this technique was first tested in the early 1990's (Keith and Greene, 1994). The proponents proposed that intelligent systems could "transform the cardiotocograph from a difficult-to-use, ineffective recorder of fetal heart rate, to an interactive and effective decision support tool capable of raising the skills of staff". They have been shown to correlate well with manual

categorisation and are available more rapidly (Liszka-Hackzell, 2001). It is thought by some (Seufert et al., 2000) that there should be no delay in implementing the computer- assisted CTG analysis to the clinical situation. An encouraging study where computer analysis was linked to alarms showed that the delay to recognize deterioration in the CTG could be reduced (Ulbricht et al., 1998). However, appraisal of this technique was limited to labour and it has not been evaluated in an antenatal setting.

Both ultrasound and the cardiotocograph use indices of cardiovascular function as a surrogate measure of fetal hypoxia and acidaemia, and indirectly cerebral hypoxia. There is limited evidence that these methods help identify vulnerable fetuses and prevent brain injury, but they are inadequate for assessing brain metabolism and function.

1.7 Summary.

The low incidence of perinatal cerebral injury in apparently well and normally grown full term neonates is because the majority mount an adequate compensatory response to the acute hypoxic stresses of labour. Conversely, insufficient or altered compensatory responses are likely to occur in those that succumb. Growth restriction and intrauterine infection are common clinical conditions that are associated with perinatal cerebral brain injury and neonatal encephalopathy. Although the systemic and cerebral haemodynamic compensatory responses to IUGR have been characterised experimentally and clinically, the cerebral energy substrate and metabolic consequences are uncertain, particularly in relation to acute hypoxia in an IUGR or infected fetus. However, the technique of magnetic resonance spectroscopy offers the

opportunity to non-invasively investigate *in-vivo* cerebral metabolism and the influences of fetal growth restriction, infection and hypoxia.

2 MAGNETIC RESONANCE AND PERINATAL CEREBRAL METABOLISM.

2.1 Historical Background.

Isidor Isaac Rabi first observed the phenomenon of nuclear magnetic resonance in a beam of lithium chloride molecules in a vacuum at Columbia University, New York, USA in 1929. In 1937, Rabi manipulated a radio frequency signal and magnetic field to observe atomic nucleus magnetic moment precession with a characteristic frequency dependant on the nucleus type and proportional to the ambient magnetic field strength. He showed a nucleus could absorb energy and "flip" to a higher energy state when a radio frequency signal matching its characteristic precession frequency was applied. Rabi was later awarded the Nobel Prize in Physics in 1944 for his method for recording the magnetic properties of atomic nuclei. In 1945, Edward Purcell (Harvard University) and Felix Bloch (Stanford University) independently observed the nuclear magnetic resonance (NMR) phenomenon in hydrogen protons in solid and bulk materials, and later went on to share the 1952 Nobel Prize in Physics for their work.

2.2 Nuclear Magnetic Resonance

2.2.1 Physics principles

An atom's nucleus comprises protons with positive charge and neutrons without charge, with negatively charged electrons in discrete orbits around the nucleus. The nucleus rotates about an axis at a constant rate, and the spin or intrinsic spin angular momentum is confined to discrete values, depending on the

number of protons and neutrons present. If the atomic number (number of protons) and atomic weight (number of protons and neutrons) are both even, then the spin is zero, and the nucleus will not interact with an external magnetic field. A nucleus has a half-integral value of spin if the atomic weight is odd, for example, a hydrogen nucleus. Spin is an integer value (e.g. 1,2,3) if the atomic weight is even and the atomic number is odd. If a nucleus has non-zero spin, it will generate a magnetic field orientated parallel to the axis of rotation. The spin of a nucleus is a vector whose orientation and manipulation by external magnetic fields and radio frequency signals is the basis of the nuclear magnetic resonance phenomenon.

The spin axis does not align exactly with the axis of an external magnetic field, but precesses about the axis of the applied magnetic field (B_o) with a frequency (ω_o) proportional to the magnetic field strength and expressed by the Larmor equation;

$$\omega_o = \gamma B_o / 2\pi$$

where ω_o = Larmor (precession) frequency (MHz)

γ = gyromagnetic ratio (MHz T^{-1})

B_o = magnetic field strength (T)

As a result, the spin vectors inside a magnetic field have a non-zero sum parallel to the axis of the magnetic field (z axis), in contrast to the zero spin vector sum of randomly orientated protons outside of a magnetic field. The

vector sum is still zero in the x and y axes that are orthogonal to the magnetic field. There is a difference in energy (ΔE) between protons aligned parallel (spin-up) and anti-parallel (spin-down) to the applied magnetic field, which is proportional to the magnetic field strength B_o. Most protons will align parallel with Bo and have a lower energy than the anti-parallel protons. The number of spin-up protons vastly exceeds the spin-down protons by about 10^6: 1. The ratio is expressed as the Boltzmann distribution;

$$N\ spin\text{-}down\ /N\ spin\text{-}up = e^{-\Delta E/kT}$$

where N *spin-down and* N *spin*-up are the number of protons in the upper and lower energy states respectively, k is Boltzmann's constant (1.381×10^{-23} J K^{-1}) and T is absolute temperature.

The vector sum of spins is non-zero because there is a gross imbalance in the number of protons at higher and lower energy levels that generates a net magnetic field M_o parallel to B_o and constant with respect to time. This is the lowest energy arrangement and the configuration to which the protons will return after any energy perturbation.

Magnetic resonance is based upon the manipulation of M_o. The spin of protons can be flipped between spin-up to spin-down by energy of the exact frequency (ω_o) contained in a short radio frequency pulse with an effective field B_1 orientated perpendicular to B_0. M_0 rotates away from its lower energy configuration by energy absorption to be perpendicular to both B_0 and B_1. M_0 will rotate into the transverse plane if the radio frequency pulse has sufficient

duration and amplitude (and is called a 90° pulse). Once the pulse ends, the protons emit energy at frequency ω_o and gradually return to the original equilibrium orientation by "relaxation". The MR signal reflects this gradual loss of energy by protons and is known as the free induction decay (FID) (Figure 2.1).

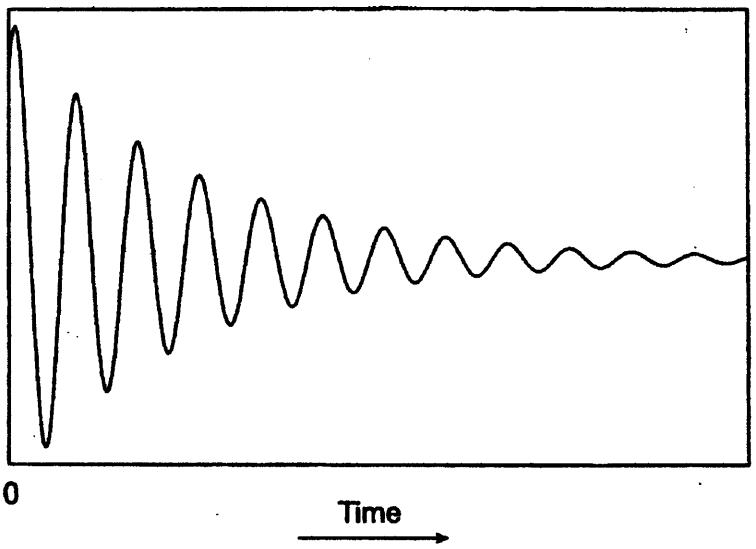

Figure 2.1 Free induction decay signal showing a decaying ($e^{-t/T2}$) sinusoid with a frequency ω_o, where T2 is the spin-spin relaxation time

The amplitude, frequency and phase (relative to the radio frequency transmitter pulse) are important characteristics of the FID. Signal amplitude is determined by M_0 immediately before the radio frequency transmitter pulse and the frequency is determined by the applied magnetic field and molecular magnetic field experienced by protons. The chemical bonds of protons and the molecular environment (termed "chemical shielding") determine the local magnetic field that is proportional to the applied magnetic field B_0. Protons in

different molecular configurations have different resonant frequencies as a result. The frequency differences are usually expressed in parts per million (ppm).

$$\omega_{i(ppm)} = (\omega_{i(Hz)} - \omega_{ref(Hz)}) / \omega_{ref\,(Hz)}$$

where $\omega_{i(Hz)}$ is the resonant frequency of the proton of interest and $\omega_{ref\,(Hz)}$ is the transmitter frequency, and the frequency differences between protons of interest are termed chemical shifts.

The raw FID signal contains many superimposed signals as a function of time. This is converted into its many frequency components relative to the transmitter frequency and expressed in the frequency domain by applying a Fourier Transformation mathematical operation to the FID signal. This separates the FID signal into its frequency components at the cost of losing information about the absolute number of protons contributing to the signal, however relative comparisons of concentrations within a spectrum can be made. Internal (e.g. water) or external reference standards are required to determine absolute proton concentrations in a specimen.

2.2.2 Factors affecting MRS spectral quality

2.2.2.1 Water suppression

The water concentration in brain tissue is about 10,000 times greater than the metabolites being studied and effective suppression of the water signal is imperative. A common method uses a frequency selective radio frequency pulse tuned at the water resonant frequency to saturate water protons, so nearly all are

in the spin-up state. Water suppression factors of 100 or more are achievable from a single pulse.

2.2.2.2 Fat suppression

The resonant frequency of lipid signals occurs at a chemical shift about 3.5ppm below the water signal, where it can overwhelm the signals from lactate and several other metabolites. Signal contamination from maternal fat is a particular problem encountered during in-utero fetal MRS studies, that has been circumvented by placing surface coils on the scalp of exteriorised fetal sheep. An alternative approach is to exploit differences in fat and metabolite relaxation and phase modulation characteristics, such as allowing a long echo time before signal acquisition and thereby attenuating the lipid signal which has a short T1 of about 250ms.

2.2.3 Computer based methods of analysing MR spectra.

MR spectral analysis can be performed in the time or frequency domain. Time domain methods operate directly on the FID or spin-echo signal and frequency domain methods process the Fourier spectrum of the original signal.

The Linear Combination Model (Provencher, 1993) analyses MR spectra in the frequency domain, using a combination of in-vitro metabolite spectra, obtained using the same acquisition characteristics (pulse sequence, echo time etc) as the in-vivo data. Using complete model spectra rather than single peaks exploits all information in the spectra.

2.2.4 Diffusion Weighted Imaging (DWI)

This MRI technique to detect random water movement using large magnetic field gradients was first described in 1986 (Le Bihan et al., 1986). Water movement or diffusion is influenced by the spatial orientation of cellular structures, such as myelin sheaths where diffusion parallel to the sheath is greater than across it. Strongly direction dependent diffusion is termed "anisotropic" and major differences in MRI contrast can occur according to the direction of the sensitising signal. Therefore, diffusion should be measured in three axes to detect diffusion anisotropy.

The Diffusion Coefficient (mm^2 s^{-1}) is influenced by the signal acquisition time because the risk of a structural barrier impeding water diffusion is proportional to the duration of observation (Td). The range of scale lengths investigated with Td = 1-100ms is 2.5-25 micrometres, which is suitable for studying central nervous system cell structures. The Apparent Diffusion Coefficient (ADC) takes account of Td, but is directionally dependent like the Diffusion Coefficient.

2.3 Magnetic Resonance and the Perinatal Brain.

2.3.1 Magnetic Resonance Spectroscopy (MRS)

Early MRS studies found cerebral metabolite concentrations varied with gestational age. For example, N-acetylaspartate (NAA) increased from 1.9mM to 3.1 mM in preterm and term babies respectively (Huppi et al., 1991) and increased in the cerebral cortex from 20 weeks gestation onwards. This gradual rise may reflect the development of axons, synapses and dendrites whilst neuron

density decreases with brain development (Kato et al., 1997). Several other metabolites such as choline, creatine and inositol appear to be unaffected by gestational age.

MRS is a valuable tool for investigating the effects of hypoxia on cerebral metabolites. Severely birth-asphyxiated infants have elevated cerebral lactate and decreased N-acetyl aspartate in the post-partum period (Penrice et al., 1996;Amess et al., 1999;Groenendaal et al., 1994) which may reflect impaired oxidative phosphorylation and neuronal damage. Abnormally low global PCr/Pi and raised Pi/ATP ratios in asphyxiated neonates with poor neurodevelopmental outcomes provides further evidence of impaired oxidative phosphorylation (Moorcraft et al., 1991a;Roth et al., 1997). By contrast, PCr/Pi gradually increases from 28 to 42 weeks gestation in normal premature and term babies.

MRS investigations of the cerebral metabolic response to acute hypoxia in neonatal and fetal animal models found increased lactate and reduced PCr/Pi and ATP in neonatal pigs during acute hypoxia which recovered a few hours after normoxia was restored. However, there was a gradual rise in lactate and fall in PCr/Pi and ATP as secondary energy failure developed about 18 hours after the initial hypoxic insult (Lorek et al., 1994;Penrice et al., 1997). A similar pattern of lactate and PCr/Pi derangement was found in human neonates with HIE.

These studies provide a valuable insight into the neonatal cerebral metabolic response to acute hypoxia. However, one cannot assume that fetal cerebral metabolism is the same as the neonate or that the metabolic responses to hypoxia observed in neonatal animal models apply to the fetus, despite some studies that report cerebral metabolite levels in fetuses and neonates of

equivalent gestational age are similar (Kok et al., 2001). Several factors affecting cerebral metabolism differ between the fetus and the neonate. Arterial oxygen and carbon dioxide partial pressures are significantly elevated and reduced respectively by the transition from intrauterine to extra-uterine life, and may influence the balance between oxidative phosphorylation and anaerobic glycolysis. Cardiac output to pulmonary and peripheral vascular beds changes significantly at delivery and may alter cerebral blood flow, pressures and metabolism.

2.3.2 Perinatal Diffusion Weighted Imaging (DWI)

Cerebral water content declines with gestational age, and if tissue barriers to water movement become closer as a result, then a secondary reduction of diffusion coefficient might occur due to this partial volume effect. Diffusion coefficient studies of the neonatal brain confirm a decrease with increasing gestational age, but the decline is greater than can be accounted for by the confounding partial volume effect (Neil et al., 1998;Tanner et al., 2000) and the cause is uncertain.

There is evidence that the cerebral DWI is affected by neonatal hypoxic ischaemic encephalopathy (HIE). However, the sensitivity of DWI to detect changes resulting from HI is variable. In one study, only 47% of term neonates with neonatal encephalopathy studied within 11 days of delivery has a decreased or abnormal DWI although they all showed abnormalities on conventional MRI (Forbes et al., 2000). These findings are supported by a DWI study of seven 36-40 weeks gestation neonates with HIE, whose DWI's were unremarkable within 24 hours of delivery, yet all four neonates examined 7 to 15 days after delivery

had marked MRI abnormalities consistent with HIE (Barkovich et al., 2001). Contradictory claims were made by two similar sized studies that found DWI abnormalities in more than 85% of neonates with HIE (Wolf et al., 2001;Takeoka et al., 2002). The inconsistent ability of DWI to detect changes due to HIE may be because changes are delayed until secondary energy failure some 18 hours after transient hypoxic ischaemia (Thornton et al., 1998).

Human and animal studies suggest DWI changes reflect disturbances of cerebral metabolism and histological responses to brain injury. Hyper-intense areas seen on DWI appear to correspond to areas of cytotoxic oedema and neuronal damage in neonates who later died (Roelants-van Rijn et al., 2001) and the areas with the greatest fall in water diffusion 3 hours after hypoxia matched areas of unilateral atrophy in cresyl violet-stained mouse brain sections 4 weeks later (Aden et al., 2002). This suggests that the early lesions detected by DWI were related to functional impairments in mice in near-adult life, but does not establish causality.

A crucial question regarding DWI is what do the changes represent? Animal models of transient middle cerebral artery occlusion have reported short term DWI abnormalities with brief occlusions and sustained ADC changes with prolonged vessel occlusion, which may reflect permanent damage (Minematsu et al., 1992). It was speculated that the ADC is sensitive to acute cytotoxic oedema (van Gelderen et al., 1994), however it does not accurately reflect neuronal shrinkage and astrocyte swelling found in response to acute hypoxic-ischaemia. The morphological changes in neurones and astrocytes that occur with decreased ADC during ischaemia do not reverse but deteriorate, whereas ADC can normalise during reperfusion and resuscitation (Li et al., 2002). Similarly, Na^+-

K^+-ATPase and cytochrome c oxidase activity in 7 and 28 day old rats falls during severe HI and stays suppressed for an hour after cerebral oxygenation and ADC were restored (Qiao et al., 2002) which undermines the suggestion that ADC changes reflect the activity of energy dependant ion exchange pumps at cell membranes (Busza et al., 1992). Neurone and extracellular volume shrinkage during acute hypoxia, and water accumulation in the extracellular space after reperfusion and damage to the blood-brain barrier might account for the biphasic decrease in ADC seen in several animal studies of HI (Thornton et al., 1998;Tuor et al., 1998;Rumpel et al., 1997). Extracellular water has a higher diffusion coefficient and can restore the ADC to normal. The secondary fall in ADC that occurs 24-72 hours after a hypoxic-ischaemic insult may occur as extracellular oedema resolves while cellular oedema persists (Forbes et al., 2000). This hypothesis is supported by studies in 7 and 28 day old rats subjected to severe transient hypoxic-ischaemia that show an association between DWI signal intensity alterations and shrinkage and re-expansion of the extracellular space (Qiao et al., 2002). These observations may reflect cellular energy collapse during the acute HI event and 24-48 hours later and the resultant failure of osmoregulation (Thornton et al., 1998). However, some studies have shown ADC tends to fall when PCr/Pi is less than 70% of normal and before changes in cell ATP levels, which suggests cell swelling may occur because of reduced Na^+-K^+-ATPase pump activity to conserve ATP levels (Back et al., 1994;Decanniere et al., 1995). Therefore, alternative mechanisms other than changes of Na^+-K^+-ATPase pump activity such as decreased temperature in ischaemic tissues, decreased apparent proton motion and increased tissue osmolality due to ischaemia, or a combination of these factors may account for the early cell

volume changes detected with diffusion-sensitive MR imaging (Le Bihan et al., 1986;Busto et al., 1987;Baker et al., 1991). Regardless of the precise cause of changes of ADC, it is potentially, a sensitive indicator of early ischaemic damage when it may be salvageable.

2.3.3 Human fetal magnetic resonance spectroscopy (MRS)

The feasibility of human fetal proton magnetic resonance spectroscopy at 36 – 41 weeks gestational age has been demonstrated by the quantification of the four dominant MRS detectable cerebral metabolites, inositol, creatine, N-acetyl-aspartate and choline (Kok et al., 2001), and well-resolved spectral peaks have been detected in the human fetus as early as 32 weeks gestation (Robinson et al., 2001). Spectrometer field strengths of 1.5 Tesla are currently used in human fetus MRS studies, although stronger fields would allow faster data acquisition and the interrogation of smaller tissue volumes, and thereby reduce signal corruption from maternal subcutaneous fat and fetal movement. The teratogenic potential of magnetic fields strengths is likely to be negligible as studies of the effects of 1.5 Tesla fields during embryonic development in the chick and mouse are reassuring or inconclusive (Tyndall and Sulik, 1991;Yip et al., 1995). However, caution should be exercised at later gestations as fetal growth restriction has been observed in mid gestation pregnant mice after only 16 hours exposure to a 0.35 Tesla magnetic field (Heinrichs et al., 1988).

If the cerebral MRS characteristics of normal, compensated and de-compensated hypoxic fetuses could be defined, then this non-invasive clinical technique could be used to manage the timing and mode of delivery of compromised fetuses to avoid additional hypoxic stress. Delivery by elective

caesarean section may be advocated for these fetuses as it is associated with a significantly reduced risk of newborn encephalopathy (OR 0.17) (Badawi et al., 1998b). Fetuses with normal cerebral metabolism could have the time and route of their delivery determined by other obstetric factors.

3 THE CHICK EMBRYO.

Animal models of perinatal hypoxic ischaemia are developed as simplified versions of systems that are too complex to investigate as a whole. Studying isolated components of a system using appropriate animal models allows the workings of the whole system to be deduced. The physiological and pathological responses to experimental cerebral hypoxic ischaemia of several mammalian fetal and neonatal animal models have been extensively investigated to elucidate the processes present in human perinatal brain injury. Contrary to first impressions, the chick embryo possesses many physiological and experimental qualities that make it eminently suitable as an animal model for studying factors that affect human perinatal brain injury

3.1 Physiology and development.

Fertilised White Leghorn (*Gallus gallus*) hen eggs incubate at 38°C and 60% humidity for 21 days before hatching spontaneously. The chick embryo is surrounded by amniotic fluid, the chorioallantoic membrane and the inner and outer shell membranes and the porous shell.

During its development the daily weight gain of embryo increases from day 6 to day 14 of incubation as the chick embryo derives energy for growth and maintenance from the yolk sac and protein from the albumen via the vitelline veins. The respiratory organ of the chick embryo is the chorioallantoic membrane (CAM), which is distributed over the inner surface of the egg. Gases diffuse between vessels in the CAM and the ambient atmosphere through micropores in the egg shell and across the inner and outer shell membranes (Figure 3.1).

Oxygen reaches the chick embryo via the chorioallantoic vein and carbon dioxide and water leave through the shell micropores.

Figure 3.1 A chick embryo and internal egg structures

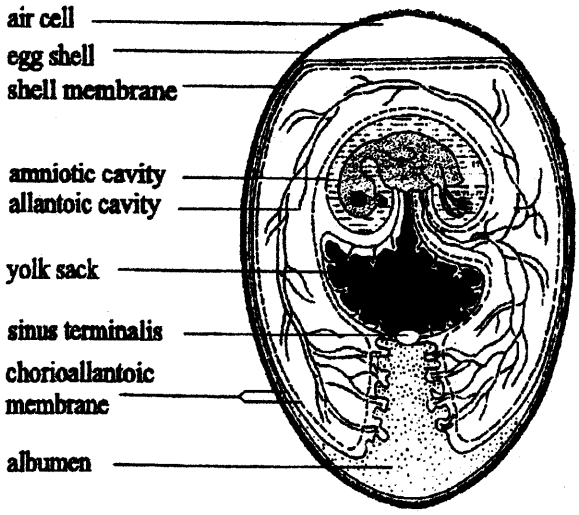

(with acknowledgements to (van Golde, 1999))

A compensatory bicarbonate metabolic alkalosis develops during the latter stages of the incubation period to ensure the diffusion capability of the egg shell is sufficient to meet the oxygen demands of the chick embryo. After day 19 of incubation, the chick embryo's oxygen demands stimulate it to break the membrane adjacent to the air cell ("internal pipping") and establish pulmonary respiration. External pipping through the axial equator of the egg shell occurs a day or so later, followed by hatching within 24 hours.

3.2 Neurodevelopment.

There are inevitably differences between human, mammalian and avian cerebral structure and neurodevelopment that need to be acknowledged. Fetuses of different species display differences in neurological maturity at equivalent fractions of gestation. Indirect indicators of the fetal stage of neurodevelopment are somatic movements, breathing rhythms and eye movements that occur in some species before birth. Several animal models such as the fetal sheep, guinea pig and chick are relatively precocious at the end of gestation compared to the human fetus, whereas the rat and mouse have similar neurodevelopment to the human at parturition. This provides an algorithm for comparing neurodevelopment between species at different gestations and ages. The neurodevelopmental maturity of a fetal model compared to a human fetus is important when considering the applicability of findings in an animal model to humans.

Another consideration is the function and development of cerebral structures that can differ greatly between species. For example, Broca's area in the left frontal lobe is crucial for human speech, and is not found in other species. Conversely, the avian visual system is capable of assimilating information faster than humans and has good visual acuity of 1.5 minutes of arc over a visual field of 70-80° compared with humans whose higher visual acuity of 0.5 minute of arc is limited to a visual field of 2.5° (Pearson R, 1972). Differences in cerebral function and development in mammals and birds are also reflected in their brain/body weight ratios. The mammalian fetal brain is significantly greater as a proportion of body weight than the avian embryo brain i.e. 100g/Kg compared to 22g/Kg. Nevertheless, there are many common cerebral embryological and

neurological processes, such as the functional organisation of the telencephalon (Macphail, 1996), dorsal migration of neurons from the basal telencephalon to populate the cerebral cortex or pallium (Cobos et al., 2001;Tuorto et al., 2003), and shared neurotransmitters (Juorio and Vogt, 1967;Gruss et al., 1999).

3.3 Cardiovascular response to hypoxia.

The chick embryo's cardiac output of 500ml/kg/min and its cardiovascular response to hypoxia are similar to the mammalian fetus (Mulder et al., 1998). The mammalian fetus shows a redistribution of the cardiac output in favour of the heart and brain during acute hypoxia. This is aided by peripheral vasoconstriction which is partly mediated by catecholamines released by sympathetic stimulation and by the direct effect of hypoxia on chromaffin cells. Mulder and colleagues (Mulder et al., 1998) used fluorescent microspheres injected in the chorioallantoic vein to demonstrate a similar redistribution in favour of the heart (up to 160% above baseline) and brain (up to 57% above baseline) in the chick embryo during the second half of incubation, which increased in magnitude with incubation time. This group also showed that embryo heart rate decreased during hypoxia and recovered on restoration of normal oxygen concentration in a manner similar to the human fetus (van Golde et al., 1997). There are further similarities in the *in-ovo* and mammalian intrauterine environments in terms of gas partial pressures and pH (Table 3-1) (Olszowka et al., 1988;Rahn and Paganelli, 1985).

Table 3-1 Gas partial pressures and pH in the mammalian fetus and chick embryo at day 14 – 15 of incubation.

	Day 14-15 chick embryo	Mammalian fetus
PH	7.37 – 7.53	7.34 – 7.4
pCO_2 (kPa)	4.5 – 5.8	5.8 - 6.7
pO_2 (kPa)	2.9 – 4.8	3 – 3.4

With acknowledgement to (Olszowka et al., 1988;Rahn and Paganelli, 1985).

3.4 Absence of maternal influences.

The ovine fetal neonatal model is a paradigm for mammalian acute hypoxia and it has the advantage of being similar in size and maturation to the human fetus. Although the fetal sheep is a good model for investigating acute hypoxia, experimental procedures performed on the pregnant ewe can cause maternal physiological stress and lead to acidosis, hypercapnia and catecholamine and corticosteroid release which may affect the fetal lamb response to hypoxia (Guissani DA et al., 1994;Rudolph, 1984). In contrast, the chick embryo has by its nature, the advantage of being independent of maternal influences.

3.5 Model of fetal hypoxia

3.5.1 Preparation for acute hypoxia.

The chick embryo does not require any invasive preparatory procedures before administration of a hypoxic insult, apart from simply applying an anaesthetic agent to the chorioallantoic membrane if magnetic resonance

spectroscopy is planned. By contrast, surgical procedures are necessary to prepare the two most popular animal models of fetal hypoxia before imposing a hypoxic insult. Caesarean section, fetal vascular catheterisation, placement of umbilical or uterine occluders, and up to 72 hours post-operative recovery before starting an experiment are usual for the ovine fetal model. Naturally, these procedures are associated by both maternal and fetal post-operative morbidity and mortality that can compromise sample sizes and increase expense. Similarly, the day 7 neonatal rat requires surgical unilateral or bilateral common carotid artery ligation to achieve a sufficient cerebral hypoxic insult.

3.5.2 Control of acute hypoxia.

Although control of the scale of hypoxic insult is achievable in the ovine, rat and chick embryo models, it is both reversible and easier to apply in the chick embryo by regulating the oxygen concentration of the ambient atmosphere. In contrast, a variable level of hypoxia is attained in the fetal lamb by using umbilical or uterine artery occluders and ventilating the pregnant ewe with hypoxic gases, although measurements of gas partial pressures in cannulated fetal arteries can be used to alter vessel occlusion to achieve a precise degree of hypoxia. The day 7 rat fetal model of hypoxia comprises common carotid ligation or obstruction with balloon catheters under light anaesthesia and respiration of 8% oxygen (Hattori et al., 1989;Rice, III et al., 1981). Regrettably, the effect of collateral blood supply through vertebral arteries is unpredictable, although this may be overcome by ligation or balloon obstruction at the expense of increased surgical complexity.

3.5.3 Susceptibility to hypoxia.

There is evidence to suggest that birds are more tolerant of cerebral hypoxia than mammals (Faraci, 1986). Firstly, there is a significant increase in cerebral blood flow that occurs at oxygen arterial partial pressures (pO_2) less than 75mm Hg, and which can increase the normal cerebral blood flow seven-fold when pO_2 drops below 30mm Hg (Grubb et al., 1978). Secondly, vasoconstriction does not occur during hypoxic hypocarbia in response to hyperventilation as in the mammal (Rosenberg, 1988) and hence there is a significant improvement of in cerebral oxygen delivery during hypoxia (Faraci, 1986;Grubb et al., 1978). Nevertheless, the chick brain is susceptible to hypoxia and demonstrates both cytological and histological responses (Lee et al., 2001;Vacotto et al., 2003).

3.6 Chick embryo model of fetal growth restriction.

Miller et al (2001) reported reproducible growth restriction of the chick embryo and accompanying evidence of brain sparing, by removing 10% of egg albumen volume at the start of incubation and incubating in an atmosphere with 14% oxygen concentration from day 10, (Miller et al., 2002). Albumen accounts for about 63% of the weight of a hen's egg and 54% of the total protein content of an egg. It comprises water (87%), protein (10%), carbohydrates (1%) and minerals for the embryo during development (Whittow, 2000). The principal effects of aspirating 10% of the egg albumen are to remove about 8% of the water and 5% of the protein available to the embryo during development. The chick embryo model of fetal growth restriction has the advantages of technical simplicity and avoidance of hazardous surgery.

In contrast, intrauterine growth restriction (IUGR) has been replicated by selective cotyledon embolisation in the fetal sheep (Trudinger et al., 1987) and uterine artery ligation with/out maternal hypoxia in the rat (Thordstein et al., 1992), but the level of growth restriction is poorly governed in both. Growth restriction in the rat model is proportionate to the position of the fetus in the uterus and its distance from the obliterated uterine artery. Therefore, fetuses manifest differing degrees of growth restriction as they are subject to dissimilar hypoxic and nutritional conditions.

3.7 Summary

The chick embryo is a suitable model of fetal hypoxia and growth restriction, with the advantages that the hypoxic insult can be accurately regulated by alteration of the ambient oxygen concentration, maternal confounding factors are eliminated, and the influence of hypoxia and nutrient restriction can be investigated separately. In addition, it is inexpensive compared to many commonly used animal models.

4 METHODS AND MATERIALS.

4.1 Chick embryo preparation.

4.1.1 Normal day 19 chick embryos.

Fertile White Leghorn hens' eggs (*Gallus gallus*) were supplied from a commercial flock of approximately 1000 hens and 100 cockerels (Henry Stewart & Co Ltd, Louth, England) and stored at 10-12°C and used within 7 days. An identification number was written in pencil on all eggs before being weighed and placed in an incubator (Polyhatch incubator, Brinsea Ltd, Sandford, N. Somerset, England). Eggs were turned automatically and kept at 38°C and 60% humidity in air within the incubator. Egg viability was checked every week by holding the egg in front of a bright point light source ("candling") and inspecting the vascular pattern in the chorioallantoic membrane (CAM). The successful incubation rate of normally grown embryos to day 21 and hatching without experimental intervention was 83% (SD 15%).

Experiments were performed on the 19th incubation day when chick embryos relied on the CAM for gaseous exchange and not pulmonary ventilation. By contrast, on the 20th - 21st day, chick embryos peck through the chorioallantoic membrane into the air cell at the blunt end of the egg ("internal pipping") and chick respiratory physiology is changed from the fetal to the adult form.

4.1.2 Growth restricted day 19 chick embryos.

Fertile hens' eggs were supplied from the same source and stored at 10-12°C and used within 7 days. Eggs were uniquely identified, weighed and the albumen content was calculated using Equation 4-1 (derived from (Finkler et al., 1998)).

Equation 4-1.

$$Albumen\_volume = \{ (Weight(g) x 0.7(ml/g)) - 8.6 \}$$

The pointed end of the shell was cleaned with 100% ethanol. A small hole was made near the pointed end of the shell with a small burr drill. The egg membranes were breached with an 18G needle attached to 5ml syringe held horizontally, and 10% of the albumen volume was aspirated. The hole was closed with a single drop of sterile cyanoacrylate glue (RS Components Ltd, Northants, U.K.). The egg weight after albumen removal was recorded before starting incubation in air at 38°C and 60% humidity. On the tenth day of incubation, eggs were transferred to an incubator with an ambient oxygen concentration of 14% and 60% humidity produced by an air/nitrogen mixture flowing at 3Litres/minute. The oxygen concentration was measured continuously with an oxygen analyser (Servomex 570A, Sussex, UK). The successful incubation rate of growth restricted embryos to day 21 without experimental intervention was significantly reduced at 15% (SD 14%) ($p < 0.001$) compared to normally grown embryos. Growth restricted embryos did not hatch spontaneously and had to removed from their shells.

Intrauterine growth restriction in the mammalian fetus often involves impaired nutrient and oxygen delivery. Both factors are duplicated in the chick model of fetal growth restriction by withdrawal of 10% of albumen (which is equivalent to 5% of total egg protein) (Whittow, 2000) and incubation in 14% ambient oxygen concentration from day 10 respectively.

4.1.3 Inoculation of day 18 chick embryos with lipopolysaccharide.

The vitality of chick embryos on the 18th day of incubation was confirmed by the presence of full and prominent CAM vessels and embryo movement seen by "candling". The air cell margins and positions of large vessels were identified. A small hole was made in the shell just above the CAM/air cell interface at a location clear of large vessels, and then extended to 6mm x 6mm with small forceps. 1-2 small drops of sterile saline were dripped onto the CAM to highlight blood vessels. A 0.4ml solution containing lipopolysaccharide (LPS) in normal saline was injected 2-3 mm below the CAM surface through a 0.33mm x 13mm needle. Haemostasis was confirmed, the shell hole was covered with a small square of impervious tape, and the egg was returned to the incubator.

4.2 Magnetic Resonance Spectroscopy (MRS) Methods

4.2.1 Sedation of chick embryo

On the 19th day of incubation, all embryos were anaesthetised with 5mg ketamine applied topically on the CAM through a hole in the shell overlying the air cell. A nonmagnetic thermistor wire (Luxtron 3100 fluoroptic thermometer,

Luxtron Corporation, USA) was placed into the air-cell for continuous monitoring of temperature *in ovo*. The egg was put into a sturdy 150ml self-seal plastic bag, adapted with an inlet and an outlet tubing system for gas supply and exhaust, through which air flowed at 3L/minute.

4.2.2 Chick embryo brain location.

The plastic bag and egg were placed on an inductively-coupled (balanced-matched) elliptical NMR surface coil (major axis 7 cm, minor axis 5.5 cm) made from a single loop of 6 mm copper tube. A neonatal sphygmomanometer cuff was secured over the bag and egg through which water at 50°C was circulated to maintain the egg at approximately 35-36°C. The egg was secured inside the bore of a 7T Biospec imaging spectrometer system (Bruker Medzin Technik GmBH, Karlsruhe, Germany; 20 cm clear bore; ^{1}H 300.5 MHz) equipped with actively shielded gradients (Bruker S-260; 11.5 cm aperture). The surface coil was tuned for the proton frequency. An adjacent single-turn secondary coil inductively coupled the sample coil to the spectrometer via a variable matching capacitor: the function of the latter was to match the sample coil impedance to the 50 Ω pre-amplifier input of the spectrometer thereby ensuring maximum transfer of radio-frequency power. This coil was used in transmit/receive mode to acquire multi-slice gradient-echo MR scout images in three orthogonal planes to enable accurate determination of the position of the chick's head within the egg (Figure 4.1).

The egg was transferred within the bag to a 2.5 cm diameter circular surface coil with the known head position placed immediately over the coil centre for acquisition of MRS data (Figure 4.2 and Figure 4.3). This coil was

made from a single-turn of copper wire (2.5 mm diameter) and was also inductively coupled (balanced-matched) and tuned for protons. An adjacent two-turn secondary coil and a series variable match capacitor inductively-coupled and impedance-matched the sample coil to the spectrometer. The coil was used in the transmit/receive mode. Global shimming (optimisation of the magnetic field homogeneity) was performed and further gradient-echo scout images were acquired to establish geometrical locations for subsequent acquisitions.

4.2.3 Proton (^{1}H) spectroscopy (relative signal amplitudes).

High-resolution images of the embryo brain in orthogonal planes were used to define a 6.6mm x 6mm x 6mm voxel (Figure 4.4). Global shimming (optimisation of the magnetic field homogeneity) was performed and further gradient-echo scout images acquired to establish geometrical locations for the subsequent acquisitions. A PRESS (Point RESolved Spectroscopy) double spin-echo localisation with an echo time (TE) of 30ms was employed to shim the voxel. The amplitudes of the 90° and 180° selective pulses were optimised by maximising the signal from brain water in the voxel. All shim currents were set to zero and the magnetic field homogeneity within the voxel was optimised by adjusting only the X, Y and Z shim currents whilst maintaining the signal from brain water. For ^{1}H MRS it is necessary to suppress the large tissue water signal in order to study the much smaller signals from metabolites of interest. For this reason three water-suppressed pulses with amplitudes optimised by minimising the signal from brain water in the voxel, were applied before the PRESS sequence. Volume-localised ^{1}H MRS spectra were acquired using a PRESS sequence (Bottomley, 1987) with a TE of 270 ms, repetition time (TR) 5s, from

the voxel located mostly in the cerebral hemispheres. 256 and 128 summed echoes were acquired for baseline measurements (total acquisition times 21.3 and 10.7 minutes respectively), and 128 summed echoes in subsequent acquisitions.

After the baseline ^{1}H spectra were acquired, air supplied to the egg was mixed with nitrogen (combined flow rate was maintained at 3L/min) to decrease the ambient oxygen concentration to 8%, as measured by an oxygen analyser (Servomex 570A, Sussex, UK). Hypoxia was maintained for 40 minutes, during which time two ^{1}H spectra were acquired at times 11-22 and 33-44 minutes. Normoxia was restored and ^{1}H spectra were acquired at 22 minutes intervals for a further 2 hours.

The proton magnetic resonance spectra were analysed by an automated Linear Combination Modelling method, whereby *in-vivo* spectrum are fitted with a weighted sum of spectra from *in-vitro* solutions of the compounds (the basis set). The basis set was acquired using the same pulse sequence, echo time, and other conditions as in the in-vivo spectrum, to ensure that effects due to J-modulation, eddy currents, partial volume etc. were modelled correctly. This model was originally described by Provencher (Provencher, 1993) and has been applied to neonates (Cady et al., 1997). The magnetic resonance spectral signal contributions of choline, N-acetylaspartate, lactate, alanine, taurine, β-hydroxybutyrate, aspartate, glutamate, glutamine, inositol, taurine and GABA (gamma amino butyrate) were ascertained.

4.2.4 Diffusion Weighted Magnetic Resonance Imaging.

Orthogonal MRI images of the chick brain were used to define a symmetrical diffusion weighted image (DWI) plane that included cerebra, optic

tecti, and brain stem. ADC values were measured in this selected plane using a diffusion-weighted stimulated-echo acquisition mode (STEAM) sequence (Merboldt et al., 1991). The sequence timing parameters were: TR 2s, TE 34ms, mixing time (TM) 183ms, acquisition time 2.2 minutes per image. The slice thickness was 2 mm, the field of view 3 cm and the image matrix (128 x 64) was zero-filled to 128 x 128 to give an in-plane pixel resolution of 0.23 mm. Diffusion-sensitising gradient pulses of 5ms duration and 200 ms separation were applied along the direction of the readout gradient. Two images were acquired at each time point, with 1.0 mT/m and 40 mT/m diffusion gradient strengths providing diffusion- weighting factors of 160 and 940 s.mm^2 respectively. Two averages were acquired resulting in a 2.13 minutes acquisition time for each measurement. ADC maps were calculated by performing a log/linear fit for each image pixel.

4.2.5 Phosphorus (^{31}P) spectroscopy (relative amplitudes).

High-resolution images of the embryo brain in orthogonal planes were used to define an 8.6mm x 6.0mm x 6.8mm voxel (section 4.2.2). Localised, single voxel phosphorus (^{31}P) spectra were acquired using point-resolved spectroscopy (PRESS). To enable the acquisition of short echo time (TE) spectra (and thereby reduce phase modulation of the adenosine triphosphate (ATP) multiplets) the 90^{o} and 180^{o} radio-frequency (RF) transmitter pulses were only 333 μs and spoiler gradient pulses only 1 ms in duration. This enabled TE to be reduced to 10 ms. The short RF transmitter pulse duration ensured both the RF bandwidth was large enough to excite the entire ^{31}P spectrum (covering about 23.5 ppm or 2,850 Hz) and ensure chemical-shift artefact effects would be minimised by the higher gradient strength. The voxel (8.6mm x 6.0mm x 6.8

mm) was centred on, and contained within, the chick embryo brain using axial, sagittal, and coronal scout MR images. With the spectrometer set to the proton (^{1}H) resonance frequency (300 MHz), RF transmitter pulse amplitudes were set by maximising the returned water signal and then the homogeneity of the magnetic field in the voxel was optimised ("shimmed") by monitoring the tissue-water signal. The spectrometer frequency was then adjusted to be exactly that of the water resonance. The spectrometer was then set to ^{31}P mode (resonance frequency 121.63 MHz) with a frequency offset such that the spectrometer frequency was at the centre of the ^{31}P spectrum (i.e. midway between the γ- and α-ATP doublets at about -5 ppm and phosphocreatine at 0 ppm) so as to minimise the maximum deviation (i.e. that for the phosphomonoester and β-ATP resonances in this PRESS implementation) from the nominal voxel spatial position as a result of chemical shift artefact. ^{31}P RF transmitter pulse amplitudes were determined from those for ^{1}H using a calibration obtained previously. It was impossible to determine these directly because, unlike the water signal, the ^{31}P signal was too small to visualise. The receiver amplification was then set to maximum and ^{31}P spectra were acquired with 2048 complex data points, TR 2s and 5 dummy scans before starting acquisition (steady state). For baseline measurements 1024 echoes were summed, and for experimental acquisitions 320 echoes.

4.2.6 Proton MRS cerebral metabolite quantitation method.

4.2.6.1 Basic Physics:

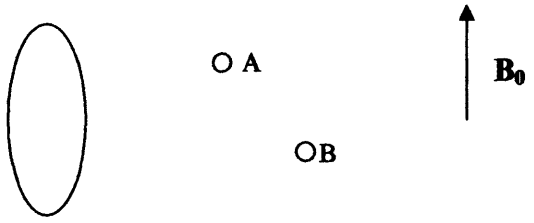

The basis behind the quantification technique is the use of the principle of reciprocity. If an alternating current, I, is set up in the coil then the amplitude of the magnetic field in the plane perpendicular to $\mathbf{B_0}$ (the transverse plane), B_{1A} and B_{1B} at points A and B in this example, is proportional to I with the proportionality constant dependent on position:

$$B_{1A} = k_A I$$
$$B_{1B} = k_B I$$

Assume a uniform sample is placed near to the coil such that points A and B are enclosed within it. If the sample is excited such that its net magnetisation, M_A and M_B at points A and B in this example, is flipped into the transverse plane, a voltage will be induced in the coil. The induced voltage due to the contributions at points A and B, U_{indA} and U_{indB}, can be given by:

$$U_{indA} = M_A \omega_0 k_A$$
$$U_{indB} = M_B \omega_0 k_B$$

ω_0 is the Larmor frequency. It can be seen that the proportionality constants k_A and k_B appear in both sets of expressions above. Thus, for a transmit/receive coil, a generalised expression can be constructed that incorporates the coil current, I_{trans}, during the transmit phase and the transmitted B_1 at point r, B_{1r}, to yield the induced voltage in the coil due to the magnetisation flipped into the transverse plane at point r, M_r:

$$U_{indr} = M_r \omega_0 \frac{B_{1r}}{I_{trans}}$$

This is the basis of the principle of reciprocity.

4.2.6.2 Quantifying spectra.

The transmit coil voltage, U_{trans}, is simply related to the transmit current by $U_{trans} = ZI_{trans}$ where Z is the coil impedance. By using the above expression, relating B_1 to flip angle and relating spectroscopy peak area A_0 to the induced voltage it can be shown that:

$$\frac{A_0 U_{trans} T}{\Phi} = concentration.\text{constant}$$

T is the sample temperature. U_{trans} and Φ, the flip angle, are related via a proportionality constant and so can be replaced with the measures of the water suppression pulse voltage and flip angle that are included in the protocol. Measuring the first and second suppression voltages allows calculation of the flip angle of the first for use in the above expression. The above expression is valid

for both phantoms and *in vivo* samples so an expression can be constructed for the absolute quantification of *in vivo* metabolites using an external water phantom as a reference; the subscript w denotes the water phantom whereas the subscript m denotes a given metabolite:

Equation 4-2

$$conc_m = \frac{A_{0m}}{A_{0w}} \frac{U_m}{U_w} \frac{T_m}{T_w} \frac{\Phi_w}{\Phi_m} conc_w$$

Adding in corrections for T2 decay of the metabolite signal and the CSF fraction of the yields;

Equation 4-3

$$conc_m = \frac{\frac{A_{0m}}{A_{0w}} \frac{U_m}{U_w} \frac{T_m}{T_w} \frac{\Phi_w}{\Phi_m} conc_w \frac{1}{e^{-TE/T2_m}}}{\left(1 - \frac{conc_{CSF}}{conc_w}\right)}$$

The CSF fraction = $conc_{CSF}$ / $conc_w$; $conc_{CSF}$ is worked out by separating brain water and CSF from the un-suppressed acquisitions using a double decaying exponential fit to a plot of peak area vs. TE and then using Equation 4-2. Brain water concentrations are calculated as per the metabolite concentrations. Brain water T2's are calculated from the double exponential fit (Danielsen and Henriksen, 1994).

4.2.6.3 Proton (^{1}H) spectroscopy (absolute concentrations).

High-resolution images of the embryo brain were used to define a 6.6mm x 6mm x 6mm voxel (Figure 3). Global shimming was performed and further gradient-echo scout images were acquired to establish geometrical locations for the subsequent acquisitions. A 3 x 3 x 3mm smaller voxel was specified near the centre of the larger voxel, and formed the source of the cerebral metabolite quantification data. The small voxel was shimmed using the PRESS (Point RESolved Spectroscopy) double spin-echo localisation with a TE 10ms. Amplitudes of the 90° and 180° selective pulses were optimised by maximising the signal from brain water in the voxel. All shim currents were set to zero and the magnetic field homogeneity within the voxel was optimised by adjusting only the X, Y and Z shim currents whilst maintaining the signal from brain water. The localised water peak was shimmed to a signal full-width at half maximum height of < 30Hz.

It was necessary to suppress the large signal from tissue water in order to study the much lower amplitude signals from cerebral metabolites. This was achieved by imposing three water-suppressed pulses with amplitudes optimised to minimise the signal from brain water in the voxel before the PRESS sequence. The water suppression pulse duration was set to 5000μs, its amplitude was increased from a minimum and the first and second water suppression voltages that achieved maximal water suppression were recorded and used to determine the flip angle in Equation 4-2.

Water suppression pulse duration was increased to 20000μs and the optimum water suppression pulse amplitude was determined and recorded.

Acquisition conditions of cerebral spectra data from the 3 x 3 x 3mm voxel were: TE 25ms, TR 5s, and 128 summed echoes.

Sequential unsuppressed data under acquisition conditions: TE = 10, 25, 35, 45, 65, 85, 105, 130, 200, 300 and 400ms, TR = 10s, and 4 summed echoes, were obtained to determine the relative concentrations of brain water and CSF.

Metabolite T2 values were determined from two water suppressed spectra obtained from the 6.6mm x 6mm x 6mm voxel using acquisition conditions: TE 135ms, TR 5s, 128 summed echoes and TE 270ms, TR 5s, 256 summed echoes respectively.

Figure 4.1 Sagittal MRI of day 19 chick embryo *in-ovo* showing spine and brain.

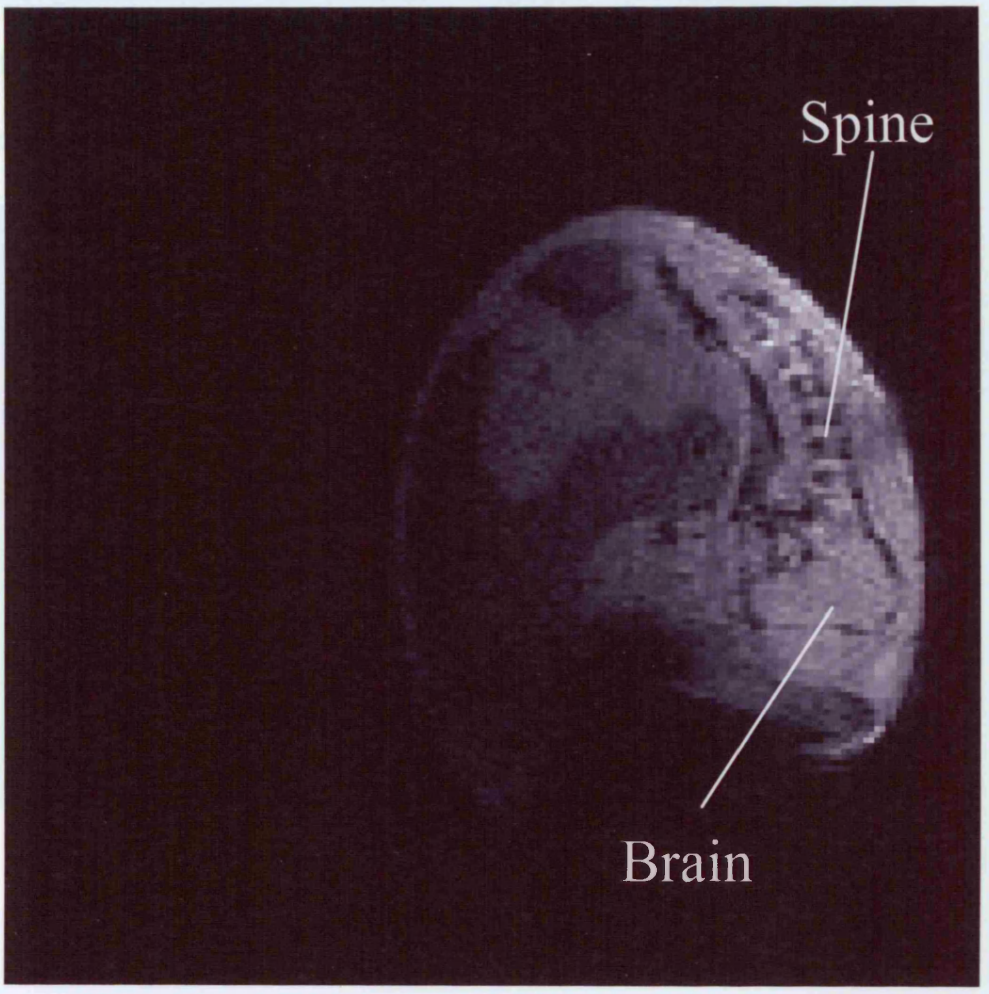

Figure 4.2 Components required for chick embryo cerebral MRS: chick embryo *in-ovo*, a 2.5 cm diameter circular surface coil, neonatal sphygmomanometer cuff (attached to opaque white tubing), fluoroptic thermistor (black wire) and 150ml plastic bag (attached to transparent green tubing).

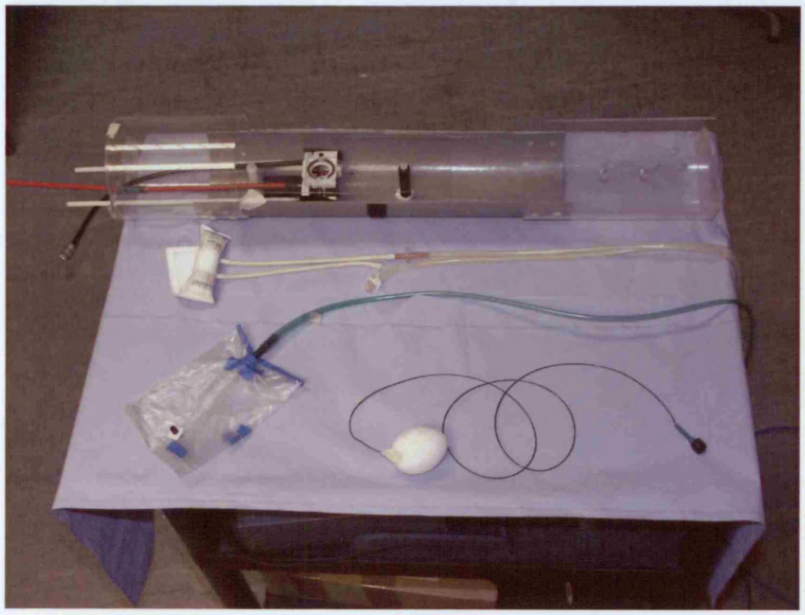

Figure 4.3 Assembled components required for chick embryo cerebral MRS, with the chick embryo brain was fixed over the centre of the circular surface coil.

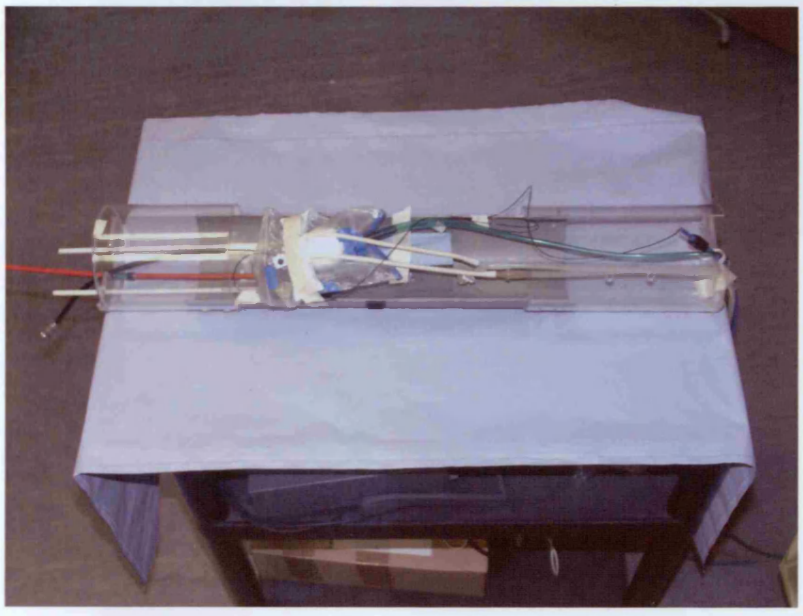

Figure 4.4 MRI of chick embryo brain with superimposed 6mm x 6mm x 6.6mm sampling voxel.

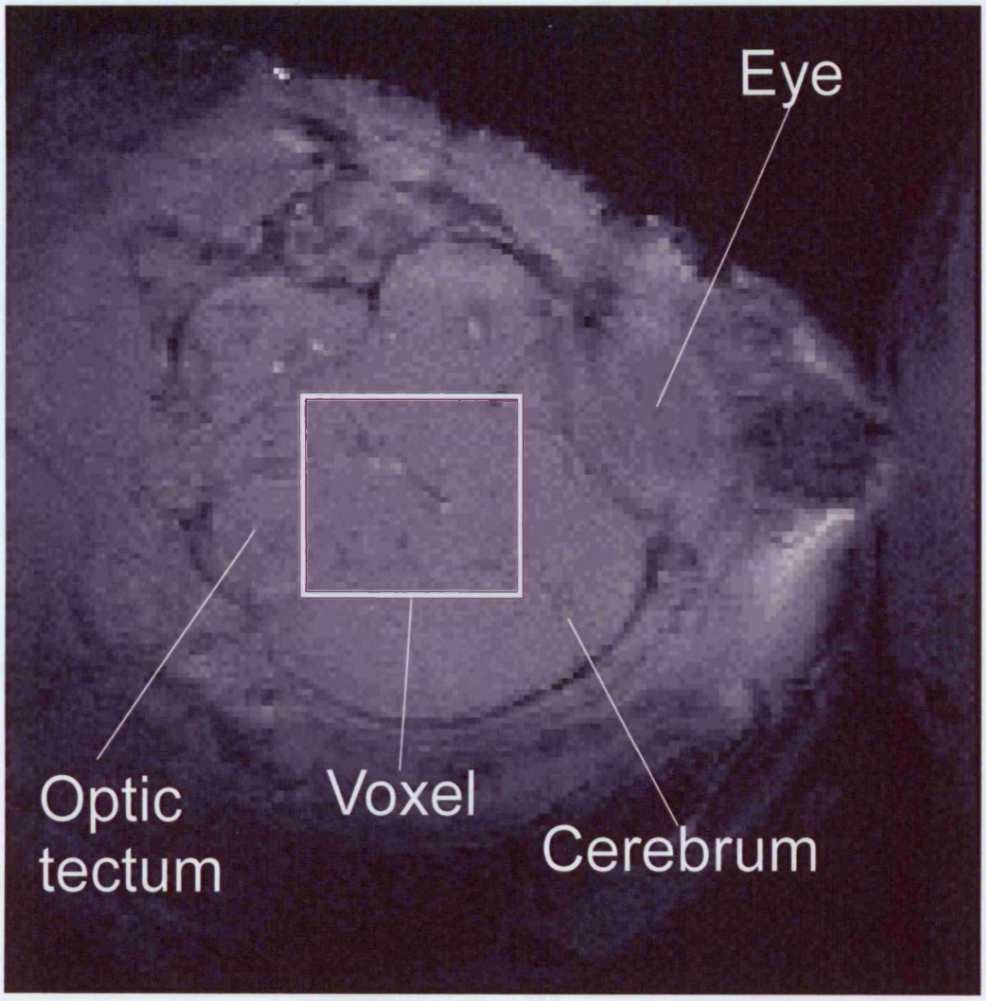

4.3 Chick embryo brain histology.

4.3.1 Fixation protocol.

On day 21, chick embryos and hatched chicks were weighed after anaesthesia by intra-peritoneal injection of 40mg pentabarbitone sodium (Euthatal (200 mg/ml pentabarbitone sodium) Rhone Merieux, Harlow, UK). The chest and abdomen were opened by sharp dissection. A small cut, slightly left and posterior to the apex of the heart, was made with scissors. A 17 gauge cannula was inserted into the left ventricle with its opening positioned beneath the major cardiac outlet vessels, and the right atrium was opened. The cannula position was adjusted and clamped when the major outlet vessels are seen to dilate with perfusate (Figure 4.5).

150ml of phosphate buffered saline followed by 200 ml of 4% paraformaldehyde were perfused at 5 ml/min. The cranium was opened and the brain was dissected out and placed in 1% paraformaldehyde and rotated at 4°C for two hours. The brain was transferred to 30% sucrose solution and rotated at 4°C overnight, until the brain sunk in the sucrose solution. The brain was cut in the coronal plane between the cerebral hemispheres and the optic tecti/cerebellum. The cut surfaces were placed on filter paper in a histology cassette, frozen on dry ice for 30 minutes and stored in a –80°C freezer.

Figure 4.5 Clamped cannula in heart during brain perfusion and fixation. A 17G cannula was inserted through the apex of the heart into the left ventricle, with its opening beneath the major cardiac outlet vessels causing them to dilate with perfusate.

4.3.2 Cryostat cutting protocol.

20 micron sections were cut on a Leica CM1900 cryostat (Leica, Nussloch, D-69222, Germany). The cabinet and specimen holder temperature were set to –20°C and –15°C respectively.

4.3.2.1 Cerebral hemispheres (Anterior brain).

The anterior-posterior depth of the specimen was measured to determine the appropriate cutting protocol for obtaining 2 sections from 8 equidistant planes (Table 4-1). The posterior face of the specimen was secured on the specimen holder with OCT compound (Tissue Tek, Sakura Finetek, Europe B.V. (NL), Netherlands). The brain was cut from left to right, starting anteriorally and moving sequentially backwards.

Table 4-1 Microtome protocol for 20micron tissue sections to sample 8 and 7 tissue planes in the anterior and posterior brain specimens respectively.

Microtome protocol	Anterior brain depth	Posterior brain depth
Discard 28, keep 2	4.9 – 5.7mm	4.3 – 5.0mm
Discard 33, keep 2	5.7 – 6.5mm	5.0 – 5.7mm
Discard 38, keep 2	6.5 – 7.3mm	5.7 – 6.4mm
Discard 43, keep 2	>7.3mm	>6.4mm

4.3.2.2 Optic tecti, cerebellum and brain stem (Posterior brain).

The anterior-posterior depth of the specimen was measured to determine the appropriate cutting protocol for obtaining 2 sections from 7 equidistant planes (Table 4-1). The anterior face of the specimen was secured on the specimen holder with OCT compound. The brain was cut from right to left, starting posteriorally and moving sequentially forwards.

Tissue sections were transferred to gelatinised microscope slides from the cryostat knife, spread in distilled water, dried at ambient room temperature overnight and stored in a dust proof microscope slide box.

4.3.3 Fixation and dehydration of tissue sections.

Cut tissue sections were fixed to gelatinised glass microscope slides by immersion in 4% formaldehyde solution (38% formaldehyde solution (Merck, Poole, United Kingdom) and distilled water) for 24 hours at 4°C and dehydrated by immersion in 70% ethanol solution (100% ethanol (Merck, Poole, United Kingdom) and distilled water) overnight at 4°C.

4.3.4 Staining protocol.

Tissue sections were stained in batches of 10 using the protocol described in Table 4-2. The extent of de-staining in 96% ethanol and glacial acetic acid solution was assessed visually during the process to avoid excessive de-staining. A cover slip was secured with Depex (Merck, Poole, United Kingdom) on top of the stained tissue specimen on completion of the staining sequence.

Table 4-2 20 micron tissue section cresyl violet staining protocol.

	Sequence of solutions	Duration of immersion
1	Nissl stain (60mls)	10 minutes
2	Distilled water (200mls)	2 minutes
3	Distilled water (200mls)	2 minutes
4	70% ethanol (200mls)	2 minutes
5	90% ethanol (200mls)	2 minutes
6	96% ethanol (200mls)	2 minutes
7	96% ethanol (200mls) and 5–7drops glacial acetic acid	3 – 10 minutes
8	100% ethanol (200mls)	2 minutes
9	Isopropan-2-ol (200mls)	2 minutes
10	Xylene (200mls)	2 minutes
11	Xylene (200mls)	2 minutes
12	Xylene (200mls)	2 minutes

4.4 Nissl stained chick embryo brain cell counting protocol.

Chick brain anatomy was identified using a stereotaxic atlas of the domestic chick brain (Kuenzel and Masson, 1998).

Pyknotic cell and neuron densities are markers of neuronal injury and death, whereas the hyperchromatic neuron density reflects the proportion of functional neurons. Current theories of neuron death after a hypoxic ischaemic insult describe a continuum between apoptosis and necrosis. Pyknosis, whereby the nucleus shrinks and becomes intensely basophilic is generally associated with

necrosis. However, neurons with uniformly dense and regularly shaped, round chromatin aggregates and uniformly condensed cytoplasm are also found in the later stages of apoptosis. Therefore, differentiating between necrosis and apoptosis on cell morphology alone is difficult, although it does reflect the incidence of cell death, irrespective of the mode.

4.4.1 Cerebral hemispheres.

Neurons (total and hyperchromatic) in the hippocampus and hyperstriatum ventralis were counted in a 500 micron x 50 micron area at x40 magnification, and pyknotic cells at the same locations were counted in a 500 micron x 100 micron grid at the same magnification (

Table 4-3).

4.4.2 Optic tectum and cerebellum.

Purkinje (total and hyperchromatic) and pyknotic cells in a 500 micron x 50 micron area orientated parallel to the Purkinje layer in the midline of the tissue section were counted at x40 magnification in each fold of the cerebellum in each tissue plane. Neurons (total and hyperchromatic) and pyknotic cells in 500 micron x 50 micron and 500 micron x 100 micron areas respectively, parallel to the axis of the Stratum griseum centrale in the optic tectum were counted at x40 magnification (

Table 4-3).

4.4.3 Sample size

It was assumed that apparently detrimental factors such as growth restriction, acute hypoxia and infection would alter pyknotic, hyperchromatic and neuron cell counts markedly, by a factor of 3 to 4. That is, the difference (δ) of the means of normal (μ_2) and affected (μ_1) brain cell counts can be expressed as, $\delta = \mu_2 - \mu_1 = \mu_2(1 - \frac{1}{3}) = \frac{2}{3}\mu_2$. Assuming the standard deviation (σ) is approximately $\mu_2/4$, to detect such a difference with 0.05 significance level and 80% power, the sample size required (N) is;

$N = 2 \times 7.849 \times \sigma^2 / \delta^2$ (Campbell and Machin, 1992)

$= 15.698 \times (\mu_2/4)^2 / (\frac{2}{3}\mu_2)^2$

$= 2.2$

Therefore, a sample size of 3 was used to evaluate the effect of growth restriction, acute hypoxia and lipopolysaccharide on cerebral histology.

Table 4-3 Brain areas and cell types counted in day 21 chick embryo brain.

Cell type	Area			
	cerebellum	hippocampus	hyperstriatum ventralis	optic tectum
pyknotic cells	√	√	√	√
neurons		√	√	√
hyperchromatic neurons		√	√	√
Purkinje cells	√			
hyperchromatic Purkinje cells	√			

5 A COMPARISON OF THE ABSOLUTE AND RELATIVE CONCENTRATIONS OF CEREBRAL METABOLITES OF DAY 19 NORMALLY GROWN AND GROWTH RESTRICTED CHICK EMBRYOS *IN-OVO* INVESTIGATED BY PROTON AND PHOSPHORUS MAGNETIC RESONANCE SPECTROSCOPY.

5.1 Introduction.

Fetal growth restriction affects up to 10% of pregnancies and is an important antenatal risk factor associated with neonatal encephalopathy (Badawi et al., 1998a). It often arises because of abnormal placental function secondary to aberrant trophoblastic invasion of the spiral arterioles in the myometrium or placental infarction secondary to maternal thrombophilia, vascular disease (e.g. poorly controlled diabetes mellitus) or hypoxia (e.g. smoking), which in turn lead to impaired oxygen and nutrient delivery to the fetus.

Several studies have suggested that important fetal metabolic changes accompany the clinically obvious alterations in growth present in growth restricted (GR) fetuses. Fetal rat model studies have demonstrated associations between growth restriction and metabolic perturbations such as hypoglycaemia, acidosis, hypercapnia and hypoxia (Jansson and Persson, 1990;Ogata et al., 1985;Ogata et al., 1986). Surprisingly, despite systemic metabolic disturbance in IUGR fetuses, the effect on cerebral glucose may be minimal, as studies of IUGR rat fetuses have reported that brain glucose and glycogen concentrations are maintained within normal limits despite systemic hypoglycaemia (Brown and

Vannucci, 1978;Vannucci et al., 1994), although others have shown reduced cerebral glucose and adenosine triphosphate (ATP) (Lin et al., 1998). Human studies in healthy normal and SGA infants using non-invasive phosphorus (^{31}P) magnetic resonance spectroscopy (MRS) failed to show differences in phosphocreatine (PCr), ATP, and intracellular pH. This suggests that cerebral intracellular energy reserves and the balance between oxidative and anaerobic glycolysis are similar in the SGA infants (Azzopardi et al., 1989b).

Glucose, fatty acids and amino acids are potential fetal cerebral energy substrates as well as vital anabolic substrates. It is speculated that fetal cerebral energy metabolism as well as brain development may be affected by the altered in-*utero* environment present in severe cases of fetal growth restriction. If alternative energy substrates are increased in association with growth restriction, then the question arises whether they fully compensate for the energy substrate scarcity or whether cellular energy reserves are compromised.

5.2 Materials and Methods.

Normal and growth restricted White Leghorn chick embryos were incubated for 19 days (sections 4.1.1 and 4.1.2). Studies were performed on day 19 of incubation (hatching occurs on day 21) and all procedures were performed in accordance with the Animals (Scientific Procedures) Act 1986, United Kingdom.

The chick embryo was anaesthetised (section 4.2.1), its brain was located within the egg and placed at the centre of a 2.5 cm diameter circular surface coil (Section 4.2.2). The part of the brain to be interrogated by MRS (voxel) was defined (Section 4.2.3).

Three experiment protocols were used to gather absolute and relative metabolite concentrations data in normally grown and growth restricted embryos.

In the first, multiple proton spectra were acquired from 7 normally grown and 8 growth restricted chick embryos to determine the absolute concentration of cerebral metabolites in a 3mm x 3mm x 3mm voxel (Section 4.2.6.3). To provide these embryos, 9 normally grown and 53 growth restricted eggs were incubated.

In the second, single proton spectra from 25 normally grown and 20 growth restricted chick embryo brains using PRESS pulse sequences with a TE 270 ms, TR 5 s and 256 summed echoes were obtained for determining the relative signal amplitudes (weighted by the spin-spin relaxation time T_2) of cerebral metabolites in a 6.6mm x 6mm x 6mm voxel (Section 4.2.3). To provide these embryos, 30 normally grown and 167 growth restricted eggs were incubated.

In the last experiment, single phosphorus spectra from 11 normally grown and 10 growth restricted chick embryos were collected using a PRESS pulse sequences with TE 10ms, TR 2 s, 2048 complex data points and 5 dummy scans, to determine the relative signal amplitudes of cerebral phosphocreatine and inorganic phosphate (Pi) in a 8.6mm x 6.0mm x 6.8mm voxel (Section 4.2.5). The chemical shift between PCr and Pi can be used as a non-invasive indicator of cerebral pH, as the chemical shift of Pi alters according to the ambient pH (Petroff et al., 1985). To provide these embryos, 14 normally grown and 67 growth restricted eggs were incubated.

The proton magnetic resonance spectra were analysed by an automated Linear Combination Modelling method, whereby *in-vivo* spectrum are fitted with

a weighted sum of spectra from *in-vitro* solutions of the compounds (the basis set). The basis set was acquired using the same pulse sequence, echo time, and other conditions as in the in-vivo spectrum, to ensure that effects due to J-modulation, eddy currents, partial volume are modelled correctly (Provencher, 1993); (Cady et al., 1997). The relative signal amplitudes (weighted by the spin-spin relaxation time T_2) of choline, N-acetylaspartate (NAA), lactate (Lac), total creatine (Cr), alanine, β-hydroxybutyrate (βHB), aspartate, glutamate, glutamine, inositol and taurine were obtained.

31P phosphorus spectra were analysed by a best fit method of free induction decay using jMRUi (Magnetic Resonance User interface) and AMARES (Naressi et al., 2001b;Naressi et al., 2001a).

T-test comparisons of absolute and relative cerebral metabolite concentrations in NG and GR embryos were performed using Sigmastat Version 2.0 (Jandel Scientific). As these were multiple tests of association of metabolites that are assumed to be independent, it is appropriate to apply the Bonferroni Correction to reduce the risk of rejecting the null hypothesis too readily (Type I error).

5.3 Results.

A representative cerebral proton magnetic resonance spectrum of a growth restricted chick embryo is shown in Figure 5.1.

Growth restriction was associated with a significant reduction in the mean absolute concentration of NAA, whereas other cerebral metabolites appeared unaffected (Table 5-1). However, this apparently significant finding ($p = 0.02$) may be erroneous once the Bonferroni correction is applied.

Growth restricted (GR) embryos had lower mean T_2-weighted inositol/Cr and NAA/Cr, and higher β–hydroxybutyrate/Cr compared with normally grown embryos, but there were no significant differences in choline/Cr, glutamate+glutamine/Cr, taurine/Cr, alanine/Cr and lactate/Cr between the brains of normally grown and GR chick embryos (Table 5-2).

Mean cerebral phosphocreatine/inorganic phosphate (PCr/Pi) was significantly reduced in growth restricted chick embryos, but the mean chemical shift between PCr and Pi was unaffected (Table 5-3).

5.4 Discussion.

The baseline ^{1}H spectra obtained during normoxia exhibited peaks similar in amplitude and chemical shift to those obtained from the brain of the human neonate (Penrice et al., 1996) and fetal sheep (van Cappellen van Walsum AM et al., 1998). Similar data have been obtained from the human fetus *in-utero* using a PRESS sequence (TE 135ms, TR 2500ms) (Kok et al., 2002), whereas in the fetal ^{1}H spectra acquired using half Fourier acquisition single shot turbo spin–echo (HASTE) sequence, the peaks for both lactate and NAA were previously contaminated by maternal tissue (Kok et al., 2001). In contrast, the presence of a

large peak ascribed to NAA that is found almost exclusively in neurones, confirmed that the signal obtained from the chick embryo was substantially cerebral in origin. Other prominent peaks were due to choline-containing compounds, creatine and lactate. In contrast to the mammalian neonate, the evident cerebral lactate signal seen in the normoxic chick embryo may be due to the relative hypoxaemia at this stage of incubation, which provides the stimulus for insertion of the beak into the air cell at 20 days of incubation.

Similar relative cerebral lactate concentrations and PCr-Pi chemical shift differences in normally grown and growth restricted embryos suggest that cerebral cellular energy requirements are satisfied under normoxic conditions without recourse to anaerobic glycolysis. However, the significantly reduced PCr/Pi ratio in growth restricted chick embryos suggests that cerebral oxidative metabolism is impaired, despite the increased β–hydroxybutyrate/Cr which might be used as an alternative cerebral energy substrate to glucose. If this speculation is correct, it would be consistent with reports in several species of an association between ketosis and reduced blood glucose concentration (Harding and Evans, 1991) (Marteniuk and Herdt, 1988;Pegorier et al., 1978), and increased cerebral uptake of ketone bodies (Daniel et al., 1977). Raised βHB has been reported in the human fetus during maternal starvation, presumably as a result of passage of ketone bodies from mother to fetus (Shambaugh, III, 1985). Ketone bodies are also increased in starved 2 weeks old rats, where their contribution to cerebral energy generation nearly doubles to supply 40% of requirements (Dahlquist, 1976). βHB inhibits lactate and glucose oxidation and spares glucose for biosynthetic deposition in the human fetus (Shambaugh, III, 1985). It has been suggested that cerebral use of ketone bodies including βHB steadily decreases as

the brain matures and co-ordinated motor activity becomes manifest (Booth et al., 1980). Notably, between 12-20 weeks gestation, the human fetal brain molar uptake of βHB is 50% greater than that of glucose (Adam et al., 1975). Ketone body use as a cerebral substrate is relatively greater in altricial species such as humans, baboons and rat than in precocial species such as the dog, cow and sheep (Cremer, 1982). The chick is a precocial species and one might expect cerebral βHB to be low. However, the raised β-HB in GR chick embryos may be due to delayed brain development secondary to nutrient deprivation, possibly by inhibiting cerebral synthesis of purine as observed in the fetal rat (Shambaugh, III et al., 1984). Brain histology and behavioural studies may help to identify the cause.

Although hyperlacticaemia and anaerobic glycolysis are commonly associated with intrauterine growth restriction, this was not found in growth restricted chick embryos. One explanation is that the cerebral lactate produced during chronic hypoxia, subsequently underwent oxidative phosphorylation when the ambient atmosphere was changed to air for the experiment. Alternatively, cerebral metabolism might be reduced, just as observed in fetal sheep and llama as a result of chronic hypoxia (Llanos et al., 2002;Newman et al., 2001). In such circumstances, total metabolism is reduced to match the available oxygen rather than attempting to fully compensate by increased anaerobic glycolysis (Bjonnes et al., 1987).

Growth restriction is associated with significant reductions in cerebral NAA/Cr and inositol/Cr, and possibly absolute NAA concentration. As the majority of NAA is found in neurones (Govindaraju et al., 2000) and inositol is a putative marker of glial cells (Brand et al., 1993), their reduced concentrations

may reflect a decline in neuronal and glial cell densities or dendrite branching that may have adverse consequences for brain development.

The observations of reduced cerebral NAA/Cr and inositol/Cr in association with increased βHB/Cr in the GR group, are evidence that the creatine concentration is unaffected by growth restriction.

Choline/Cr was similar in both normally grown and GR groups. Phosphorylcholine, glycero-phosphorylcholine and free choline are the main contributors to the choline resonance signal and are important components of cell membranes. Phosphatidylcholine (lecithin), which is also a major component of cell membranes did not contribute significantly to the signal in this study because its T_2 is very short. Although brain growth is relatively spared compared to other organs in IUGR, brain maturation is impaired and forebrain weight, total lipids and myelin are reduced in a rat pup model (Bourre et al., 1981). As changes in the in-vivo MRS signal are generally associated with alterations in membrane composition, either chick embryo brain development is unaffected by growth restriction or the choline resonance signal does not reflect changes in lipids or myelin in this model.

The metabolite concentrations of the most prominent cerebral metabolites detected by MRS in chick and mammalian brain are comparable, and suggest that the underlying metabolic processes and cell components are alike (Table 5-4). The total creatine concentration in chick embryos is similar to human grey (6.4 – 9.7 mmol/Kg ww) and white matter (5.2 – 5.7) (Pouwels and Frahm, 1998;Wang and Li, 1998). Also, the MRS observable human cerebral choline concentration is 1 – 2mmol/Kg ww (Pouwels and Frahm, 1998;Tan et al., 1998;Wang and Li, 1998) and 2.16 mmol/Kg ww in the chick embryo. However,

the N-acetylaspartate concentration in the chick embryo, which includes a contribution from N-acetylaspartylglutamate, is about half the concentration reported in humans (Kreis, 1997).This may be due to a lower neurone density in the chick embryo brain or reduced NAA in neurons, as the concentration can differ between neuron types (Simmons et al., 1991).

5.5 Conclusions.

Under normoxic conditions, growth restriction is associated with increased cerebral β–hydroxybutyrate, and reduced cerebral NAA, inositol and PCr/Pi.

Figure 5.1 Cerebral proton MR spectrum of a day 19 growth restricted chick embryo in air.

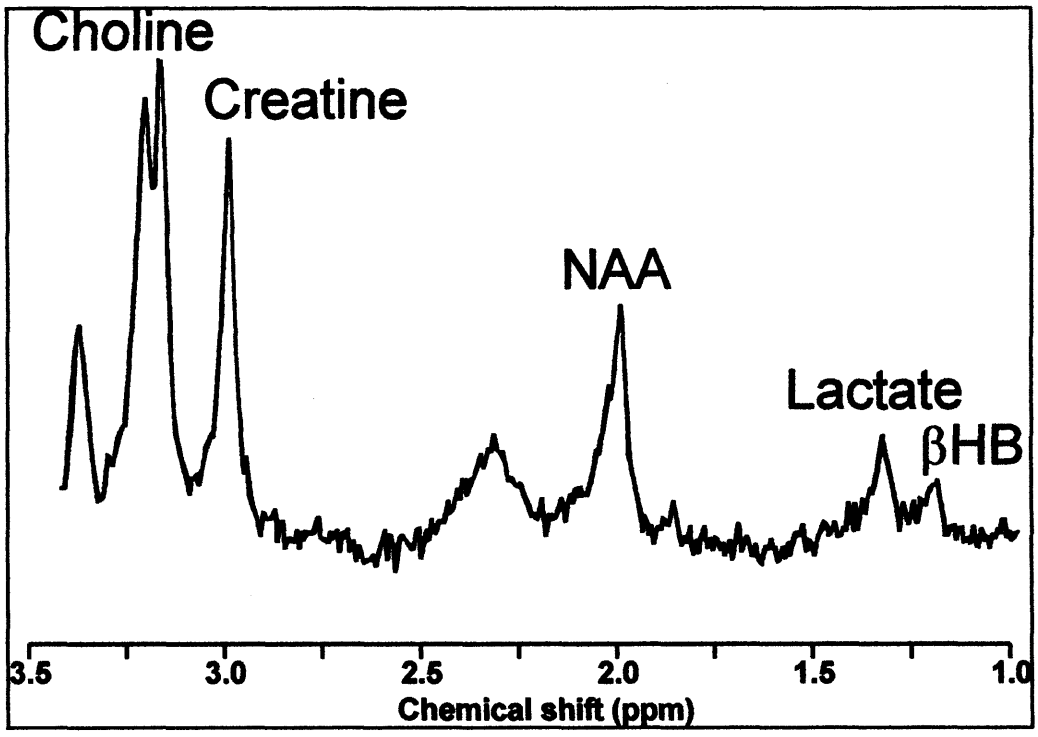

Spectral peaks corresponding to choline, creatine, N-acetylaspartate (NAA), lactate and β-hydroxybutyrate (βHB) are identified.

Table 5-1 Mean cerebral metabolite concentrations (mmols/Kg ww) and standard deviation (SD) of day 19 normally grown (NG) and growth restricted (GR) chick embryos measured by proton MRS.

Metabolite	NG mean concentration (mmols/Kg ww) (n = 7)	SD	GR mean concentration (mmols/Kg ww) (n = 8)	SD	t-test p value
Creatine	5.73	1.35	5.51	1.18	0.75
Choline	2.16	0.23	2.22	0.49	0.75
Total N-acetyl-aspartate	4.72	0.49	3.83	0.81	**0.02**
Glutamate (Glu)	5.07	1.41	5.63	0.64	0.36
Glutamine (Gln)	5.31	1.70	5.78	0.87	0.54
Glu+Gln	10.38	3.00	11.41	1.40	0.44
Taurine	3.90	0.89	4.82	1.58	0.25
Brain Water	0.71	0.13	0.71	0.05	0.93

Bonferroni corrected α level = (0.05 divided by the number of tests (8)) = **0.00625**

Table 5-2 T_2-weighted mean cerebral metabolite/Cr and standard deviation (SD) of day 19 normally grown (NG) and growth restricted (GR) chick embryos measured by proton MRS.

Metabolite /Cr	NG (n = 25)		GR (n = 20)		t-test p value
	Mean	SD	Mean	SD	
Choline	0.77	0.12	0.69	0.19	0.12
Glutamine and glutamate	1.94	0.39	1.98	0.1	0.78
Inositol	1.61	0.42	1.15	0.52	**0.002**
NAA	0.89	0.17	0.743	0.17	**0.005**
Taurine	1.65	0.44	1.62	0.51	0.86
Alanine	0.12	0.1	0.21	0.23	0.21
βHB	0.25	0.24	0.57	0.38	**<0.001**
Lactate	0.51	0.34	0.44	0.24	0.86

Bonferroni corrected α level = (0.05 divided by the number of tests (8)) = **0.00625**

Table 5-3 Mean cerebral phosphocreatine/inorganic phosphate (PCr/Pi) and mean chemical shift between PCr and Pi and standard deviations (SD) of day 19 normally grown (NG) and growth restricted (GR) chick embryos measured by phosphorus MRS.

	NG (n = 11)		GR (n = 10)		t-test
	Mean	SD	Mean	SD	p value
PCr/ Pi	2.83	1.71	1.31	0.64	**0.01**
Chemical shift (ppm)	5.13	0.078	5.15	0.095	0.38

Table 5-4 Cerebral metabolite concentrations (mmols/Kg ww) in the chick embryo and human.

	Metabolite concentration (mmols/Kg ww)	
	Chick embryo	**Human**
Creatine	5.73	5.2 – 9.7
Choline	2.16	1- 2
Total N-acetylaspartate	4.72	7 – 16

References (Kreis, 1997;Pouwels and Frahm, 1998;Tan et al., 1998;Wang and Li, 1998)

6 THE CEREBRAL METABOLIC RESPONSE TO ACUTE HYPOXIA OF THE DAY 19 CHICK EMBRYO *IN-OVO* MEASURED BY PROTON MAGNETIC RESONANCE SPECTROSCOPY.

6.1 Introduction.

Effective haemodynamic and metabolic compensatory mechanisms are thought to make the fetal brain less vulnerable to hypoxia-ischaemia than at later stages of development (Mallard et al., 1994;Newman et al., 2001). These mechanisms are important because their failure, due for instance to prolonged, severe hypoxia-ischaemia during labour, can result in brain injury with the debilitating long term consequence of cerebral palsy (Gaffney et al., 1994). The fetal haemodynamic response to hypoxaemia that acts to increase cerebral blood flow and maintain oxygen delivery, has been well-characterised in the human, sheep and more recently the chick embryo (Guissani DA et al., 1994;Mulder et al., 1998;Sutterlin et al., 1999). However, less is known about fetal cerebral metabolic responses. Therefore, proton magnetic resonance spectroscopy (^{1}H MRS) was proposed to determine changes in relative cerebral metabolite concentration during acute hypoxia in the chick embryo at day 19 of incubation.

Animal studies of the effect of acute hypoxic ischaemia on cerebral histology have used comparatively profound insults. For example, four vessel occlusion in rats (Busto et al., 1987), bilateral carotid artery occlusion (Cai et al., 2001), unilateral common carotid artery ligation and systemic hypoxia in neonatal rats (Hudome et al., 1997) and uterine artery occlusion to achieve a arterial oxygen concentration < 1.5mmol/l in fetal sheep (Gunn et al., 1992) have

been used. By comparison, 8% oxygen for 40 minutes in day 19 chick embryos was considered moderate hypoxia and no histological evidence of brain injury was anticipated.

6.2 Materials and Methods.

6.2.1 MRS

Twenty three fertilised hens eggs were incubated for 19 days in air (Section 4.1.1), at which time 19 embryos were alive. Studies were performed on day 19 of incubation (hatching occurs on day 21) and all procedures were performed in accordance with the Animals (Scientific Procedures) Act 1986, United Kingdom.

The chick embryo was anaesthetised (Section 4.2.1). The chick embryo brain was located within the egg and placed at the centre of a 2.5 cm diameter circular surface coil (Section 4.2.2). The part of the brain to be interrogated by MRS (voxel) was defined (Section 4.2.3).

After a baseline ^{1}H spectrum was acquired in air, additional nitrogen was supplied to normally grown chick embryos in the acute hypoxia group (n=11) (combined flow rate was maintained at 3L/min) to decrease the ambient oxygen concentration to 8%, as measured by an oxygen analyser (Servomex 570A, Sussex, UK). Hypoxia was maintained for 40 minutes, during which two ^{1}H spectra were acquired at times 11-22 and 33-44 minutes. Normoxia was restored and ^{1}H spectra were acquired at 22 minutes intervals for a further 2 hours. A "control" group of normally grown chick embryos (n=8) were subjected to a similar protocol but remained in air for the duration of the experiment.

Proton spectra were analysed using a technique of linear combination modelling (Provencher, 1993) and relative cerebral metabolite signal amplitudes (weighted by the spin-spin relaxation time T_2) were obtained.

For statistical analysis, group means of the spectra at each time point during hypoxia and recovery were compared with the equivalent normoxic controls. Data sets were tested for normality and equal variance before statistical comparison. Parametric and non-parametric data comparisons were performed using the t-test and Mann-Whitney Rank Sum Test respectively. Statistical analyses were performed using Sigmastat Version 2.0 (Jandel Scientific).

6.2.2 Histology

The effect of moderate hypoxia on day 21 chick embryo neuron morphology and density was investigated by incubating 29 chick embryos for 19 days in air (Section 4.1.1), by which time 4 had died. On day 19, 25 eggs were put in a sealed plastic bag located inside an incubator, supplied with air at 3L/min through an inlet hose connected to a gas mixer and regulator, and kept warm by a radiant heater within the incubator. Two experimental groups were exposed to air (N) and hypoxia (H) (Table 6-1) and incubated in air afterwards. All chick embryos survived to day 21, when they were euthanased, and their brains were perfused, fixed and prepared for cryopreservation (Section 4.3.1), before storage in a –80°C freezer. All procedures were performed in accordance with the Animals (Scientific Procedures) Act 1986, United Kingdom.

Ten (5 (Normoxia) + 5 (Hypoxia)) brains from chick embryos were of sufficient quality to be processed further. 20 micron sections from 3 brains in each group (a total of 6 brains) were cut, air dried and fixed onto slides (Sections

4.3.2 and 4.3.3) and stained with Nissl stain (Section 4.3.4). Counting of hyperchromatic, normal and pyknotic neurons in the hippocampus, hyperstriatum ventralis, cerebellum and optic tectum (Section 4.4) was performed by a single non-blinded individual.

Cell counts in each brain structure were averaged over all the tissue sections in which each structure was present. Statistical analysis of average cell counts in the two experimental groups was performed by One and Two Way Analysis of Variance (ANOVA) using Sigmastat Version 2.0 (Jandel Scientific).

6.3 Results.

6.3.1 MRS

There were 11 and 8 eggs in the hypoxia and control groups respectively and 3 embryos in each group died within 48 hours of the experiment. The survival rate to day 21 of incubation was similar in both groups (Fisher's Exact test $p = 1.0$).

Representative spectra collected at baseline in air, after 40 minutes of hypoxia, and at the end of recovery are shown in Figure 6.1. Signals corresponding to lactate, choline, creatine, N-acetylaspartate, taurine, β-hydroxybutyrate, aspartate, glutamate, glutamine and inositol were identified by linear combination modelling.

Hypoxia was associated with a significant rise in the lactate/Cr from 0.58 ± 0.41 (mean ± standard deviation (SD)) to 1.56 ± 0.54; this returned towards, but had not reached baseline values by the end of recovery (0.84 ± 0.48) (Table 6-2).

In addition, the alanine/Cr rose from 0.14 ± 0.14 (mean ± SD) to 0.29 ± 0.17, and then remained at this level during recovery (Table 6-3). Other metabolites did not change significantly as a result of acute hypoxia.

T2-weighted metabolite signal amplitudes were reported relative to total creatine which was assumed to be stable and a useful internal reference under the acute hypoxic conditions of this study. This assumption was justified, as the signal amplitudes of all metabolites apart from lactate and alanine were invariant with respect to inspired oxygen levels. Metabolites did not change from baseline values in the control embryos.

6.3.2 Histology

6.3.2.1 Hyperstriatum ventralis, hippocampus and optic tectum.

Mean pyknotic cell density and pyknotic cell/neuron quotient were significantly increased by hypoxia ((0.19 (N) vs. 0.5 (H); p=0.007) and (0.0054 (N) vs. 0.0154 (H); p = 0.002) respectively) (Table 6-4).

Hypoxia was associated with reduced hyperchromatic neuron density (9.4 (N) vs. 4.8 (H); p = 0.044), and there was a trend for the hyperchromatic neuron/ neuron quotient to be reduced (0.25 (N) vs. 0.13 (H); p=0.081)

The hyperchromatic neuron density was significantly greater in the hyperstriatum ventralis (HV) compared to the optic tectum (OT) (10.4 (HV) vs. 3.7 (OT); p=0.006) and hippocampus (Hi) (10.4 (HV) vs. 3.3 (Hi); p=0.004). Similarly, the neuron density is significantly greater in the HV compared to the OT (48.4 (HV) vs. 23.9 (OT); p<0.001) and Hi (48.4 (HV) vs. 34.2 (Hi); p<0.001). The hyperchromatic neuron/neuron quotient was not different in the three brain areas.

Hypoxia did not significantly affect neuron density.

6.3.2.2 Cerebellum.

Hypoxia was associated with a significant increase in pyknotic cell/Purkinje cell quotient (0.013 (N) vs. 0.021 (H); p=0.026) and a trend of increased pyknotic cell density (0.29 (N) vs. 0.45 (H); p=0.057), but was not associated with any change in dark Purkinje cell density, dark Purkinje cell/Purkinje cell quotient or Purkinje cell density.

6.4 Discussion.

Exposure to acute hypoxia in the chick embryo was associated with a rapid increase in the cerebral lactate/Cr, which peaked soon after the return to normoxia and then fell back to baseline values within two hours following acute hypoxia. It is likely that the observed increase represents intracellular lactate produced within the brain by anaerobic glycolysis, but it is not possible to exclude ingress of extra-cerebral lactate across the immature blood-brain barrier. However, increased cerebral lactate levels did not appear to relate to an increase in cerebral creatine, which is a crude indirect indicator of impaired cellular energy metabolism.

If elevation of cerebral lactate during hypoxia represents a failure of oxidative phosphorylation and consequent reliance on anaerobic glycolysis to maintain ATP levels, changes could be anticipated in the ^{1}H MRS creatine peak which includes signals from both creatine and phosphocreatine (PCr). Dephosphorylation of intracellular reserves of PCr during hypoxia will lead to increased creatine. It has been reported that the ^{1}H MRS Cr resonance has a

longer spin-spin relaxation time (T2 = 297 ± 41 ms at 1.5 T) than PCr (T2 = 143 ± 41 ms) – presumably due to greater mobility of the lighter Cr molecule (Ke Y et al., 2001). As a consequence of this and the long TE used in this study (270ms) the total creatine signal should increase if significant PCr dephosphorylation occurred, but such changes were not observed.

The increase in lactate most likely forms part of a co-ordinated metabolic response to match cellular energy demand with production rather than representing a failure of cellular energy metabolism. In addition to being a product of anaerobic glycolysis lactate is known to provide an alternative metabolic substrate for the developing brain (Jones and Rolph, 1985) and abolishing the increase in plasma lactate observed during acute hypoxia in the ovine fetus, using peripheral chemoreceptor blockade, leads to increased fetal mortality (Walker et al., 1996). Other aspects of the metabolic response are also likely to be important. Whilst both the embryo and newly hatched chicken produce lactate to the same degree during hypoxia, the embryo can reduce its total metabolic rate to a much greater degree than the chick (to 19% of baseline values vs. 78% respectively) (Bjonnes et al., 1987). This ability of the developing brain to reduce its metabolic rate may explain why the decline in ATP concentration, measured by ^{31}P MRS during acute hypoxia, was much slower in the rat fetus compared with the adult (O'Shaughnessy et al., 1991) and why creatine remained stable in this study. In the light of these findings it is not surprising that the lactate concentration in umbilical cord blood correlates poorly with neurological damage (Kruger et al., 1999).

The alanine/Cr showed a significant increase during acute hypoxia. This response has also been observed after cerebral ischaemia in the rat (Brulatout et

al., 1996;Higuchi et al., 1997;Smart et al., 1994) (Higuchi et al., 1997)and in the cerebro-spinal fluid of fetal lambs subjected to mild hypoxia (van Cappellen van Walsum AM et al., 2001). The role of alanine in cerebral metabolism is unclear. It has the potential to act as both a substrate for glutamate production and as a product of anaerobic glycolysis. In this latter role, pyruvate can be converted to alanine in the cytosol via a readily reversible transamination reaction, in a manner similar to the reduction of pyruvate to lactate. Such a conversion during severe hypoxia has been observed in an in-vitro superfused guinea pig cortex study (Griffin et al., 1998) and incubated cerebral-cortex slices (Ben Yoseph et al., 1993). The reaction is enhanced by increased concentrations of adenosine diphosphate (ADP) and guanosine diphosphate (GDP), and inhibited by ATP and guanosine triphosphate (GTP). The source of the pyruvate for conversion to alanine may be intracellular, but an in-vitro cortical neurone study suggested it was likely to be extracellular (Cruz et al., 2001).

T_2-weighted metabolite signal amplitudes are expressed relative to creatine, which makes the assumption that the H^1 creatine resonance remains stable throughout the experimental period. The creatine resonance observed by ^1H MRS arises from both phosphocreatine (PCr) and creatine (Cr). During hypoxia some PCr will be converted to Cr in order to maintain cerebral ATP levels and during recovery Cr will be re-phosphorylated to PCr. The total Cr (i.e. PCr plus Cr) concentration should remain constant unless transient hypoxia produces an insult severe enough to cause disruption of cellular membranes and consequent loss of intracellular contents. Under the mild hypoxic conditions of this study, such membrane disruption is not expected and hence, total Cr should be a useful internal reference for the purpose of comparison of the levels of other

metabolites. Furthermore, the total Cr signal amplitude is relatively resistant to change except in destructive pathologies such as malignant tumour and stroke (Govindaraju et al., 2000). However, PCr and Cr have different T_2 decay time constants of about 143 ms and 297 ms respectively (Ke Y et al., 2001). Substantial utilisation of PCr (resulting in an increase in Cr) would result in a longer effective Cr T_2 and, consequently, greater total Cr signal amplitude when observed by spin-echo techniques such as PRESS. However, this effect was probably negligible in this experiment as, relative to Cr, the signal amplitudes of several metabolites such as taurine, inositol, and N-acetylaspartate did not change with respect to inspired oxygen levels.

The group sample size (n = 3) used for histological investigation of the effects of hypoxia on chick embryos' brain was constrained by chick embryo survival to day 21 and technical difficulties achieving a uniformly well fixed chick brain. Although an acceptable 68% of chick embryos subjected to MRS investigation survived to day 21, the quality of perfusion and fixation was of sufficient quality for histological examination in only 45% of brains. Therefore, separate cohorts of chick embryos exposed only to acute hypoxia or normoxia on day 19, but not MRS, were produced in sufficient quantities to overcome the effective 70% loss rate of specimens suitable for histological examination.

The findings of increased pyknosis and reduced hyperchromatic neuron density 3 days after acute hypoxia imply neuronal injury, as reduced Nissl staining is found in dead and compromised neurons. However, neuron density was not affected and this may indicate either very few neurons were damaged or the assessment was performed before the complete neuronal response was accomplished. As the observer performing the cell counting was aware of each

specimen's history (non-blinded), these cerebral histological findings should be interpreted with caution.

Whether antenatal risk factors for neonatal encephalopathy, such as chronic hypoxia, fetal malnourishment or exposure to infection alter the observed cerebral metabolic response to acute hypoxia is investigated in subsequent experiments.

6.5 Conclusions.

Day 19 chick embryo cerebral lactate/Cr and alanine/Cr were significantly elevated as a result of acute hypoxia, and gradually declined towards their baseline levels after normoxia was restored. There were no significant changes in other observed metabolites in response to this level of acute hypoxia.

Figure 6.1 Cerebral proton MR spectra from the brain of a day 19 normally grown chick embryo before, after 40 minutes of acute hypoxia and at the end of a 2 hour recovery period in air. Spectral peaks corresponding to choline, creatine, N-acetylaspartate (NAA) and lactate are identified.

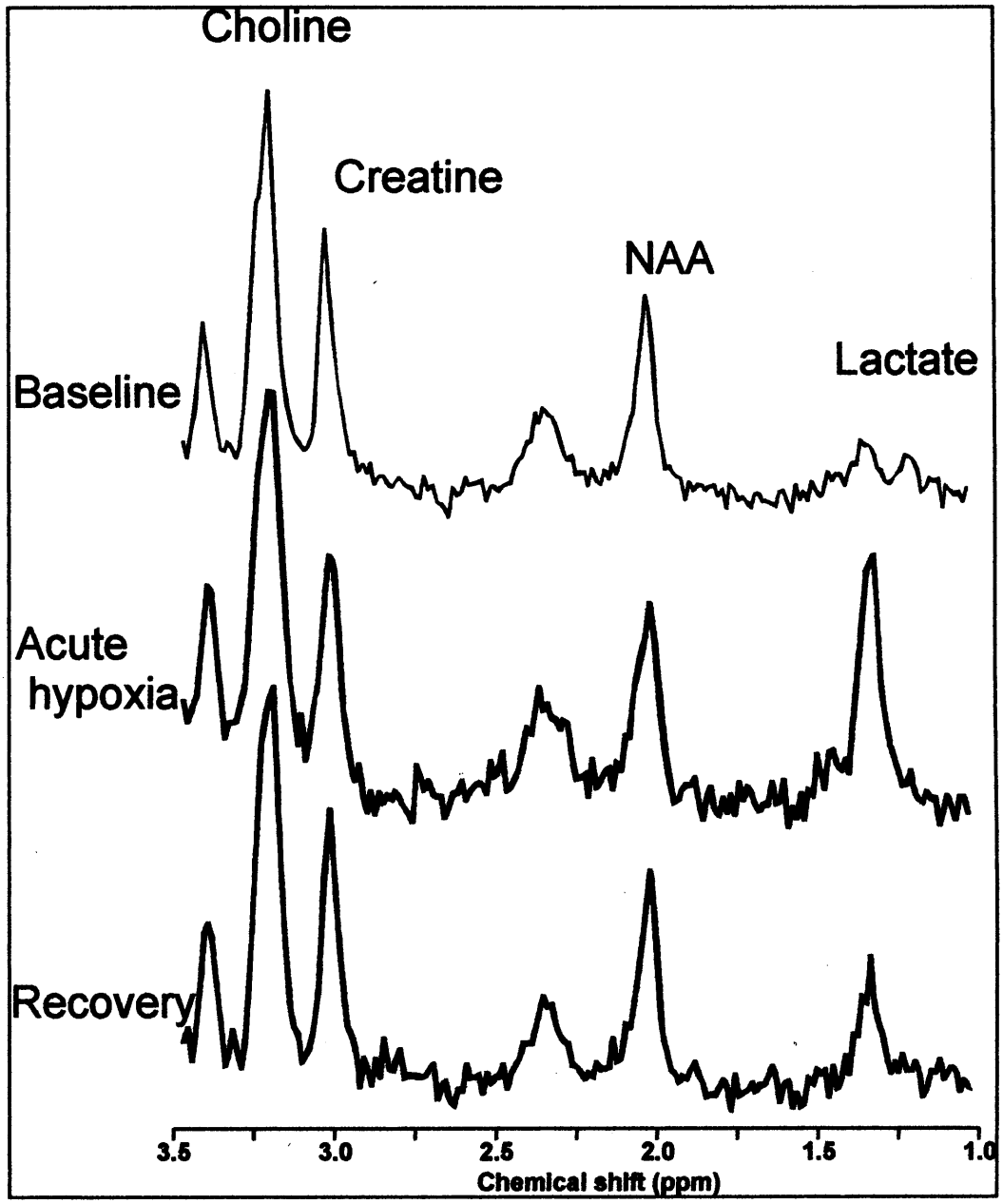

Table 6-1 Gas mixture and duration of supply in two groups of day 19 chick embryos.

Group	Ambient atmosphere	Oxygen concentration (%)	Duration (minutes)	Number of eggs
Normoxia (N)	air	21	40	14
Hypoxia (H)	air/nitrogen	8	40	11

Table 6-2 Cerebral mean lactate/Cr T_2-weighted signal amplitudes and standard deviation (SD) of chick embryos at Day 19 of incubation, before, during and after hypoxia (H) and in embryos that remained in air (N).

time (hr:mm)	H lactate/Cr (n = 11)		N lactate/Cr (n = 8)		p value
	Mean	SD	Mean	SD	
00:00 Normoxic baseline	0.58	0.41	0.38	0.22	0.23
00:11 Hypoxia	1.08	0.59	0.41	0.28	**0.004**
00:33 Hypoxia	1.56	0.54	0.50	0.38	**<0.001**
00:55 Recovery	1.51	0.53	0.48	0.32	**<0.001**
01:17 Recovery	1.19	0.34	0.50	0.30	**<0.001**
01:39 Recovery	0.98	0.32	0.48	0.32	**0.003**
02:01 Recovery	0.88	0.4	0.52	0.34	0.06
02:23 Recovery	0.84	0.48	0.37	0.33	**0.02**

Table 6-3. Cerebral mean alanine/Cr T_2-weighted signal amplitudes and standard deviation (SD) of chick embryos at Day 19 of incubation, before, during and after hypoxia (H) and in embryos that remained in air (N).

time (hr:mm)	H alanine/Cr (n = 11)		N alanine/Cr (n = 8)		p value
	Mean	SD	Mean	SD	
00:00 Normoxic baseline	0.14	0.14	0.093	0.068	0.37
00:11 Hypoxia	0.22	0.12	0.068	0.075	**0.005**
00:33 Hypoxia	0.29	0.17	0.064	0.07	**0.007**
00:55 Recovery	0.22	0.11	0.10	0.10	**0.036**
01:17 Recovery	0.27	0.18	0.091	0.09	**0.015**
01:39 Recovery	0.26	0.13	0.08	0.08	**0.003**
02:01 Recovery	0.21	0.1	0.092	0.091	**0.02**
02:23 Recovery	0.22	0.14	0.1	0.1	0.08

Table 6-4 Cerebral cell densities (cells/ unit area) in the hyperstriatum ventralis, hippocampus and optic tectum of day 21 chick embryos exposed to air (N) and acute hypoxia (H) on day 19 of incubation.

	N (n = 3)	H (n = 3)	p value
Pyknotic cell density	0.19	0.5	**0.025**
Hyper-chromatic neuron density	9.4	4.5	**0.044**
Neuron density	35.4	33.2	0.24

7 A COMPARISON OF THE CEREBRAL METABOLIC RESPONSE TO ACUTE HYPOXIA OF DAY 19 NORMALLY GROWN AND GROWTH RESTRICTED CHICK EMBRYOS *IN-OVO* MEASURED BY PROTON MAGNETIC RESONANCE SPECTROSCOPY.

7.1 Introduction.

Several studies have suggested that important fetal metabolic changes accompany the alterations of growth present in growth restricted (GR) fetuses. Fetal hypoglycaemia, hyperlacticaemia, acidosis, hypercapnia and hypoxia are associated with growth restriction in human and animal studies (Jansson and Persson, 1990;Ogata et al., 1985;Ogata et al., 1986;Economides and Nicolaides, 1989;Nicolaides et al., 1989;Soothill et al., 1986). Whether these changes affect cerebral glucose supply and requirements is uncertain, as brain glucose and glycogen concentrations are maintained within normal limits despite systemic hypoglycaemia in the IUGR rat fetus (Brown and Vannucci, 1978;Vannucci et al., 1994), but reduced cerebral glucose and adenosine triphosphate (ATP) have also been reported (Lin et al., 1998). Studies of healthy normal and small-for-gestational age (SGA) human infants using non-invasive phosphorus (^{31}P) magnetic resonance spectroscopy (MRS) failed to show differences in phosphocreatine (PCr), ATP, and intracellular pH. This suggests that cerebral intracellular energy reserves and the balance between oxidative and anaerobic glycolysis are similar in normal and SGA infants (Azzopardi et al., 1989b).

Findings of preserved cerebral metabolism in SGA infants, together with fetal ultrasound studies showing redistribution of cardiac output in favour of the

brain, heart and adrenal glands in the presence of growth restriction (Dubiel et al., 2002) suggest that cerebral oxidative metabolism is initially maintained by increased cerebral blood flow (thus protecting the 'oxygen margin of safety') despite utero-placental insufficiency and impaired blood gas exchange. Further protection by increased oxygen extraction is provided if the increased cerebral blood flow is inadequate (Flecknell et al., 1983;Richardson et al., 1996). These compensatory responses partly account for the relatively normal head growth ("brain sparing") but impaired abdominal and lower limb growth in asymmetrical IUGR, as opposed to proportionately impaired head, abdomen and lower limb growth in symmetrical IUGR. The utilisation of alternative energy substrates and reduced metabolic demand are further adaptive mechanisms that can minimise the deleterious effects of utero-placental insufficiency. It is reasonable to expect essential metabolic functions are maintained by these adaptive responses that appear to be cerebro-protective.

It has been speculated that the threshold of fetal brain safety may be significantly lowered with severe growth restriction, and thereby increase the risk of impaired cerebral energy metabolism and consequent cerebral injury even during the normal physiological stresses of uneventful delivery.

The earlier proton (^{1}H) MRS study of the cerebral metabolic response to acute hypoxia of day 19 normal chick embryos (Chapter 6), showed significant rises in cerebral lactate and alanine during acute moderate hypoxia that gradually recovered after restoration of normoxia (Peebles et al., 2003).

As there is evidence that cerebral metabolism is disturbed in the GR chick embryo (Chapter 5), it was speculated that it's cerebral metabolic response to acute hypoxia may also differ from that of the normally grown (NG) chick

embryo. The objective of this study was to compare the cerebral metabolic and neurone morphological responses to acute hypoxia of normally grown and GR chick embryos *in-ovo* using proton MRS and histology respectively.

7.2 Materials and Methods.

7.2.1 MRS

One hundred and fourteen GR White Leghorn chick embryos were incubated for 19 days (Section 4.1.2). On day 19, 17 remained alive and acute hypoxia experiments identical to those described in Chapter 6 were performed. All procedures were performed in accordance with the Animals (Scientific Procedures) Act 1986, United Kingdom

The chick embryo was anaesthetised (Section 4.2.1) then its brain was located within the egg and placed at the centre of a 2.5 cm diameter circular surface coil (Section 4.2.2). The part of the brain to be interrogated by MRS (voxel) was defined (Section 4.2.3).

After a baseline ^{1}H spectrum was acquired in air, additional nitrogen was supplied to growth restricted chick embryos in the acute hypoxia group (n=9) (combined flow rate was maintained at 3L/min) to decrease the ambient oxygen concentration to 8%, as measured by an oxygen analyser (Servomex 570A, Sussex, UK). Hypoxia was maintained for 40 minutes, during which two ^{1}H spectra were acquired at times 11-22 and 33-44 minutes. Normoxia was restored and ^{1}H spectra were acquired at 22 minutes intervals for a further 2 hours. A "control" group of growth restricted chick embryos (n=8) were subjected to a similar protocol but remained in air for the duration of the experiment.

Proton spectra were analysed using a technique of linear combination modelling (Provencher, 1993).

For statistical analysis, NG (data from Chapter 6) and GR group means of the spectra at each time point during hypoxia and recovery were compared with equivalent normoxic controls. Data sets were tested for normality and equal variance before statistical comparison. Parametric and non-parametric data comparisons were performed using the t-test and Mann-Whitney Rank Sum Test respectively. Statistical analyses were performed using Sigmastat Version 2.0 (Jandel Scientific).

7.2.2 Histology

Ninety six growth restricted chick embryos were incubated for 19 days (Section 4.1.2), by which time 58 had died. On day 19, 36 of the remaining viable eggs were put in a sealed plastic bag located inside an incubator, supplied with air at 3L/min through an inlet hose connected to a gas mixer and regulator, and kept warm by a radiant heater within the incubator. Two experimental groups were exposed to air (N) and acute hypoxia (H) and incubated in air afterwards (Table 7-1). Twenty one (11 (Normoxia) + 10 (Hypoxia)) chick embryos survived to day 21, when they were euthanased and their brains were perfused, fixed and prepared for cryopreservation (Section 4.3.1), before storage in a –80°C freezer. All procedures were performed in accordance with the Animals (Scientific Procedures) Act 1986, United Kingdom.

Ten (4 (Normoxia) + 6 (Hypoxia)) brains from growth restricted embryos were of sufficient quality to be processed further. 20 micron sections from 3 brains in each group (a total of 6 brains) were cut, air dried and fixed onto slides (Sections 4.3.2 and 4.3.3) and stained with Nissl stain (Section 4.3.4). Counting

of hyperchromatic, normal and pyknotic neurons in the hippocampus, hyperstriatum ventralis, cerebellum and optic tectum (Section 4.4) was performed by a single non-blinded individual.

Cell counts in each brain structure were averaged over all the tissue sections in which each structure was present. Statistical analysis of average cell counts by brain area in two normally grown (data from Chapter 6) and two growth restricted groups (Table 7-1) was performed by Two and Three Way Analysis of Variance (ANOVA) using Sigmastat Version 2.0 (Jandel Scientific).

7.3 Results.

7.3.1 MRS

A representative sequence of metabolite spectra from a growth restricted chick embryo brain acquired before, during acute hypoxia, and during recovery in air is shown in Figure 7.1 with annotated peaks corresponding to choline, creatine, N-acetylaspartate (NAA), lactate and β-hydroxybutyrate (βHB).

There was no significant difference in the normoxic baseline mean lactate/Cr for any group. During transient hypoxia, lactate/Cr rose in NG embryos from 0.5 ± 0.38 (mean ± SD) to 1.56 ± 0.54 ($p<0.001$), then gradually declined to 0.84 ± 0.48 ($p=0.02$) at the end of the experiment (Figure 7.2). A significant increase also occurred in the GR group, from a baseline of 0.46 ± 0.19 to 0.92 ± 0.43 ($p=0.02$) during hypoxia (Table 7-2). However, the rise was significantly attenuated and shorter lasting in the brains of GR compared to NG embryos (Figure 7.3 and Figure 7.4), with a maximal change of 0.66 ± 0.34 in GR compared to 0.98 ± 0.25 in NG embryos ($p< 0.027$).

Mean alanine/Cr significantly increased in NG embryos during acute hypoxia, from 0.14 ± 0.14 (p=0.37) to 0.29 ± 0.17 (p=0.01), and recovered by the end of the experiment 0.22 ± 0.14 (p=0.08) (Figure 7.5). Unlike NG embryos there was no significant change in alanine/Cr associated with acute hypoxia in GR embryos (Figure 7.6).

In growth restricted chick embryos, βHB/Cr was significantly elevated throughout the experiment (Figure 7.7). However, acute hypoxia was not associated with any change in βHB/Cr in either NG or GR chick embryos.

The T_2 weighted signal amplitudes of N-acetylaspartate, choline and inositol relative to creatine did not change during acute hypoxia. Poor spectral resolution prevented analysis of aspartate and GABA data. All metabolites were stable with respect to time in the control groups.

T2-weighted metabolite signal amplitudes were reported relative to total cerebral creatine that was assumed to be stable and a useful internal reference under the acute hypoxic conditions of this study. This assumption was justified, as the signal amplitudes of all metabolites apart from lactate were invariant with respect to inspired oxygen levels in growth restricted chick embryos.

Four growth restricted and 3 normal chick embryos died within 48 hours of acute hypoxia and their survival rates were similar (Fisher's Exact test p = 0.38).

7.3.2 Histology

7.3.2.1 Hyperstriatum ventralis, hippocampus and optic tectum.

Hypoxia was associated with a significant increase in pyknotic cell density (0.11 (normoxia (N)) vs. 0.45 (hypoxia (H)); p<0.005) and pyknotic cell/

neuron quotient (0.0025 (N) vs. 0.012 (H); p=0.004). Growth restriction had no significant affect on neuron pyknosis, hyperchromatic neuron density or hyperchromatic neuron/neuron quotient.

Growth restriction was associated with a significant increase in neuron density (34.5 (NG) vs. 40.4 (GR); p=0.007), whereas hypoxia was not (38.2 (N) vs. 36.7 (H); (p= 0.45).

7.3.2.2 Cerebellum.

Hypoxia was associated with a significant increase in pyknotic cell density (0.29 (N) vs. 0.42 (H); p=0.014) and pyknotic cell/Purkinje cell quotient (0.012 (N) vs. 0.019 (H); p=0.002).

Hypoxia was associated with a significant reduction of hyperchromatic Purkinje cell density (6.43 (N) vs. 4.02 (H); p=0.02) and a non-significant reduction of hyperchromatic Purkinje cell/Purkinje cell quotient (0.25 (N) vs. 0.18 (H); p=0.07). Growth restriction did not affect the hyperchromatic Purkinje cell density (5.7 (N) vs. 4.8 (GR); p=0.38).

Hypoxia, but not growth restriction, was associated with a significant reduction in Purkinje cell density (25.1 (N) vs. 21.9 (H); p<0.001).

The effects of hypoxia and growth restriction on histology in the hyperstriatum ventralis, hippocampus, optic tectum and cerebellum were independent and there was no evidence of an interaction.

7.4 Discussion.

These findings show that embryonic growth restriction, induced by chronic hypoxia for the last half of incubation and protein deprivation from the beginning of incubation, results in an altered metabolic response to acute hypoxia in the chick embryo *in-ovo*. Compared with NG embryos, GR embryos had an attenuated alanine and lactate response to acute hypoxia with increased baseline levels of βHB. These differences in cerebral energy metabolism, which are broadly in agreement with observations of impaired human fetal cerebral glucose oxidation due to ketosis (Bhasin and Shambaugh, III, 1982;Shambaugh, III, 1985)(Bhasin and Shambaugh, III, 1982), suggest mechanisms by which growth restriction in the human fetus might contribute to an increased incidence of hypoxic ischaemic encephalopathy, seizures and neurological dysfunction.

Baseline (normoxic) cerebral lactate levels were similar in the brains of normal and GR embryos. In addition the pattern of change in lactate during acute hypoxia was alike in the two groups, with an increase that peaked at the end of hypoxia and returned toward baseline values during the recovery period. However, the size of the lactate rise was significantly reduced in the growth restricted group. This is in contrast to data from the growth restricted human fetus where baseline lactate is increased and lactate rises in response to hypoxia more rapidly and by a greater degree than observed in normally grown fetuses (Trudinger et al., 1987) (Lin et al., 1980;Marconi et al., 1990). A possible explanation for these differences is that the chick embryo does not have a placenta; the placenta transfers lactate from the fetal to the maternal circulation during hypoxia (Hooper, 1995). Part of the increase in fetal lactate observed in the growth restricted human fetus during acute hypoxaemia may be due to

placental insufficiency and impaired clearance of lactate. Measurements from the chick embryo brain will not be effected by placental or maternal changes and allow direct assessment of the fetal response.

There are several reasons why the increase of lactate during hypoxia may be attenuated by growth restriction. Prolonged growth restriction has been shown to decrease glycogen storage in the liver (Hsu et al., 1993). It is possible that glycolysis is limited in this model by depletion of substrate. It is speculated that an impaired anaerobic response may decrease the ability of the brain to maintain ATP levels and so make it more susceptible to the effects of acute hypoxia. The fact that chick embryos exposed to chronic hypoxia (as in the GR group) may reduce their total metabolic rate (Beattie and Smith, 1975) suggests an alternative explanation; decreased energy requirement could limit the need for anaerobic glycolysis during acute hypoxia and so attenuate the rise in lactate. Reduced cerebral metabolism in response to hypoxia has also been observed in fetal sheep and llamas (Llanos et al., 2002;Newman et al., 2001). (Llanos et al., 2002;Newman et al., 2001)Although lactate has been shown to be an alternative substrate for cerebral metabolism in a variety of animals (Dombrowski, Jr. et al., 1989;King et al., 1997;Thurston et al., 1983), increased lactate clearance is unlikely to account for the smaller rise in lactate observed in GR embryos. This is because oxygen is required for breakdown of lactate and so increased lactate clearance is unlikely to be observed during acute hypoxia.

In NG embryos, cerebral alanine/Cr showed a significant increase during acute hypoxia whereas the response was absent in GR embryos. As with lactate, this may be the result of reduced availability of glucose or reduced basal cerebral metabolism.

NAA, inositol and choline (putative markers of neurons, glial cells and cell membranes respectively) were stable with respect to the inspired oxygen level in both NG and GR chick embryos, which suggests the level of hypoxia used was insufficient to cause immediate cerebral injury or change in cell membrane composition.

It is unclear whether these metabolic responses to acute hypoxia are neuro-protective or harmful since the hatch rates of normally grown and growth restricted chick embryos were similar.

Histological examination suggests growth restriction was associated with a significant increase in neuron cell density in the combined Hi, HV and OT area, however the Purkinje cell density in the cerebellum was unaffected. These findings should be interpreted cautiously as the observer performing the cell counting was aware of each specimen's history (non-blinded). A similar previous study reported reduced Purkinje cell density in chronically hypoxic chick embryos towards the end of incubation (Lee et al., 2001;Mancini et al., 1985). However, this discrepancy might occur because of different experimental conditions; growth restricted embryos in this experiment were exposed to an ambient oxygen concentration of 14% from day 10 of incubation, whereas the Lee et al (2001) and Mancini et al (1985) experiments used eggs that were half painted with impermeable wax at the onset of incubation and the level of hypoxia was indeterminable. Apparent associations between hypoxia and reduced Purkinje cell density and hyperchromatic Purkinje cell density were found in this experiment, but these findings are inconsistent with those in Chapter 6 and should be interpreted with caution.

The increased neuron density associated with growth restriction may be due partly to reduced brain size. Growth restriction in chick embryos is associated with a reduction in brain weight (0.838g (NG) vs. 0.791g (GR); p=0.02) (Miller et al., 2002), which would account for only 6% of the 16% increase in neuron density. Larger studies are necessary to confirm these histological findings and investigate their cause.

7.5 Conclusions.

The day 19 GR chick embryo brain has increased βHB/Cr and exhibits a significantly attenuated increase in lactate/Cr and alanine/Cr in response to transient hypoxia compared to its NG counterpart. These findings are consistent with enhanced ketosis in the late gestation growth restricted chick embryo.

Figure 7.1 Cerebral proton MR spectra from the brain of a day 19 growth restricted chick embryo before, after 40 minutes of acute hypoxia and at the end of a 2 hour recovery period in air. Spectral peaks corresponding to choline, creatine, N-acetylaspartate (NAA), lactate and β–hydroxybutyrate (βHB) are identified.

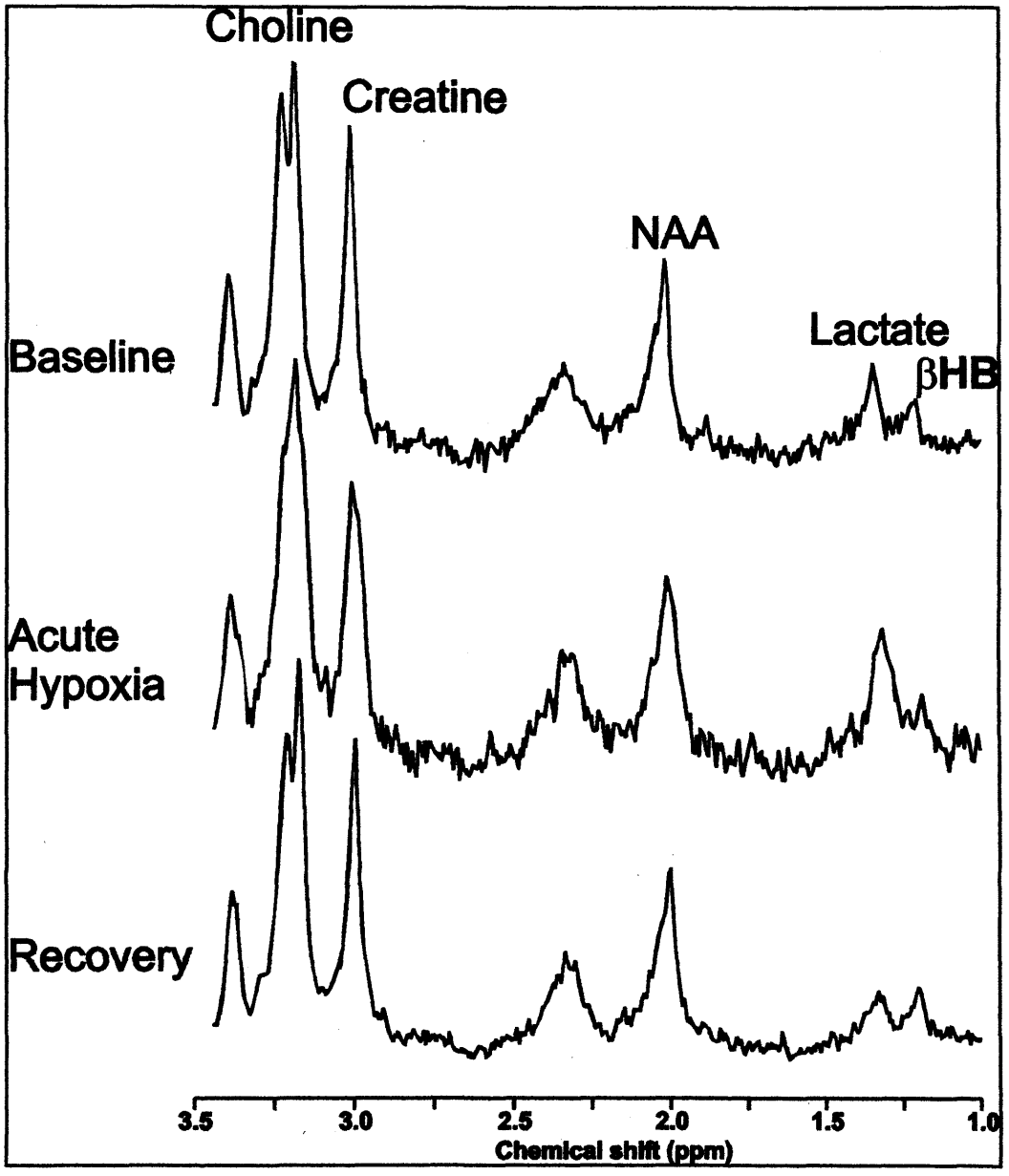

Figure 7.2 Mean cerebral lactate/Cr (±SD) in normally grown chick embryos exposed to hypoxia (black bars) and normoxia (grey bars). ** signifies p<0.001 and * p<0.01.

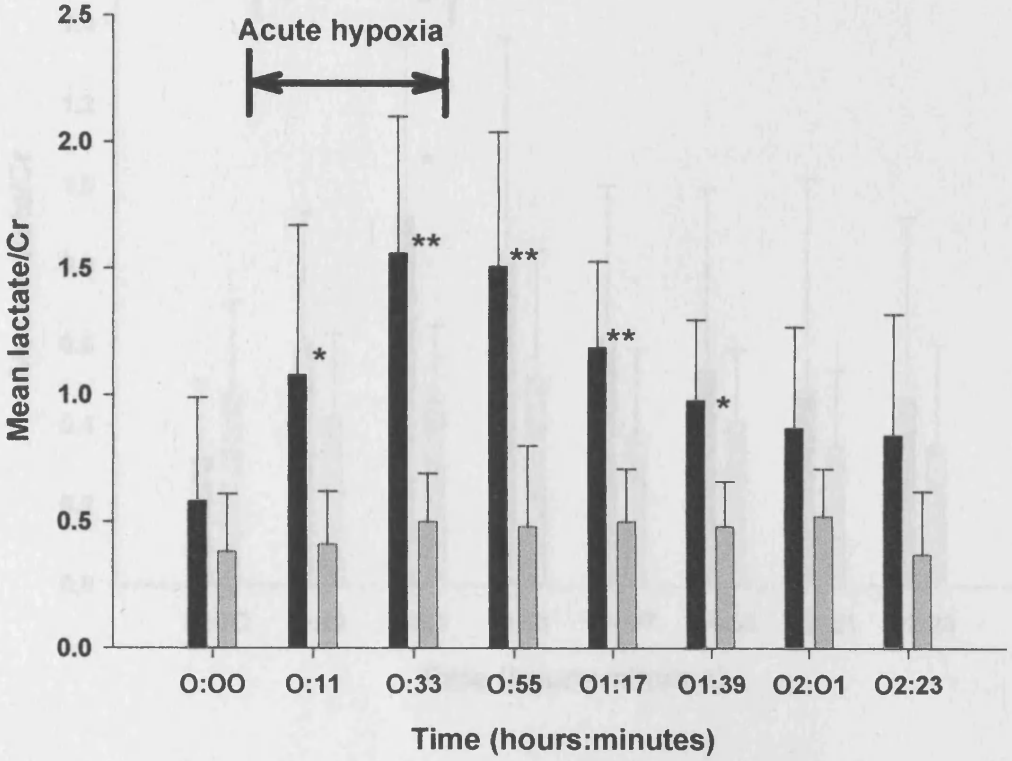

Figure 7.3 Mean cerebral lactate/Cr (±SD) in growth restricted chick embryos exposed to hypoxia (black bars) and normoxia (grey bars).

*** signifies p=0.02.**

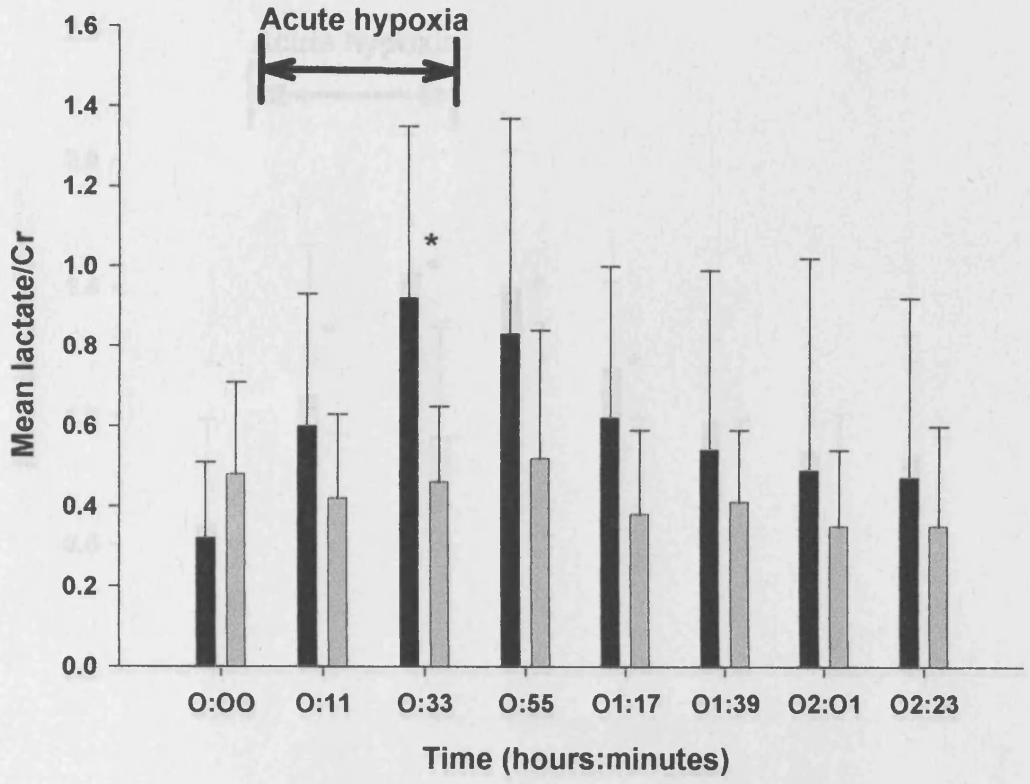

Figure 7.4 Mean cerebral lactate/Cr (±SD) of normally grown (black bars) and growth restricted (grey bars) chick embryos exposed to hypoxia.

*** signifies $p < 0.02$.**

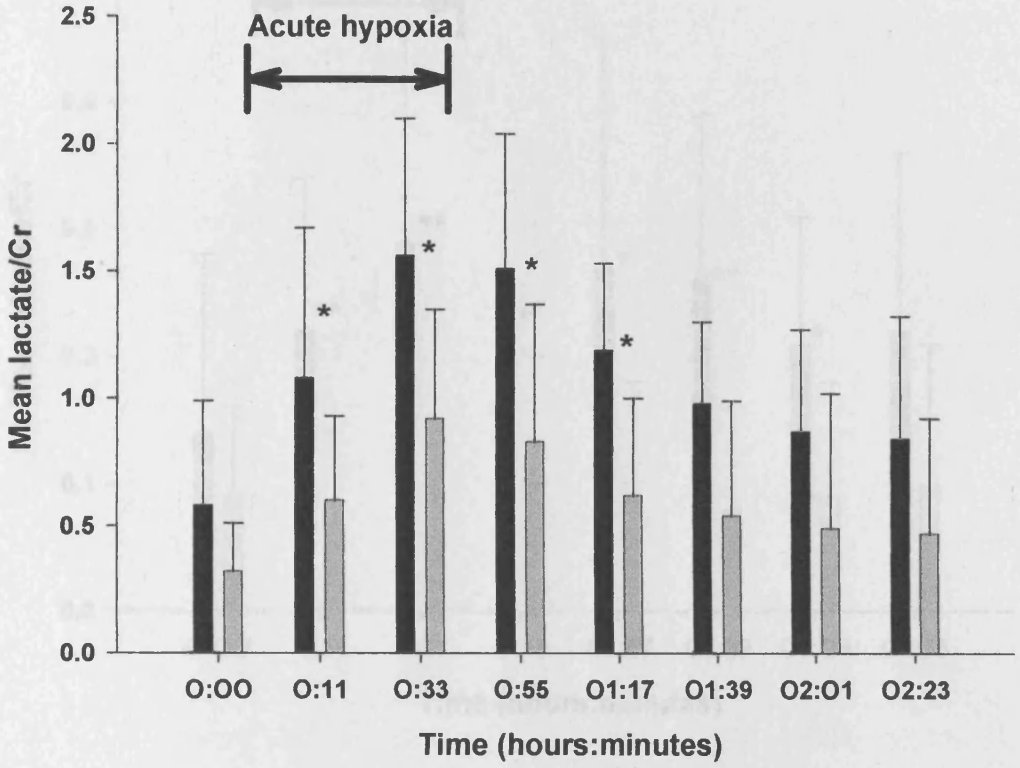

Figure 7.5 Mean cerebral alanine/Cr (±SD) in normally grown chick embryos exposed to hypoxia (black bars) and normoxia (grey bars). ** signifies p <0.01 and * p < 0.05.

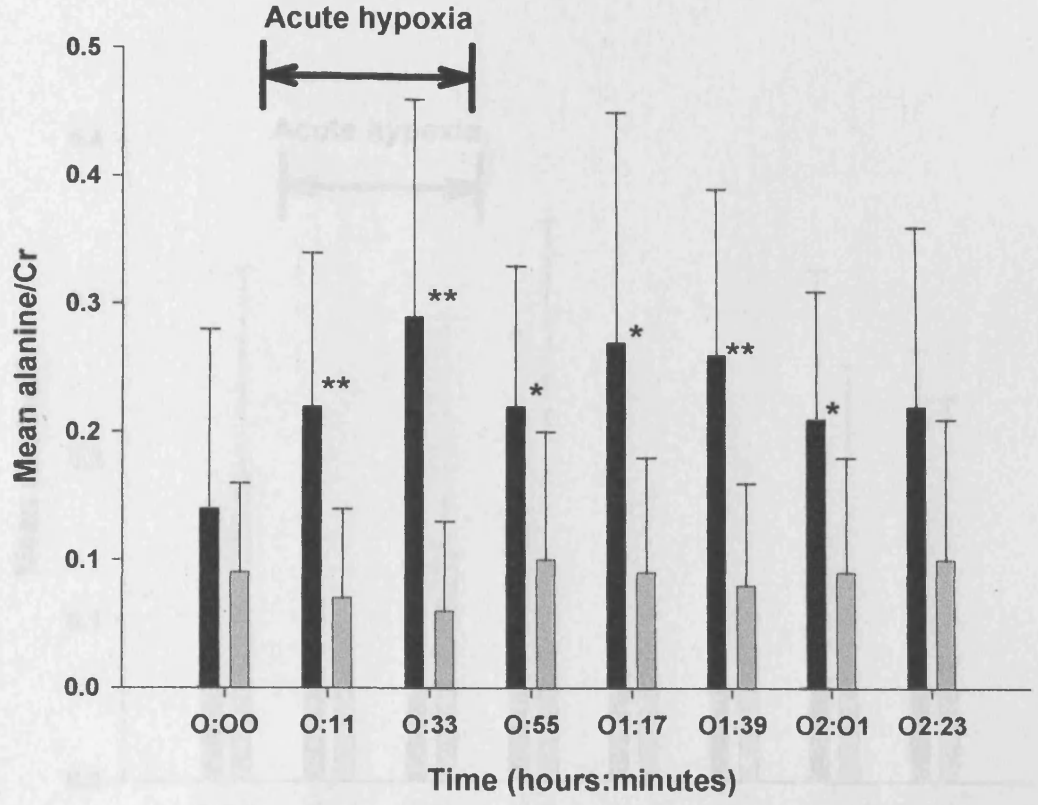

Figure 7.6 Mean cerebral alanine/Cr (±SD) in growth restricted chick embryos exposed to hypoxia (black bars) and normoxia (grey bars).

Mean alanine/Cr was similar in both groups and unaffected by acute hypoxia.

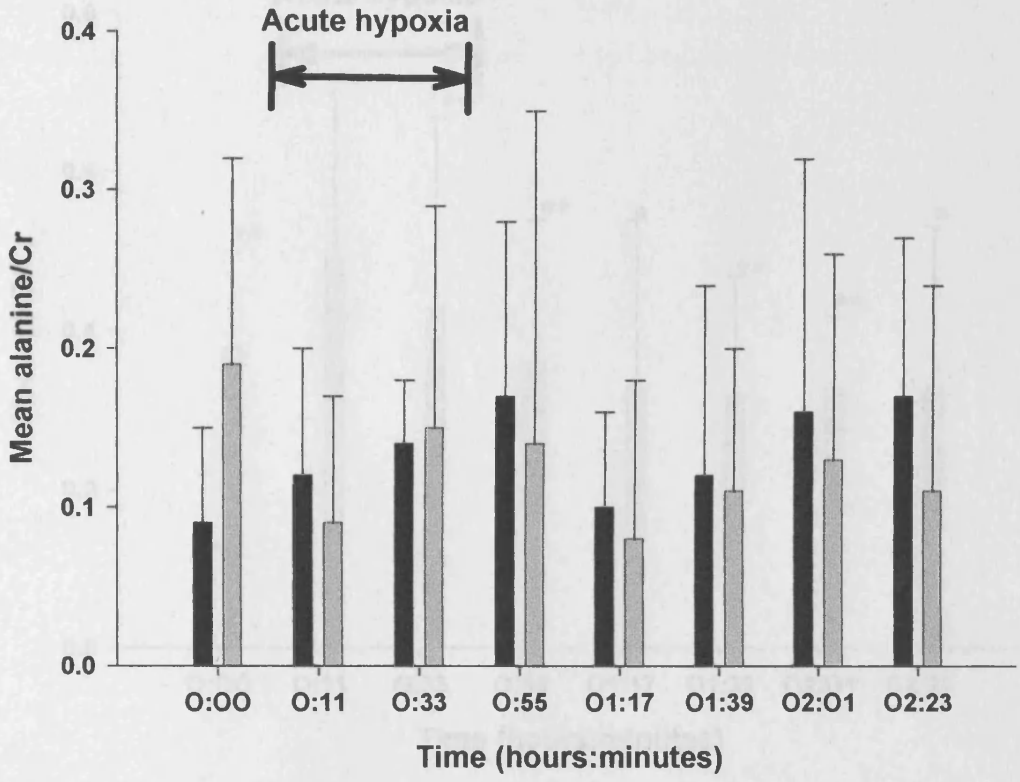

Figure 7.7 Mean cerebral β–hydroxybutyrate/Cr (±SD) in normally grown (black bars) and growth restricted (grey bars) chick embryos exposed to hypoxia.

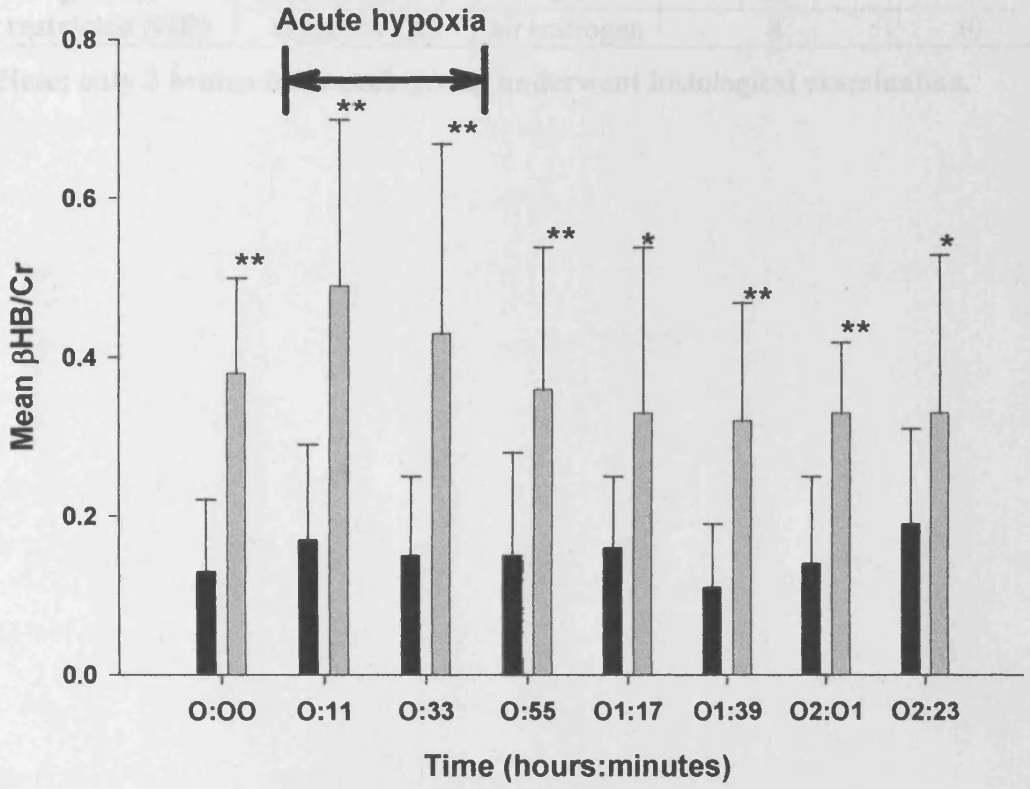

* signifies $p<0.05$ and ** $p<0.001$.

Table 7-1 Gas mixture and duration of supply in four groups of day 19 chick embryos.

Group		Ambient atmosphere	Oxygen concentration (%)	Duration (minutes)	Number of eggs
normally grown (NG)	Normoxia (N)	air	21	40	14
	Hypoxia (H)	air+nitrogen	8	40	11
growth restricted (GR)	Normoxia (N)	air	21	40	21
	Hypoxia (H)	air+nitrogen	8	40	15

Note: only 3 brains from each group underwent histological examination.

Table 7-2 Mean cerebral lactate/Cr T_2-weighted signal amplitudes (±SD) of normally grown (NG) and growth-restricted (GR) chick embryos during acute hypoxia and recovery in air (H), and during continuous normoxia (N).

H			N			t-test p-value		
time (hh:mm)	NG[1] (n=11)	GR[2] (n=9)	time (hh:mm)	NG[3] (n=8)	GR[4] (n=8)	[1]vs.[3]	[2]vs.[4]	[1]vs.[2]
00:00 Normoxic baseline	0.58 (0.41)	0.32 (0.19)	**00:00 Normoxic baseline**	0.38 (0.22)	0.48 (0.23)	0.23	0.07	0.076
00:11 Hypoxia	1.08 (0.59)	0.60 (0.33)	**00:11 Normoxia**	0.41 (0.28)	0.42 (0.21)	**0.004**	0.22	**0.015**
00:33 Hypoxia	1.56 (0.54)	0.92 (0.43)	**00:33 Normoxia**	0.50 (0.38)	0.46 (0.19)	**<0.001**	**0.02**	**0.013**
00:55 Recovery	1.51 (0.53)	0.83 (0.54)	**00:55 Normoxia**	0.48 (0.32)	0.52 (0.32)	**<0.001**	0.18	**0.013**
01:17 Recovery	1.19 (0.34)	0.62 (0.38)	**01:17 Normoxia**	0.50 (0.30)	0.38 (0.21)	**<0.001**	0.13	**0.003**
01:39 Recovery	0.98 (0.32)	0.54 (0.45)	**01:39 Normoxia**	0.48 (0.32)	0.41 (0.18)	**0.003**	0.72	**0.02**
02:01 Recovery	0.87 (0.4)	0.49 (0.53)	**02:01 Normoxia**	0.52 (0.34)	0.35 (0.19)	0.06	0.51	0.089
02:23 Recovery	0.84 (0.48)	0.47 (0.45)	**02:23 Normoxia**	0.37 (0.33)	0.35 (0.25)	**<0.02**	0.51	**0.023**

8 THE EFFECT OF GROWTH RESTRICTION ON CEREBRAL INTRACELLULAR ENERGY RESERVES IN THE CHICK EMBRYO *IN-OVO* DURING ACUTE HYPOXIA MEASURED BY PHOSPHORUS MAGNETIC RESONANCE SPECTROSCOPY.

8.1 Introduction.

Fetal growth restriction is associated with significant changes of energy substrate availability, intracellular energy reserves and amino-acid concentrations, as well as the clinically obvious alterations of growth parameters such as birth weight and ponderal index. For example, hypoglycaemia is associated with human IUGR (Economides and Nicolaides, 1989;Soothill et al., 1987), and neonatal IUGR puppies have significantly reduced cerebral oxidative metabolism and cerebral energy reserves in response to 3 hours of neonatal fasting (Kliegman, 1986). These findings are supported by earlier experiments that demonstrated an association between growth restriction and significantly reduced cerebral PCr/Pi in the day 19 chick embryo (Chapter 5).

In addition, cerebral amino acid metabolism is disturbed in intrauterine growth mouse fetuses, who have reduced aspartate and increased alanine concentrations in the striatum compared to appropriately grown littermates (Thordstein et al., 1992).

Phosphorus magnetic resonance spectroscopy (MRS) is a non-invasive technique for monitoring cerebral energy metabolism in-vivo. Three adenosine triphosphate peaks representing the α, β, and γ phosphate molecules,

phosphocreatine (PCr) and inorganic phosphate (Pi) are present in the spectrum in the chemical shift range between +5 and –20ppm. The chemical shift of Pi is affected by pH whereas the chemical shift of PCr is stable. Therefore, the chemical shift difference between PCr and Pi is an indicator of tissue pH. PCr is an intracellular energy buffer, with a high energy phosphate bond similar to ATP, which can regenerate ATP from ADP.

Equation 8-1.

$$ADP + PCr \Leftrightarrow ATP + Pi$$

From Equation 8-1. PCr/Pi ratio is proportional to ATP/ADP and is an indicator of intracellular energy reserve.

The potential of phosphorus MRS to investigate the effect of hypoxic ischaemia on cerebral intracellular energy reserves has been demonstrated by several studies of perinatal cerebral energy metabolism that found reduced PCr/Pi in human neonates with clinical evidence of hypoxic-ischaemic brain injury (Moorcraft et al., 1991b;Azzopardi et al., 1989a;Hope and Reynolds, 1985;Hamilton et al., 1986;Hope et al., 1984). Complementary studies in a piglet neonatal model showed cerebral PCr/Pi declined during acute hypoxia and recovered promptly during resuscitation, but showed a secondary fall 24-48 hours later (Lorek et al., 1994).

As intrauterine growth restriction significantly affects several aspects of cerebral metabolism it was proposed to study its influence on changes of intracellular energy reserves in response to acute hypoxia using phosphorus

MRS. The hypothesis was that fetal growth restriction would be associated with a faster decline of intracellular energy reserves during acute hypoxia than in normally grown fetuses.

8.2 Materials and Methods.

Normally grown (n=7) and growth restricted (n=5) chick embryos were incubated for 19 days (Section 4.1.1 and 4.1.2). Studies were performed on incubation day 19 (hatching occurs on day 21) and all procedures were performed in accordance with the Animals (Scientific Procedures) Act 1986, United Kingdom. To provide these embryos, 9 normally grown and 34 growth restricted eggs were incubated.

The chick embryos were anaesthetised (Section 4.2.1) and the brain was located within the egg and placed at the centre of a 2.5 cm diameter circular surface coil (Section 4.2.2).

The spectrometer was set to acquire phosphorus spectra from an 8.6mm x 6.0mm x 6.8 mm voxel located entirely in the brain (Section 4.2.5).

After a baseline ^{31}P spectrum (TE=10ms, TR=2s, NS=320, acquisition time 11 minutes) (Figure 8.1) was acquired in air, additional nitrogen was added (combined flow rate was maintained at 3L/min) to rapidly decrease the ambient oxygen concentration to 4%, as measured by an oxygen analyser (Servomex 570A, Sussex, UK). Hypoxia was maintained for 60 minutes, during which time six sequential ^{31}P spectra were acquired. After 60 minutes, normoxia was restored and surviving chick embryos were returned to the incubator. The severity of acute hypoxia in this experiment was considerably greater than in Chapters 6 and 7 to ensure alterations in PCr and Pi.

Phosphorus spectra were analysed using jMRUI (Java-based Magnetic Resonance User Interface)(Naressi et al., 2001a;Naressi et al., 2001b) and AMARES (advanced method for accurate, robust, and efficient spectral fitting), a sophisticated nonlinear least-squares algorithm method for estimating the spectral components of magnetic resonance spectroscopy signals in the time domain (Vanhamme et al., 2001) (Vanhamme et al., 1997).

For statistical analysis, group means of cerebral PCr/Pi signal amplitude, change of PCr/Pi (ΔPCr/Pi) and PCr-Pi chemical shift at each time point during hypoxia were compared between normally grown and growth restricted chick embryos by Two Way ANOVA using Sigmastat Version 2.0 (Jandel Scientific).

8.3 Results.

Baseline cerebral PCr/Pi was similar in normally grown and growth restricted chick embryos (Table 8-1), and after declining significantly in response to acute hypoxia, PCr/Pi was similar in the NG and GR embryos at the end of hypoxia (Table 8-1). The rate of decline PCr/Pi (ΔPCr/Pi) was initially faster in normally grown embryos ($p=0.04$), but was similar there afterwards in both groups (Figure 8.2 and Figure 8.3). The chemical shift between PCr and Pi was similar in NG and GR embryos initially, and then decreased steadily from 5.1 to 4.32 with hypoxia (Table 8-2), which is equivalent to a fall of pH from 7.26 to 6.7. Growth restriction was associated with a significantly reduced chemical shift at the end of hypoxia ($p=0.007$).

Spectrum peaks corresponding to α,β and γ phosphates of ATP could not be resolved with sufficient accuracy to allow an assessment of relative ATP concentrations to be made.

There was no significant difference in the 60% survival rate in the two groups (Fishers Exact test $p = 1.0$).

8.4 Discussion.

Unlike the larger study of 21 embryos (Chapter 5) which found a significant difference of baseline PCr/Pi in NG and GR embryos, this study of 12 chick embryos did not confirm the findings. This was probably because the group sizes were too small and the analysis had insufficient power to detect a significant difference.

PCr/Pi fell sharply after the onset of hypoxia in both groups and stabilised by the end of the hypoxic period at 10%-25% of the baseline value. There was no

evidence of a significant difference between the groups in the rate of decline of absolute and normalised PCr/Pi, except at the very onset of hypoxia when PCr/Pi declined faster in the NG group ($p = 0.04$). Overall, these findings suggest the balance between energy production and demand is similar in both groups, despite the different lactate responses to transient hypoxia observed with proton MRS (Chapter 7). If the basal cerebral metabolic rate was less in GR embryos, as suggested by studies of the influence of chronic hypoxia on chick embryo metabolism (Beattie and Smith, 1975) (Bjonnes et al., 1987), it might account for both the attenuated lactate response and the similar decline of PCr/Pi during hypoxia compared to normally grown embryos. Alternatively, the similar decline of PCr/Pi in NG and GR embryos may be due to the severity of the hypoxic episode, whereas it is possible that subtle differences might be present in response to mild hypoxia.

The chemical shift between PCr and Pi spectral peaks decreases as the ambient pH falls (Table 8-2). By using this phenomenon, it was evident that the cerebral pH was similar in both groups before the onset of hypoxia (pH = 7.26) (Petroff et al., 1985) and fell during hypoxia to reach a nadir at 55 minutes (pH = 6.9 (normally grown) and pH= 6.7 (growth restricted)). The lower minimum chemical shift in the GR group ($p=0.007$) was unexpected, since it was assumed cerebral pH would be higher in growth restricted embryos as it has previously been shown to produce less cerebral lactate in response to hypoxia (Chapter 7). This apparent paradox may be accounted for by a reduced bicarbonate buffering capacity or increased base deficit in growth restricted embryos (Andres et al., 1999;Baschat et al., 1999).

8.5 Conclusions.

Growth restriction is associated with reduced cerebral chemical shift and pH at the end of severe hypoxia, but does not appear to affect the rate of decline of cerebral energy reserves.

Table 8-1 Mean PCr/Pi (±SD) in normally grown (NG) and growth restricted (GR) day 19 chick embryos before and at the end of acute hypoxia (4% oxygen concentration for 60 minutes).

	Baseline (t = zero)	**End of hypoxia (t = 55 mins)**
NG (n = 7)	1.89 (0.7)	0.36 (0.21)
GR (n = 5)	1.54 (0.36)	0.22 (0.17)
t-test p value	0.13	0.56

Table 8-2 Mean chemical shift between PCr and Pi (ppm) (±SD) in normally grown (NG) and growth restricted (GR) day 19 chick embryos before and at the end of acute hypoxia (4% oxygen concentration for 60 minutes).

	Baseline (t = zero)	**End of hypoxia (t = 55 mins)**
NG (n = 7)	5.11 (0.07)	4.67 (0.16)
GR (n = 5)	5.1 (0.1)	4.32 (0.48)
t-test p value	0.92	**0.007**

Figure 8.1 Cerebral phosphorus MR spectrum of a day 19 growth restricted chick embryo in air. The spectral peaks corresponding to phosphocreatine (PCr), inorganic phosphate (Pi), phosphomonoesters (PME), phosphodiesters (PDE), α,β and γ phosphates of ATP are identified.

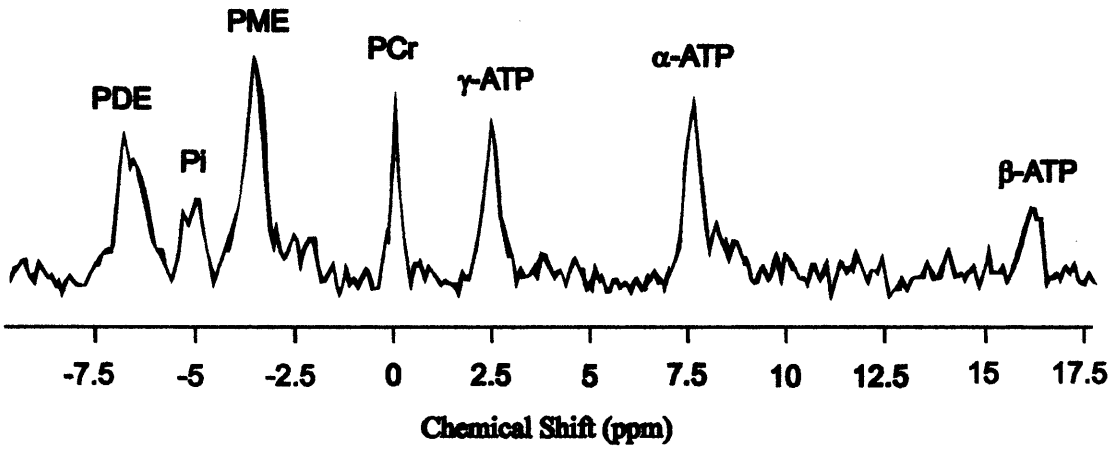

Figure 8.2 Mean cerebral PCr/Pi (±SD) in normally grown (black bars) and growth restricted (grey bars) day 19 chick embryos during acute hypoxia (4% oxygen concentration for 60 minutes).

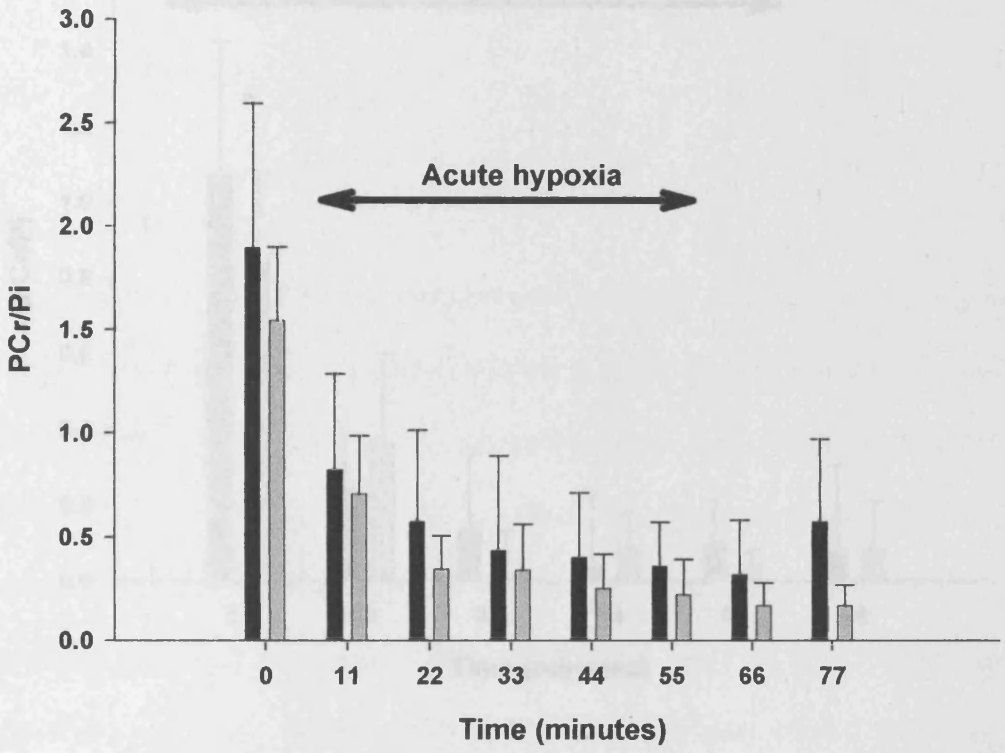

Figure 8.3 Mean cerebral ΔPCr/Pi (±SD) in normally grown (black bars) and growth restricted (grey bars) day 19 chick embryos during acute hypoxia (4% oxygen concentration for 60 minutes). * signifies p=0.04.

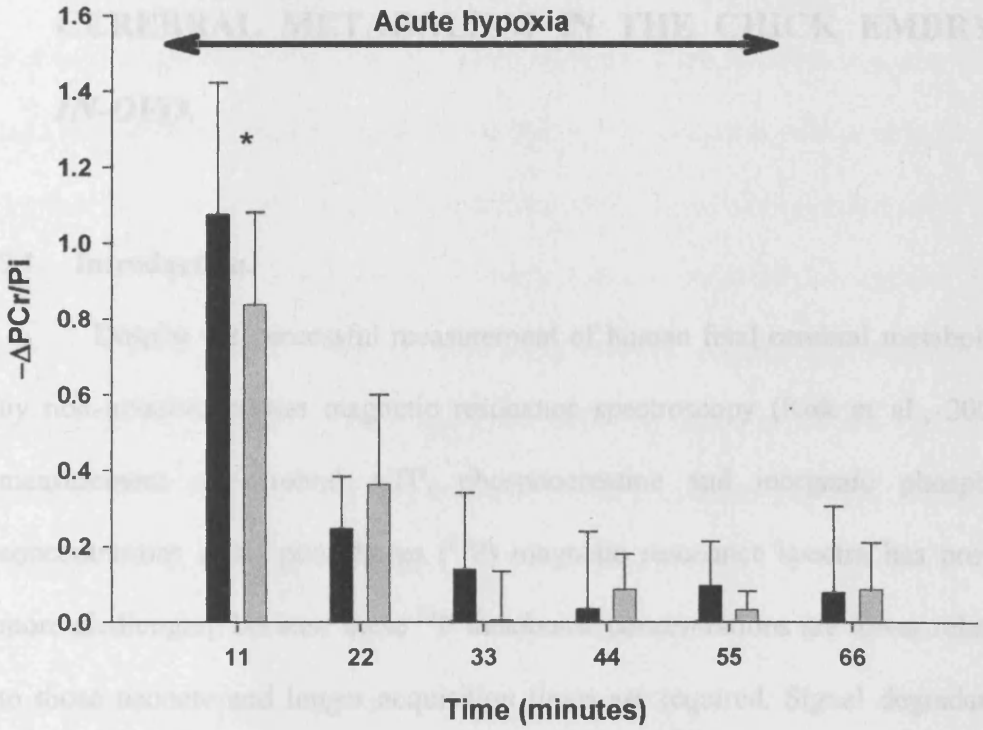

9 A DIFFUSION WEIGHTED MAGNETIC RESONANCE IMAGING STUDY OF THE EFFECT OF ACUTE HYPOXIA AND GROWTH RESTRICTION ON CEREBRAL METABOLISM IN THE CHICK EMBRYO *IN-OVO.*

9.1 Introduction.

Despite the successful measurement of human fetal cerebral metabolites by non-invasive proton magnetic resonance spectroscopy (Kok et al., 2002), measurement of cerebral ATP, phosphocreatine and inorganic phosphate concentrations using phosphorus (^{31}P) magnetic resonance spectra has proved more challenging because these ^{31}P metabolite concentrations are lower relative to those neonate and longer acquisition times are required. Signal degradation secondary to fetal movement becomes an important consideration as a consequence.

An alternative approach is to use diffusion-weighted magnetic resonance imaging to assess the cerebral energy status by measuring changes of the apparent diffusion coefficient (ADC) of tissue water. ADC decreases during and after cerebral ischaemia in both animal and human studies, however the exact mechanism responsible is not known (Cady et al., 1997;Hope et al., 1984). A nett shift of water from the extracellular to the intracellular space during hypoxic ischaemia, as a result of cell energy failure and consequent cell membrane depolarisation is a prevailing and plausible explanation. Certainly, studies in the

adult rat and neonatal piglet show a close correlation between reduction of ADC and ATP depletion, measured by ^{31}P spectroscopy or biochemically (Hoehn-Berlage et al., 1995;Olah et al., 2001).

Previous experiments (Chapters 7 and 8) showed growth restricted embryos have an attenuated lactate response to acute hypoxia, but their rate of decline of cellular energy reserves during severe acute hypoxia was similar to normally grown embryos. These observations are consistent with a reduction of cerebral metabolic rate in growth restricted embryos. ADC is speculated to be a marker of cellular osmoregulation and a putative indicator of cellular ATP reserves of the fetus. The association of growth restriction with neonatal encephalopathy and neurodevelopmental delay, suggests it should affect the cerebral ADC response to acute hypoxia, unless a counteracting factor, such as reduced metabolic rate, intervenes.

9.2 Materials and Methods.

Normally grown (NG) and growth restricted (GR) White Leghorn chick embryos were incubated for 19 days (Sections 4.1.1 and 4.1.2). Studies were performed on incubation day 19 (hatching occurs on day 21) and all procedures were performed in accordance with the Animals (Scientific Procedures) Act 1986, United Kingdom.

The chick embryo was anaesthetised (Section 4.2.1) and its brain was located within the egg and placed at the centre of a 2.5 cm diameter circular surface coil (Section 4.2.2). A symmetrical magnetic resonance image (MRI) of the embryo brain that included cerebra, optic tecti, and brain stem was defined using orthogonal MRI images of the chick brain. ADC values were measured in the

defined plane using a diffusion-weighted stimulated-echo acquisition mode (STEAM) sequence (Section 4.2.4).

After a baseline diffusion-weighted image (DWI) was acquired in air, additional nitrogen was added and supplied to normally grown (n=11) and growth restricted (n=9) chick embryos (combined flow rate was maintained at 3L/min) to decrease the ambient oxygen concentration to 8%, as measured by an oxygen analyser (Servomex 570A, Sussex, UK). Hypoxia was maintained for 40 minutes, during which time two DWI were acquired at times 0-11 and 22-33 minutes. Normoxia was restored and DWI's were acquired at 22 minute intervals for a further 2 hours. Two "control" groups of normally grown (n=6) and growth restricted (n=6) chick embryos were subjected to a similar protocol but remained in air for the duration of the experiment. DWI data and the proton MRS data described in Chapters 6 and 7, were collected simultaneously from the same chick embryos.

For each set of diffusion weighted images, ADC maps were computed using source images that were free of motion artefact. The mean ADC was computed for each cerebral hemisphere excluding the cerebellum. CSF has a high ADC and an attempt was made to exclude its contribution by eliminating pixels with an ADC that exceeded an arbitrary value of $1.2\ 10^{-9}\ m^2.s^{-1}$

In a second experiment, performed to demonstrate that cerebral ADC is altered in response to hypoxia, a group of four normally grown day 19 chick embryos were subjected to a prolonged and severe hypoxic insult of 4% oxygen for 110 minutes followed by 2.5% oxygen for 44 minutes. After a baseline DWI and a proton magnetic resonance spectrum were acquired in air, alternate DWI's and proton spectra (Section 4.2.3) were acquired at 11 minutes intervals during

hypoxia. The mean ADC was computed for each cerebral hemisphere excluding the cerebellum and an attempt was made to exclude the contribution of CSF as described earlier. Proton spectra were analysed using a technique of linear combination modelling (Provencher, 1993) to determine the relative T_2 weighted signal amplitudes of lactate, N-acetylaspartate (NAA), choline and creatine. To provide these embryos, 5 normally grown eggs were incubated.

In the statistical analysis of the first experiment, group means of the ADC at each time point during hypoxia and recovery were compared with the equivalent normoxic controls. Data sets were tested for normality and equal variance before statistical comparison using the t-test were performed. In the second experiment, a One Way ANOVA was performed to examine the effect of severe hypoxia on cerebral ADC and metabolite/creatine quotient. Statistical analyses were performed using Sigmastat Version 2.0 (Jandel Scientific).

9.3 Results.

Data from 17% and 34% scans were contaminated by movement artefact in the hypoxia and control groups respectively and were discarded.

An acute reduction of oxygen concentration to 8% for 40 minutes followed by recovery in air did not significantly change cerebral ADC in normally grown or growth restricted chick embryos (Table 9-1).

The cerebral ADC of normally grown chick embryos declined gradually and was significantly reduced by an ambient oxygen concentration of 2.5%, 121 minutes after the start of the second experiment (One Way ANOVA $p = 0.006$). Conversely, lactate/Cr increased significantly 99 minutes after the start of the second experiment (One Way ANOVA $p = 0.016$) and then stabilised (Figure

9.1). Similar rises of choline/Cr and NAA/Cr occurred but were not statistically significant (Figure 9.2).

9.4 Discussion.

Mean cerebral ADC was unaffected by acute hypoxia (8% oxygen concentration for 40 minutes) in normal and growth restricted embryos (Table 9-1), and there were no cases of a precipitous reduction of ADC in response to hypoxia. These findings suggest osmoregulation was maintained during the hypoxic challenge and cell homeostasis was unaffected. It is possible these unidirectional ADC measurements were prone to anisotropy and failed to detect a change as a result of the orientation of the specimen and the myelinated axons within it, although this is unlikely as ADC was calculated over a relatively large area. Diffusion measurements in 3 orthogonal axes would overcome this potential problem and enable a directionally averaged diffusion coefficient independent of specimen orientation to be calculated.

There was a rapid rise of mean cerebral lactate/Cr during severe hypoxia that reached a maximum after 99 minutes exposure to 4% oxygen, probably because of anaerobic glycolysis. It is notable that mean ADC only decreased significantly as mean lactate/Cr peaked (Figure 9.1). This may reflect a failure of osmoregulation because cellular ATP reserves could not be maintained by anaerobic glycolysis. The pronounced fall in ADC in 4 chick embryos subjected to prolonged severe hypoxia validates the use of DWI in the chick embryo.

The marked rise in cerebral lactate during severe hypoxia is likely to reflect a failure of oxidative phosphorylation and increased reliance on anaerobic glycolysis to generate ATP. Both creatine and phosphocreatine (PCr) contribute

to the creatine proton MRS signal. PCr is dephosphorylated to creatine to generate ATP so the contribution of the creatine signal should increase if energy requirements are not met. The T2 relaxation time of PCr is shorter than creatine (Ke Y et al., 2001) therefore, at the TE used in this study, the creatine signal should change as a consequence of significant PCr dephosphorylation (Cady et al., 1994). The coincident declines of the T_2 weighted signal amplitudes of lactate, choline and N-acetylaspartate relative to creatine (Figure 9.1 and Figure 9.2) after prolonged hypoxia are consistent with an increased creatine signal, although the decrease did not reach statistical significance in this small study.

The rise in cerebral lactate observed during hypoxia is likely to be part of a coordinated metabolic response to maintain cell membrane function and homeostasis, and represents a successful adaptation of ATP generation to meet energy demand. The significant fall in cerebral ADC in the chick embryo in response to a prolonged severe hypoxic insult appears to be linked to a rise in free creatine when lactate concentration is maximal, which is consistent with a failure of cellular energy generation and cell membrane depolarisation.

9.5 Conclusions.

8% oxygen for 40 minutes does not significantly alter cerebral ADC in normally grown and growth restricted chick embryos. ADC is a relatively insensitive indirect measure of cerebral intracellular energy reserves.

Table 9-1 Mean cerebral ADC (± SD) in day 19 normally grown (NG) and growth restricted (GR) chick embryos during acute hypoxia and recovery in air (H) and during continuous normoxia (N).

time (hh:mm)	H			N		p-value	
	N^1 (n= 11)	GR^2 (n=9)		N^3 (n=6)	GR^4 (n=6)	^{1}vs.^{3}	^{2}vs.^{4}
00:00 Normoxic baseline	0.954 (0.09)	0.96 (0.11)		0.94 (0.09)	0.84 (0.1)	0.73	**0.02**
00:33 Hypoxia	0.92 (0.08)	0.95 (0.12)		0.96 (0.1)	0.89 (0.05)	0.38	0.27
00:55 Recovery	0.995 (0.11)	0.93 (0.13)		0.96 (0.06)	0.88 (0.03)	0.56	0.44
02:23 Recovery	0.97 (0.06)	0.94 (0.13)		0.91 (0.09)	0.9 (0.09)	0.17	0.5

Figure 9.1. Mean cerebral ADC (x100) (black bars) and lactate/Cr (x10) (grey bars) (±SD) of day 19 normally grown chick embryos in response to 4% oxygen for 110 minutes followed by 2.5% oxygen for 44 minutes (n=4).

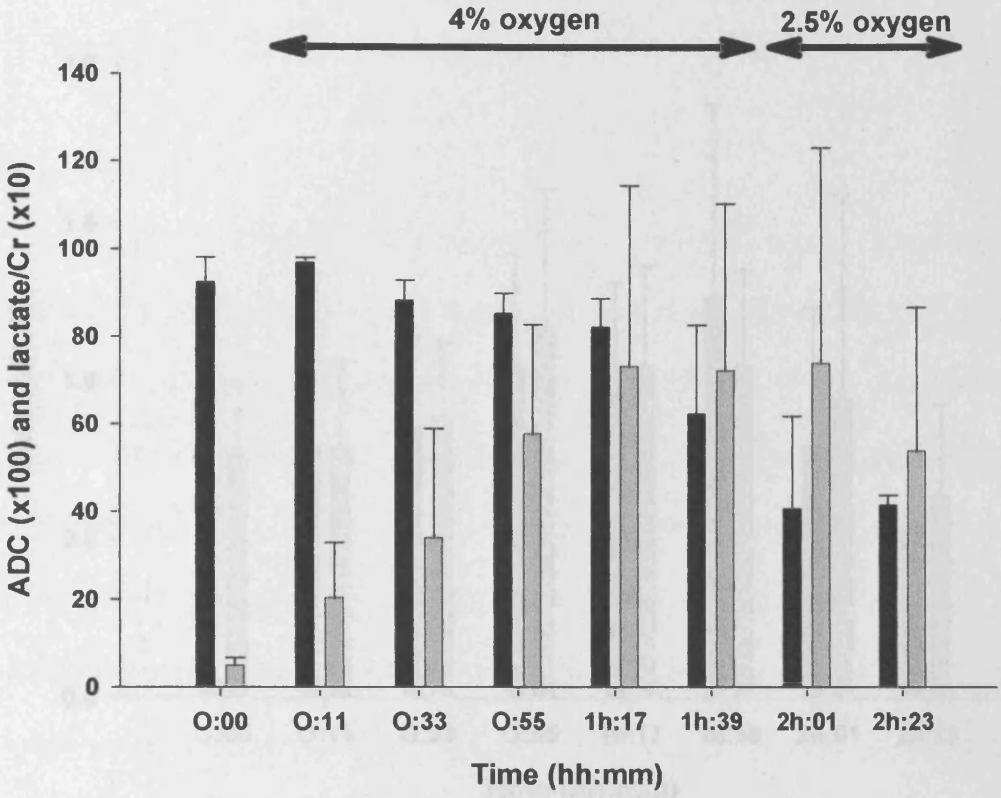

Figure 9.2 Mean cerebral choline/Cr (black bars) and N-acetylaspartate/Cr (grey bars) (±SD) of day 19 normally grown chick embryos in response to 4% oxygen for 110 minutes followed by 2.5% oxygen for 44 minutes (n=4).

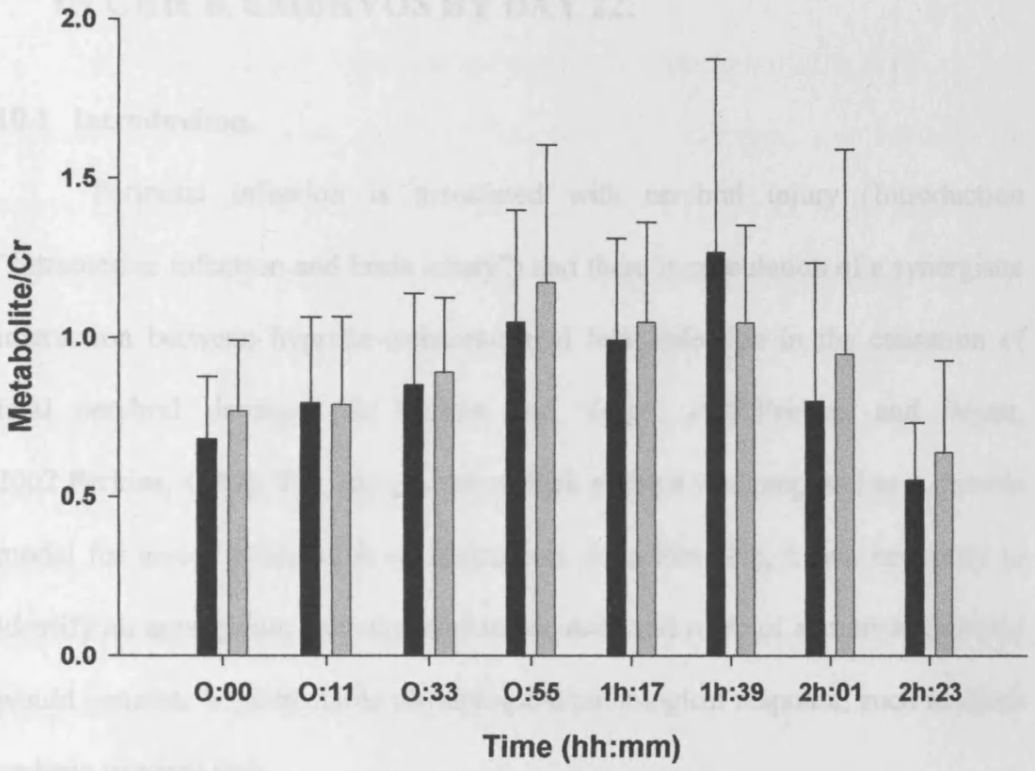

10 AN EXPERIMENT TO DETERMINE THE REQUIRED DOSE OF SALMONELLA TYPHI LIPOPOLYSACCHARIDE ADMINISTERED ON DAY 18 OF INCUBATION TO CAUSE 50% MORTALITY (LD50) IN CHICK EMBRYOS BY DAY 22.

10.1 Introduction.

Perinatal infection is associated with cerebral injury (Introduction "Intrauterine infection and brain injury") and there is speculation of a synergistic interaction between hypoxic-ischaemia and fetal infection in the causation of fetal cerebral damage (du Plessis and Volpe, 2002;Peebles and Wyatt, 2002;Perkins, 1987). The late gestation chick embryo was proposed as a suitable model for investigating such an interaction. As a first step, it was necessary to identify an appropriate bacterial endotoxin, dose and route of administration that would generate a quantifiable physiological/pathological response, such as chick embryo survival rate.

There is contradictory evidence regarding avian sensitivity to bacterial endotoxin, as several groups report a similar response to mammals (Sunwoo et al., 1996;Jones et al., 1983;Curtis et al., 1980;Klasing and Peng, 1987;Miller and Qureshi, 1992;Koh et al., 1996),while others have suggested they are more resistant (Roeder et al., 1989). Variable avian sensitivity to some bacterial endotoxins and resistance to others might account for these reports. Several studies have shown domestic chickens (*Gallus gallus*) are susceptible to Escherichia coli and Salmonella typhi species endotoxin, by responses such as

pyrexia (Jones et al., 1983) (Kane and Peterson, 1976), raised IL-6 and heterophils cell count (Xie et al., 2000), increased serum antibodies (Sunwoo et al., 1996)and deficits of memory–processing in day old chicks (Sell et al., 2001). Salmonella typhi endotoxin was chosen for this experiment because of its proven activation of the chick immune response (Sijben et al., 2003;Kaiser et al., 2000;Sunwoo et al., 1996).

Several routes of bacterial endotoxin administration were practiced and evaluated. The simplest was injection into the allantoic sac beneath the chorioallantoic membrane ("sub-CAM") (Figure 10.1), which is the same route used for automated inoculation of chick embryos *in-ovo*. Intravascular injection into chorioallantoic vessels as described previously (Foster and Leudke, 1968) proved technically difficult, and was often associated with excessive bleeding from the vessel after the needle was withdrawn and this adversely affected embryo survival. A study of topical bacterial endotoxin applied onto the chorioallantoic membrane showed the hatch rate was unaffected by very high concentrations equivalent to 100mg lipopolysaccharide/Kg, so this route of administration was discounted. Intraperitoneal injection under ultrasound guidance was the most difficult technique evaluated. For this, a 2cm square "window" was cut in the shell using a burr drill without perforating the shell membrane. The embryo was identified using an ultrasound probe held against the "window", and a fine needle was directed into its abdomen. Although the procedure was a technical success, it took too long to perform to be feasible. Therefore, the sub-CAM route of lipopolysaccharide administration was selected for determining the LD50 dose of Salmonella typhi LPS.

Lipopolysaccharide was administered on day 18 of incubation because several studies in chickens and rats showed cytokine, fever and cerebral blood flow responses to endotoxin 1 to 24 hours after administration (Cai et al., 2000;Eklind et al., 2001;Macari et al., 1993;Xie et al., 2000). This arrangement allowed 24 hours for absorption from the allantoic sac and systemic distribution before acute hypoxia on day 19 in a later experiment.

10.2 Materials and Methods.

White Leghorn chick embryos were incubated for 19 days (Section 4.1.1). On day 18 (of 21 days incubation) chick embryo vitality was confirmed by holding the egg against a bright light source in a darkened room ("candling") and observing full and prominent CAM vessels and embryo movement. The margins of the air cell and the position of prominent vessels were marked on the shell with a pencil. A small 6mm x 6mm hole was made in the shell just above the border of the air cell. 1 - 2 small drops of sterile 0.9% saline from a 26G needle were placed on the CAM to identify an area free of large vessels and suitable for injection. A 0.4ml solution of inoculant containing 0, 1mg, 3mg 10mg or 30 mg of Salmonella typhi LPS (Sigma Lot 071K1430) in sterile 0.9% saline was injected 2-3 mm below the CAM surface. The number of eggs in each experimental group is shown in Table 10-1. Haemostasis was confirmed, and the hole was covered with a small square of non-sterile tape. The egg was returned to the incubator to continue incubation in air for a further 4 days. Fifty eggs were incubated to provide chick embryos for this experiment.

On days 21, 22 and 23 of incubation, the number of hatched chicks, live and dead embryos in each group was recorded.

10.3 Results.

Chick embryo cumulative mortality increased with larger doses of LPS (Table 10-1 and Figure 10.2). 3mg LPS was associated with 44% cumulative mortality on day 22 of incubation.

10.4 Conclusions.

By day 22 of incubation there was a clear dose-mortality response, with a cumulative mortality in the 3mg LPS group of just less than 50%. Therefore, this dose was chosen for investigating the interaction of lipopolysaccharide and hypoxia on cerebral histology, as it has an clear pathological effect and enables the influence of other factors to be assessed.

Table 10-1 Lipopolysaccharide (LPS) dose and cumulative mortality between day 18 and 23 of incubation after LPS inoculation on day 18.

		LPS Dose				
		0mg	1mg	3mg	10mg	30mg
Day 18	No. inoculated	5	9	9	9	8
Day 21	No. surviving	5	7	6	2	0
	% cumulative mortality	0	22	33	78	100
Day 22	No. surviving	4	7	5	2	0
	% cumulative mortality	20	22	44	78	100
Day 23	No. surviving	4	6	5	2	0
	% cumulative mortality	20	22	44	78	100

Figure 10.1 Diagram of chick embryo and internal egg structures

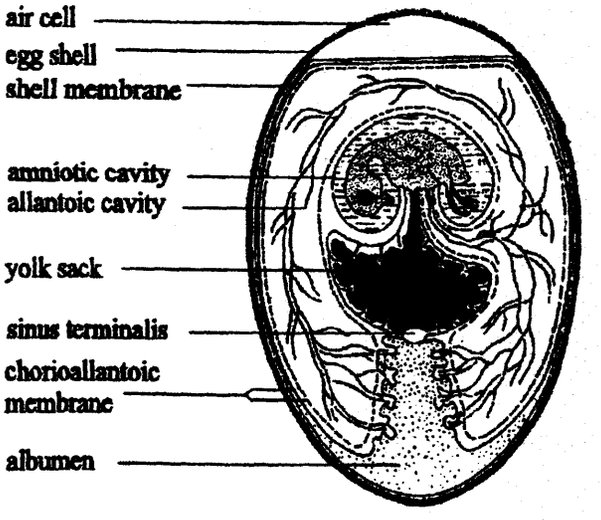

(with acknowledgements to (van Golde, 1999))

Figure 10.2 Chick embryo cumulative mortality (%) on day 22 of incubation in response to different lipopolysaccharide (LPS) doses on day 18. 3mg LPS was associated with 44% cumulative mortality.

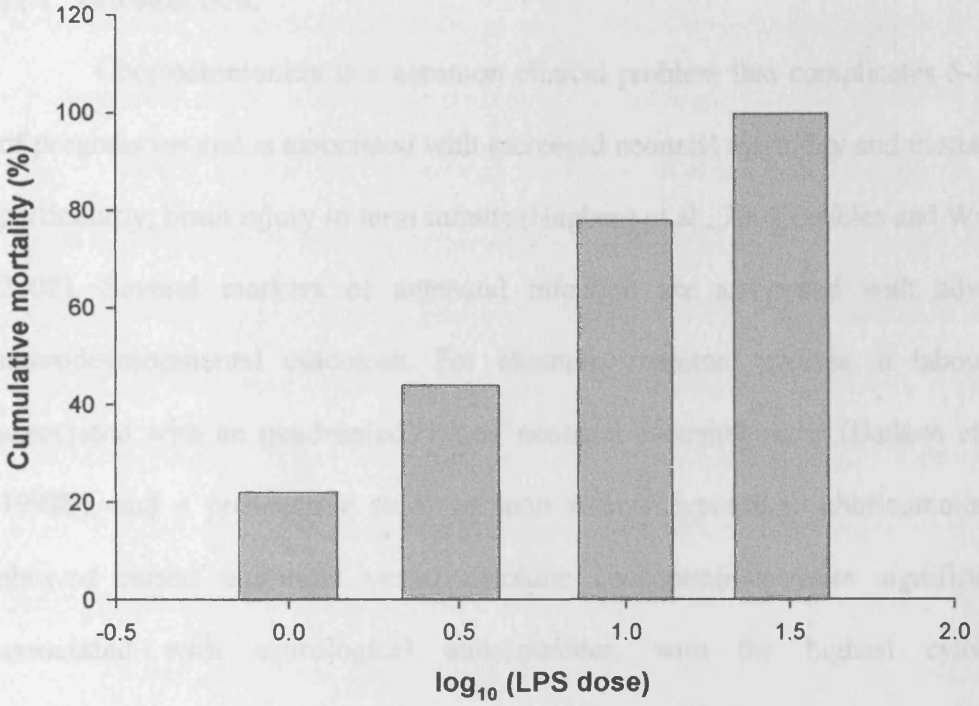

11 AN INVESTIGATION OF THE EFFECT OF SYSTEMIC SALMONELLA TYPHI LIPOPOLYSACCHARIDE AND ACUTE HYPOXIA ON DAY 21 CHICK EMBRYO CEREBRAL HISTOLOGY.

11.1 Introduction.

Chorioamnionitis is a common clinical problem that complicates 5-10% of pregnancies and is associated with increased neonatal morbidity and mortality, particularly, brain injury in term infants (Hagberg et al., 2002;Peebles and Wyatt, 2002). Several markers of antenatal infection are associated with adverse neurodevelopmental outcomes. For example, maternal pyrexia in labour is associated with an quadrupled risk of neonatal encephalopathy (Badawi et al., 1998b), and a prospective study of term infants exposed to chorioamnionitis showed raised umbilical vessel cytokine concentrations were significantly associated with neurological abnormalities, with the highest cytokine concentrations found in infants who developed hypoxic ischaemic encephalopathy and seizures (Shalak et al., 2002). In addition, premature rupture of membranes longer than 24 hours is significantly associated with cerebral palsy, mental retardation, epilepsy, severe defects of vision and hearing at 4 years of age (Holst et al., 1989).

Studies in the premature fetus and neonate have also implicated intrauterine infection and chorioamnionitis as causative factors in the pathogenesis of periventricular leukomalacia (PVL) (O'Shea, 2002;Saliba and Marret, 2001;Vigneswaran, 2000). In particular, fetal and neonatal inflammatory responses can contribute towards neonatal brain injury and neurodevelopmental

disabilities including cerebral palsy (Rezaie and Dean, 2002). An association between the inflammatory response and brain injury was demonstrated by a study of 50 infants born at 23-29 weeks' gestation in which elevated cytokines in umbilical blood predicted cerebral lesions detected by magnetic resonance imaging shortly after delivery (Duggan et al., 2001). Another study showed raised umbilical cord interleukin-6 was an independent risk factor for periventricular leukomalacia (Yoon et al., 1996). These reports suggest infants who mount an immune response in-utero are at increased risk of cerebral injury.

Animal studies of the effects of simultaneous hypoxia/ischaemia and infection have shown synergy between the two factors in causing brain injury. Two studies showed a small dose of endotoxin in day 7 neonatal rats could sensitise the immature brain to injury and induce cerebral infarction in response to a short periods of hypoxia-ischaemia that by themselves cause little or no injury (Eklind et al., 2001;Coumans et al., 2003), and another reported similar findings in fetal sheep (Peebles and Wyatt, 2002).

There has been speculation about the mechanisms involved with increased susceptibility to hypoxic/ischaemic (HI) brain injury in the presence of infection or its products. Reduced cerebral blood flow in association with infection has been reported with cerebral vessel occlusion in neonatal animal models (Fabian et al., 2000) (Froen et al., 2002), whereas the findings were not replicated in an adult animal model (Eklind et al., 2001). It has been proposed that impaired cerebral metabolism (Froen et al., 2002) and elimination of the usual fall in cerebral temperature during a HI insult (Suzuki et al., 2000) in the presence of infection also contribute to brain injury.

The hypothesis to be tested was that histological evidence of neuronal damage arising from acute hypoxia is significantly increased by systemic bacterial endotoxin administered 24 hours beforehand, and that the neuronal damage associated with bacterial endotoxin and hypoxia individually, is significantly less than when the two are combined.

11.2 Materials and Methods.

Thirty six White Leghorn chick embryos were incubated for 18 days (Section 4.1.1), by which time 6 had died. On day 18 of incubation, 30 eggs were inoculated 2-3 mm below the chorioallantoic membrane, with 3mg Salmonella typhimurium lipopolysaccharide (Sigma Lot 071K1430) (Section 4.1.3), but 1 died by day 19. These 29 eggs and an additional 25 normally grown eggs (as described in the histology section of Chapter 6) formed four groups that were put in a sealed plastic bag located inside an egg incubator on day 19, and supplied with air (N) or a hypoxic (H) mixture of air and nitrogen (8% oxygen concentration) for 40 minutes at 3L/minute and kept warm by a radiant heater within the incubator (Table 11-1).

Eggs were returned to an incubator immediately after the experiment to continue incubating in air. All inoculated embryos survived to be euthanased on day 21, when their brains were perfused, fixed and prepared for cryopreservation (Section 4.3.1), before storage in a –80°C freezer. Eleven (7 (Normoxia) + 4 (Hypoxia)) brains from embryos inoculated with lipopolysaccharide were of sufficient quality to be processed further. 20 micron sections from 3 brains in each group (a total of 6 brains) were cut, air dried and fixed onto slides (Sections 4.3.2 and 4.3.3) and stained with Nissl stain (Section 4.3.4). All procedures were

performed in accordance with the Animals (Scientific Procedures) Act 1986, United Kingdom.

Counting of hyperchromatic, normal and pyknotic neurons in the hippocampus, hyperstriatum ventralis, cerebellum and optic tectum was performed (Section 4.4) by a single non-blinded individual.

Cell counts in each brain structure were averaged over all the tissue sections in which each structure was present. Statistical analysis of average cell counts by brain area in the four experimental groups was performed by Two and Three Way Analysis of Variance (ANOVA) using Sigmastat Version 2.0 (Jandel Scientific).

11.3 Results.

11.3.1 Hyperstriatum ventralis, hippocampus and optic tectum.

Hypoxia was associated with a significant increase in pyknotic cell density (0.58 (hypoxia (H)) vs. 0.11 (air (N)); $p=0.008$) and pyknotic cell/ neuron quotient (0.014 (H) vs. 0.0052 (N); $p = 0.008$), but LPS did not affect either.

LPS significantly increased the hyperchromatic neuron density (10.9 (LPS^+) vs. 5.8 (LPS^-); $p = 0.026$), but not the hyperchromatic neuron/neuron quotient.

LPS was associated with a significantly increased neuron density (47 (LPS^+) vs. 34 (LPS^-); $p<0.001$). In addition, there was a significant interaction between the presence or absence of LPS and the ambient atmosphere, as LPS and hypoxia was associated with a significant increase in neuron density (53 (LPS^+ and H) vs. 33 (LPS^- and H); $p=0.009$).

11.3.2 Cerebellum.

LPS was associated with a significant increase in the pyknotic cell/Purkinje cell quotient (1.027 (LPS^+) vs. 0.017 (LPS^-); p= 0.03) and a tendency for increased pyknotic cell density (0.54 (LPS^+) vs. 0.37 (LPS^-); p = 0.052).

11.4 Discussion.

Functional neurons are identified by their size and shape after Nissl staining, whereas dead and compromised neurons do not take up Nissl stain because their cytoplasm is contracted and eosinophilic, and Nissl bodies are sparse. Therefore, the increased neuron and hyperchromatic neuron densities associated with LPS may be because increased rough endoplasmic reticulum protein synthesis in response to endotoxin or inflammatory cytokines makes them more discernible. Alternatively, LPS may up-regulate neurotrophic factors that control neuronal survival and death, and thereby inhibit naturally occurring neuronal death by apoptosis.

The response of Purkinje cells in the cerebellum to LPS appears different compared to neurones in other brain areas. For example, LPS and growth restriction were both associated with increased neuronal density in the hippocampus, hyperstriatum ventralis and optic tectum, yet did not affect Purkinje cells in the cerebellum. In addition, LPS was associated with a significant increase in pyknotic cell/total Purkinje cell quotient, but not Purkinje cell density, that was not seen in other brain areas. This suggests Purkinje cells may be particularly susceptible to damage by LPS.

Previous reports of synergy between hypoxia and infection to increase brain injury (Eklind et al., 2001;Peebles and Wyatt, 2002) appear to be supported by the finding of a significant interaction between hypoxia and LPS to increase neuron density in the hippocampus, hyperstriatum ventralis and optic tectum.

11.5 Conclusions.

This small study provides evidence of an association between LPS and changes of neuronal morphology and density, and supports the hypothesis that there is synergy between hypoxia and LPS in their affect on chick embryo brain histology. The small size of this study requires larger confirmatory experiments to be performed.

Table 11-1 Gas mixture and duration of supply in four groups of day 19 chick embryos.

Group		Ambient atmosphere	Oxygen concentration (%)	Duration (minutes)	Number of eggs
Normal (LPS^-)	**Normoxia (N)**	air	21	40	14
	Hypoxia (H)	air/nitrogen	8	40	11
Inoculated with LPS (LPS^+)	**Normoxia (N)**	air	21	40	14
	Hypoxia (H)	air/nitrogen	8	40	15

Note: only 3 brains from each group underwent histological examination.

12 Further work.

There is uncertainty about the origin of the impaired lactate response to acute hypoxia seen in association with growth restriction. It is unclear whether reduced cerebral basal metabolic rate or impaired cerebral glucose availability have a role. Measurement of serum glucose from chorioallantoic veins, and non-invasive evaluation of cerebral glucose and oxygen metabolism using Positron Emission Tomography (PET) with [^{18}F]-deoxyglucose and [^{15}O] oxygen respectively may provide important information to assist in solving this question.

The unanticipated smaller chemical shift between PCr and Pi after acute hypoxia in GR compared to NG embryos should be investigated by measuring serum bicarbonate and base deficit to determine the effect of growth restriction on bicarbonate buffering capacity.

Three axis DWI and ADC measurement in NG and GR embryos would overcome anisotropy and scrutinise the finding that unidirectional DWI and ADC appear to be insensitive indices of changes of cerebral metabolism.

The chick embryo model of fetal growth restriction is an opportunity to examine the independent contributions of substrate deprivation and chronic hypoxia to the observed changes of cerebral metabolism. This can be investigated by applying the previously described MRS and MRI techniques to growth impaired chick embryos induced by either chronic hypoxia or 10% albumen removal.

The interaction between infection and acute hypoxia and their effects on cerebral energy substrates, intracellular energy reserves and cerebral water diffusion can be investigated using the MRI and MRS techniques already

described. This would enable the hypothesis that systemic bacterial endotoxin alters cerebral energy substrate concentrations and decreases intracellular energy reserves which decline rapidly during acute hypoxia to be tested.

Larger group sizes are needed for histological and immunocytological studies to test the hypotheses that fetal growth restriction and infection increase neuronal susceptibility to acute hypoxia. Neuron injury can be assessed using cell morphological features and the relative contributions of necrosis and apoptosis to neuronal damage may be deduced using terminal deoxynucleotide transferase (TdT) mediated dUTP-biotin nick-end-labelling (TUNEL) staining.

Chick behavioural studies of memory and learning ability based on bead discrimination tasks offer a means to investigate the individual and combined influences of growth restriction, acute hypoxia and bacterial endotoxin on neurodevelopment.

13 Overview

Magnetic Resonance Spectroscopy investigations in day 19 growth restricted chick embryo have confirmed the hypothesis that there is an association between growth restriction and significant changes in cerebral structural metabolite (reduced NAA and inositol) and energy substrate (increased β–hydroxybutyrate and reduced PCr/ Pi) concentrations. Cerebral energy requirements appear to be met in the GR embryo as cerebral lactate and PCr-Pi chemical shift were not significantly different to NG embryos. Although an alternative cerebral energy substrate (β–hydroxybutyrate) was markedly increased, the reduced PCr/Pi (and presumed intracellular energy reserves) suggests that cerebral oxidative metabolism was impaired in the GR embryo. This would imply a reduced the margin of safety in the event of acute hypoxia. Reduced NAA and inositol may reflect changes in neuron and glial cell concentration or development.

These MRS studies have shown an association between acute hypoxia and significantly increased cerebral lactate and alanine, which recovered after normoxia was restored. These responses were clearly evident in normally grown chick embryos, but appeared significantly attenuated or absent (in the case of alanine) in growth restricted embryos as was hypothesised. Unexpectedly, growth restriction had no effect on the rate of decline of PCr/Pi during acute hypoxia. Although reduced availability of glucose substrate for anaerobic glycolytic energy production might account for the observed lactate response, reduced cerebral metabolism in association with growth restriction could account for the lactate and the PCr/Pi response to acute hypoxia.

Creatine appears to be a stable cerebral metabolite whose concentration is affected by neither growth restriction nor acute hypoxic episodes such as described in Chapters 6 and 7. Therefore it appears to be an appropriate reference metabolite to compare the concentrations of other cerebral metabolites under such conditions.

After the attenuated lactate response was identified, the smaller cerebral chemical shift between PCr and Pi (and lower intracellular pH) in GR embryos compared to NG embryos after acute hypoxia was unexpected. This observation may arise because the usual compensatory bicarbonate metabolic alkalosis towards the end of incubation may be impaired in GR embryos.

The utility of Diffusion Weighted Imaging (DWI) and Apparent Diffusion Coefficient (ADC) measurements during acute hypoxia was unsatisfactory. Images were prone to movement artefact and the unidirectional cerebral ADC was an insensitive indirect indicator of cellular energy metabolism. Only a prolonged and severe hypoxic insult accompanied by maximal relative cerebral lactate concentrations, was found to alter the DWI and significantly decrease ADC.

Further histological examination for the neuronal morphological effects of acute hypoxia and growth restriction are necessary. These initial studies suggest acute hypoxia is associated with increased pyknosis and reduced hyperchromatic neuron density, whereas growth restriction has no influence on either, but is associated with increased neuron density. There was no evidence of an interaction between acute hypoxia and growth restriction on neuronal morphology, and therefore no histological evidence to support to the hypothesis

that growth restriction is associated with increased susceptibility to neuronal injury due to acute hypoxia.

There is a logarithmic relationship between Salmonella typhi LPS administered in the latter stages of incubation via the sub-chorioallantoic membrane route and chick embryo mortality in the dose range described in Chapter 10. LPS was associated with increased neuron density and hyperchromatic neuron density, which may reflect increased rough endoplasmic reticulum protein synthesis and led to improved neuron discernability. Although there was evidence of an interaction between acute hypoxia and LPS on neuron density, this does not substantiate the hypothesis that systemic bacterial endotoxin will increase susceptibility to acute hypoxic brain injury.

The day 19 chick embryo has proved to be an effective model of fetal cerebral metabolism and eminently suitable for investigation by proton and phosphorus MRS. It has demonstrated its value as a model of fetal growth restriction and offers an opportunity to investigate the independent influences of chronic hypoxia and substrate deprivation on cerebral metabolism.

APPENDIX 1

Tissue perfusion, fixation, cryopreservation and staining solutions.

Phosphate buffered saline
Phosphate buffered saline 0.85% NaCl, 10mM Na2HPO4 pH 7.4
To make 1 litre of solution, add:
1.42g Na_2HPO_4 (mw=142)
8.5g NaCl
To: 1L distilled water.
Stir for 5 minutes
Add dilute (1:50) H_3PO_4 until pH = 7.4

Phosphate buffered saline with Magnesium chloride (10mM)
Phosphate buffered saline 0.85% NaCl, 10mM Na2HPO4 10mM MgCl pH 7.4
To make 1 litre of solution, add:
1.42g Na_2HPO_4 (mw=142)
8.5g NaCl
2.03g $MgCl_2$-6 hydrate (mw=203)
To: 1L distilled water.
Stir for 5 minutes
Add dilute (1:50) H_3PO_4 until pH = 7.4

20% paraformaldehyde
20% paraformaldehyde pH 7.4
To make 100ml of solution, add:
20g paraformaldehyde
To: 80ml distilled water with 5 drops of 0.5N NaOH
Stir and heat the solution until it is clear, then filter.
Add dilute (1:500) H_3PO_4 until pH = 7.4

4% paraformaldehyde
4% paraformaldehyde pH 7.4
To make 200ml of solution, add:
40ml 20% paraformaldehyde
160ml Phosphate buffered saline with Magnesium chloride (10mM)

1% paraformaldehyde
1% paraformaldehyde pH 7.4
To make 100ml of solution, add:
5ml 20% paraformaldehyde solution
95ml Phosphate buffered saline

30% sucrose solution
To make 100 mls of solution, add:
30g Saccharose
70ml Phosphate buffered saline
Stir the solution for 5 minutes until it is clear.

Nissl stain.

To make 100 mls of solution, add:

1 g cresyl violet

10mls 100% ethanol

Stir in a closed 50ml falcon tube standing on its lid for 15 minutes.
Add the solution to 90mls warm distilled water and mix for 20 minutes, filter for 30 minutes and use immediately.

REFERENCE LIST

1. Abuhamad AZ, Mari G, Bogdan D, Evans AT, III (1995) Doppler flow velocimetry of the splenic artery in the human fetus: is it a marker of chronic hypoxia? Am J Obstet Gynecol 172: 820-825.

2. Adam PA, Raiha N, Rahiala EL, Kekomaki M (1975) Oxidation of glucose and D-B-OH-butyrate by the early human fetal brain. Acta Paediatr Scand 64: 17-24.

3. Adamson SJ, Alessandri LM, Badawi N, Burton PR, Pemberton PJ, Stanley F (1995) Predictors of neonatal encephalopathy in full-term infants. BMJ 311: 598-602.

4. Aden U, Dahlberg V, Fredholm BB, Lai LJ, Chen Z, Bjelke B (2002) MRI evaluation and functional assessment of brain injury after hypoxic ischemia in neonatal mice. Stroke 33: 1405-1410.

5. Ahmed SH, He YY, Nassief A, Xu J, Xu XM, Hsu CY, Faraci FM (2000) Effects of lipopolysaccharide priming on acute ischemic brain injury. Stroke 31: 193-199.

6. al Mohanna FA, Caddy KW, Bolsover SR (1994) The nucleus is insulated from large cytosolic calcium ion changes. Nature 367: 745-750.

7. Altman DG, Chitty LS (1997) New charts for ultrasound dating of pregnancy. Ultrasound Obstet Gynecol 10: 174-191.

8. Ames A, III (2000) CNS energy metabolism as related to function. Brain Res Brain Res Rev 34: 42-68.

9. Amess PN, Penrice J, Wylezinska M, Lorek A, Townsend J, Wyatt JS, Amiel-Tison C, Cady EB, Stewart A (1999) Early brain proton magnetic resonance spectroscopy and neonatal neurology related to neurodevelopmental outcome at 1 year in term infants after presumed hypoxic-ischaemic brain injury. Dev Med Child Neurol 41: 436-445.

10. Amin H, Singhal N, Sauve RS (1997) Impact of intrauterine growth restriction on neurodevelopmental and growth outcomes in very low birthweight infants. Acta Paediatr 86: 306-314.

11. Anderson DF, Parks CM, Faber JJ (1986) Fetal O2 consumption in sheep during controlled long-term reductions in umbilical blood flow. Am J Physiol 250: H1037-H1042.

12. Andres RL, Saade G, Gilstrap LC, Wilkins I, Witlin A, Zlatnik F, Hankins GV (1999) Association between umbilical blood gas parameters and neonatal morbidity and death in neonates with pathologic fetal acidemia. Am J Obstet Gynecol 181: 867-871.

13. Azzopardi D, Wyatt JS, Cady EB, Delpy DT, Baudin J, Stewart AL, Hope PL, Hamilton PA, Reynolds EO (1989a) Prognosis of newborn infants with hypoxic-ischemic brain injury assessed by phosphorus magnetic resonance spectroscopy. Pediatric Research 25: 445-451.

14. Azzopardi D, Wyatt JS, Hamilton PA, Cady EB, Delpy DT, Hope PL, Reynolds EO (1989b) Phosphorus metabolites and intracellular pH in the brains of normal and small for gestational age infants investigated by magnetic resonance spectroscopy. Pediatr Res 25: 440-444.

15. Back T, Hoehn-Berlage M, Kohno K, Hossmann KA (1994) Diffusion nuclear magnetic resonance imaging in experimental stroke. Correlation with cerebral metabolites. Stroke 25: 494-500.

16. Badawi N, Kurinczuk JJ, Keogh JM, Alessandri LM, O'Sullivan F, Burton PR, Pemberton PJ, Stanley FJ (1998a) Antepartum risk factors for newborn encephalopathy: the Western Australian case-control study. BMJ 317: 1549-1553.

17. Badawi N, Kurinczuk JJ, Keogh JM, Alessandri LM, O'Sullivan F, Burton PR, Pemberton PJ, Stanley FJ (1998b) Intrapartum risk factors for newborn encephalopathy: the Western Australian case-control study. BMJ 317: 1554-1558.

18. Badawi N, Watson L, Petterson B, Blair E, Slee J, Haan E, Stanley F (1998c) What constitutes cerebral palsy? Dev Med Child Neurol 40: 520-527.

19. Baker LL, Kucharczyk J, Sevick RJ, Mintorovitch J, Moseley ME (1991) Recent advances in MR imaging/spectroscopy of cerebral ischemia. AJR Am J Roentgenol 156: 1133-1143.

20. Bal-Price A, Brown GC (2001) Inflammatory neurodegeneration mediated by nitric oxide from activated glia-inhibiting neuronal respiration, causing glutamate release and excitotoxicity. J Neurosci 21: 6480-6491.

21. Barkovich AJ, Westmark KD, Bedi HS, Partridge JC, Ferriero DM, Vigneron DB (2001) Proton spectroscopy and diffusion imaging on the first day of life after perinatal asphyxia: preliminary report. AJNR Am J Neuroradiol 22: 1786-1794.

22. Baschat AA, Gembruch U, Harman CR (2001) The sequence of changes in Doppler and biophysical parameters as severe fetal growth restriction worsens. Ultrasound Obstet Gynecol 18: 571-577.

23. Baschat AA, Gembruch U, Reiss I, Gortner L, Diedrich K (1997) Demonstration of fetal coronary blood flow by Doppler ultrasound in relation to arterial and venous flow velocity waveforms and perinatal outcome--the 'heart-sparing effect'. Ultrasound Obstet Gynecol 9: 162-172.

24. Baschat AA, Gembruch U, Reiss I, Gortner L, Harman CR, Weiner CP (1999) Neonatal nucleated red blood cell counts in growth-restricted fetuses: relationship to arterial and venous Doppler studies. Am J Obstet Gynecol 181: 190-195.

25. Baud O, Ville Y, Zupan V, Boithias C, Lacaze-Masmonteil T, Gabilan JC, Frydman R, Dehan M (1998) Are neonatal brain lesions due to intrauterine infection related to mode of delivery? Br J Obstet Gynaecol 105: 121-124.

26. Beal MF (1996) Mitochondria, free radicals, and neurodegeneration. Curr Opin Neurobiol 6: 661-666.

27. Beattie J, Smith AH (1975) Metabolic adaptation of the chick embryo to chronic hypoxia. Am J Physiol 228: 1346-1350.

28. Ben Yoseph O, Badar-Goffer RS, Morris PG, Bachelard HS (1993) Glycerol 3-phosphate and lactate as indicators of the cerebral cytoplasmic redox state in severe and mild hypoxia respectively: a 13C- and 31P-n.m.r. study. Biochem J 291 (Pt 3): 915-919.

29. Bhasin S, Shambaugh GE, III (1982) Fetal fuels. V. Ketone bodies inhibit pyrimidine biosynthesis in fetal rat brain. Am J Physiol 243: E234-E239.

30. Bjonnes PO, Aulie A, Hoiby M (1987) Effects of hypoxia on the metabolism of embryos and chicks of domestic fowl. J Exp Zool Suppl 1: 209-212.

31. Blair E, Stanley F (1990) Intrauterine growth and spastic cerebral palsy. I. Association with birth weight for gestational age. Am J Obstet Gynecol 162: 229-237.

32. Block BS, Schlafer DH, Wentworth RA, Kreitzer LA, Nathanielsz PW (1990) Intrauterine asphyxia and the breakdown of physiologic circulatory compensation in fetal sheep. Am J Obstet Gynecol 162: 1325-1331.

33. Bona E, Hagberg H, Loberg EM, Bagenholm R, Thoresen M (1998) Protective effects of moderate hypothermia after neonatal hypoxia-ischemia: short- and long-term outcome. Pediatr Res 43: 738-745.

34. Booth RF, Patel TB, Clark JB (1980) The development of enzymes of energy metabolism in the brain of a precocial (guinea pig) and non-precocial (rat) species. J Neurochem 34: 17-25.

35. Borowsky IW, Collins RC (1989) Metabolic anatomy of brain: a comparison of regional capillary density, glucose metabolism, and enzyme activities. J Comp Neurol 288: 401-413.

36. Bottomley PA (1987) Spatial localization in NMR spectroscopy in vivo. Ann N Y Acad Sci 508: 333-348.

37. Bourre JM, Morand O, Chanez C, Dumont O, Flexor MA (1981) Influence of intrauterine malnutrition on brain development: alteration of myelination. Biol Neonate 39: 96-99.

38. Bracci R, Perrone S, Buonocore G (2001) Red blood cell involvement in fetal/neonatal hypoxia. [Review] [56 refs]. Biology of the Neonate 79: 210-212.

39. Brand A, Richter-Landsberg C, Leibfritz D (1993) Multinuclear NMR studies on the energy metabolism of glial and neuronal cells. Dev Neurosci 15: 289-298.

40. Brenner B, Kupferminc MJ (2003) Inherited thrombophilia and poor pregnancy outcome. Best Pract Res Clin Obstet Gynaecol 17: 427-439.

41. Brooks KJ, Clark JB, Bates TE (1998) 3-Hydroxybutyrate aids the recovery of the energy state from aglycaemic hypoxia of adult but not neonatal rat brain slices. J Neurochem 70: 1986-1990.

42. Brown JD, Vannucci RC (1978) Cerebral oxidative metabolism during intrauterine growth retardation. Biol Neonate 34: 170-173.

43. Brulatout S, Meric P, Loubinoux I, Borredon J, Correze JL, Roucher P, Gillet B, Berenger G, Beloeil JC, Tiffon B, Mispelter J, Seylaz J (1996) A one-dimensional (proton and phosphorus) and two-dimensional (proton) in vivo NMR spectroscopic study of reversible global cerebral ischemia. J Neurochem 66: 2491-2499.

44. Bukowski R, Burgett AD, Gei A, Saade GR, Hankins GD (2003) Impairment of fetal growth potential and neonatal encephalopathy. Am J Obstet Gynecol 188: 1011-1015.

45. Busto R, Dietrich WD, Globus MY, Valdes I, Scheinberg P, Ginsberg MD (1987) Small differences in intraischemic brain temperature critically determine the extent of ischemic neuronal injury. J Cereb Blood Flow Metab 7: 729-738.

46. Busza AL, Allen KL, King MD, van Bruggen N, Williams SR, Gadian DG (1992) Diffusion-weighted imaging studies of cerebral ischemia in gerbils. Potential relevance to energy failure. Stroke 23: 1602-1612.

47. Cady EB, Amess P, Penrice J, Wylezinska M, Sams V, Wyatt JS (1997) Early cerebral-metabolite quantification in perinatal hypoxic-ischaemic encephalopathy by proton and phosphorus magnetic resonance spectroscopy. Magn Reson Imaging 15: 605-611.

48. Cady EB, Lorek A, Penrice J, Wylezinska M, Cooper CE, Brown GC, Owen-Reece H, Kirkbride V, Wyatt JS, Osmund E (1994) Brain-metabolite transverse relaxation times in magnetic resonance spectroscopy increase as adenosine triphosphate depletes during secondary energy failure following acute hypoxia-ischaemia in the newborn piglet. Neuroscience Letters 182: 201-204.

49. Cai Z, Pan ZL, Pang Y, Evans OB, Rhodes PG (2000) Cytokine induction in fetal rat brains and brain injury in neonatal rats after maternal lipopolysaccharide administration. Pediatric Research 47: 64-72.

50. Cai Z, Pang Y, Xiao F, Rhodes PG (2001) Chronic ischemia preferentially causes white matter injury in the neonatal rat brain. Brain Res 898: 126-135.

51. Caldeyro-Barcia r., Mendez-Bauer C., Posiero J.J., Escarcena L.A., Pose S.V., Bieniarz J., Arnt I., Gulin L., Althabe O. (1966) Control of human fetal heart rate in labor. In: The Heart and Circulation of the Newborn and Infant. (Cassels D.E., ed), pp 7-36. New York and London: Grune and Stratton.

52. Campbell MJ, Machin D (1992) Appendix 1 Techniques. In: Medical Statistics: A Commonsense Approach pp 147-149. Chichester: John Wiley & Sons.

53. Campbell S, Vyas S, Nicolaides KH (1991) Doppler investigation of the fetal circulation. J Perinat Med 19: 21-26.

54. Chaiworapongsa T, Romero R, Kim JC, Kim YM, Blackwell SC, Yoon BH, Gomez R (2002) Evidence for fetal involvement in the pathologic process of clinical chorioamnionitis. American Journal of Obstetrics & Gynecology 186: 1178-1182.

55. Clausson B, Gardosi J, Francis A, Cnattingius S (2001) Perinatal outcome in SGA births defined by customised versus population-based birthweight standards. BJOG 108: 830-834.

56. Cobos I, Puelles L, Martinez S (2001) The avian telencephalic subpallium originates inhibitory neurons that invade tangentially the pallium (dorsal ventricular ridge and cortical areas). Dev Biol 239: 30-45.

57. Cohn HE, Sacks EJ, Heymann MA, Rudolph AM (1974) Cardiovascular responses to hypoxemia and acidemia in fetal lambs. Am J Obstet Gynecol 120: 817-824.

58. Coumans AB, Middelanis JS, Garnier Y, Vaihinger HM, Leib SL, Von Duering MU, Hasaart TH, Jensen A, Berger R (2003) Intracisternal application of endotoxin enhances the susceptibility to subsequent hypoxic-ischemic brain damage in neonatal rats. Pediatr Res 53: 770-775.

59. Cremer JE (1982) Substrate utilization and brain development. J Cereb Blood Flow Metab 2: 394-407.

60. Cremer JE, Heath DF (1974) The estimation of rates of utilization of glucose and ketone bodies in the brain of the suckling rat using compartmental analysis of isotopic data. Biochem J 142: 527-544.

61. Cruz F, Villalba M, Garcia-Espinosa MA, Ballesteros P, Bogonez E, Satrustegui J, Cerdan S (2001) Intracellular compartmentation of

pyruvate in primary cultures of cortical neurons as detected by (13)C NMR spectroscopy with multiple (13)C labels. Journal of Neuroscience Research 66: 771-781.

62. Curtis MJ, Jenkins HG, Butler EJ (1980) The effect of Escherichia coli endotoxins and adrenocortical hormones on plasma enzyme activities in the domestic fowl. Res Vet Sci 28: 44-50.

63. Dahlquist G (1976) Cerebral utilization of glucose, ketone bodies and oxygen in starving infant rats and the effect of intrauterine growth retardation. Acta Physiol Scand 98: 237-247.

64. Dalton KJ, Dawes GS, Patrick JE (1977) Diurnal, respiratory, and other rhythms of fetal heart rate in lambs. Am J Obstet Gynecol 127: 414-424.

65. Dammann O, Dammann CE, Allred EN, Veelken N (2001) Fetal growth restriction is not associated with a reduced risk for bilateral spastic cerebral palsy in very-low-birthweight infants. Early Hum Dev 64: 79-89.

66. Daniel PM, Love ER, Moorhouse SR, Pratt OE (1977) The transport of ketone bodies into the brain of the rat (in vivo). J Neurol Sci 34: 1-13.

67. Danielsen ER, Henriksen O (1994) Absolute quantitative proton NMR spectroscopy based on the amplitude of the local water suppression pulse. Quantification of brain water and metabolites. NMR Biomed 7: 311-318.

68. Dashe JS, Rogers BB, McIntire DD, Leveno KJ (1999) Epidural analgesia and intrapartum fever: placental findings. Obstet Gynecol 93: 341-344.

69. De Smedt MC, Visser GH, Meijboom EJ (1987) Fetal cardiac output estimated by Doppler echocardiography during mid- and late gestation. Am J Cardiol 60: 338-342.

70. de Vries HE, Blom-Roosemalen MC, van Oosten M, de Boer AG, van Berkel TJ, Breimer DD, Kuiper J (1996) The influence of cytokines on the integrity of the blood-brain barrier in vitro. J Neuroimmunol 64: 37-43.

71. Decanniere C, Eleff S, Davis D, van Zijl PC (1995) Correlation of rapid changes in the average water diffusion constant and the concentrations of lactate and ATP breakdown products during global ischemia in cat brain. Magn Reson Med 34: 343-352.

72. Deshpande JK, Siesjo BK, Wieloch T (1987) Calcium accumulation and neuronal damage in the rat hippocampus following cerebral ischemia. J Cereb Blood Flow Metab 7: 89-95.

73. DeVore G.R., Horenstein J. (1993) Ductus venosus index: a method for evaluating right ventricular preload in the second-trimester fetus. Ultrasound Obstet Gynecol 3: 338-342.

74. Dietrich WD, Busto R, Valdes I, Loor Y (1990) Effects of normothermic versus mild hyperthermic forebrain ischemia in rats. Stroke 21: 1318-1325.

75. Dinarello CA (1996) Cytokines as mediators in the pathogenesis of septic shock. Curr Top Microbiol Immunol 216: 133-165.

76. Dollner H, Vatten L, Halgunset J, Rahimipoor S, Austgulen R (2002) Histologic chorioamnionitis and umbilical serum levels of pro-inflammatory cytokines and cytokine inhibitors. BJOG 109: 534-539.

77. Dombrowski GJ, Jr., Swiatek KR, Chao KL (1989) Lactate, 3-hydroxybutyrate, and glucose as substrates for the early postnatal rat brain. Neurochem Res 14: 667-675.

78. Dorrepaal CA, Berger HM, Benders MJ, Zoeren-Grobben D, Van de BM, Van Bel F (1996) Nonprotein-bound iron in postasphyxial reperfusion injury of the newborn. Pediatrics 98: 883-889.

79. du Plessis AJ, Volpe JJ (2002) Perinatal brain injury in the preterm and term newborn. [Review] [59 refs]. Current Opinion in Neurology 15: 151-157.

80. Dubiel M, Gunnarsson GO, Gudmundsson S (2002) Blood redistribution in the fetal brain during chronic hypoxia. Ultrasound Obstet Gynecol 20: 117-121.

81. Duggan PJ, Maalouf EF, Watts TL, Sullivan MH, Counsell SJ, Allsop J, Al Nakib L, Rutherford MA, Battin M, Roberts I, Edwards AD (2001) Intrauterine T-cell activation and increased proinflammatory cytokine concentrations in preterm infants with cerebral lesions.[comment]. Lancet 358: 1699-1700.

82. Economides DL, Nicolaides KH (1989) Blood glucose and oxygen tension levels in small-for-gestational-age fetuses. Am J Obstet Gynecol 160: 385-389.

83. Eklind S, Mallard C, Leverin AL, Gilland E, Blomgren K, Mattsby-Baltzer I, Hagberg H (2001) Bacterial endotoxin sensitizes the immature brain to hypoxic--ischaemic injury. European Journal of Neuroscience 13: 1101-1106.

84. Ergander U, Eriksson M, Zetterstrom R (1983) Severe neonatal asphyxia. Incidence and prediction of outcome in the Stockholm area. Acta Paediatr Scand 72: 321-325.

85. Espinoza MI, Parer JT (1991) Mechanisms of asphyxial brain damage, and possible pharmacologic interventions, in the fetus. [Review] [26 refs]. American Journal of Obstetrics & Gynecology 164: 1582-1589.

86. Fabian RH, Perez-Polo JR, Kent TA (2000) Electrochemical monitoring of superoxide anion production and cerebral blood flow: effect of

interleukin-1 beta pretreatment in a model of focal ischemia and reperfusion. Journal of Neuroscience Research 60: 795-803.

87. Faraci FM (1986) Circulation during hypoxia in birds. Comp Biochem Physiol A 85: 613-620.

88. Fattal-Valevski A, Leitner Y, Kutai M, Tal-Posener E, Tomer A, Lieberman D, Jaffa A, Many A, Harel S (1999) Neurodevelopmental outcome in children with intrauterine growth retardation: a 3-year follow-up. J Child Neurol 14: 724-727.

89. Ferreiro B, Bernal J, Potter BJ (1987) Ontogenesis of thyroid hormone receptor in foetal lambs. Acta Endocrinol (Copenh) 116: 205-210.

90. Ferriero DM (2001) Oxidant mechanisms in neonatal hypoxia-ischemia. Dev Neurosci 23: 198-202.

91. Finer NN, Robertson CM, Richards RT, Pinnell LE, Peters KL (1981) Hypoxic-ischemic encephalopathy in term neonates: perinatal factors and outcome. J Pediatr 98: 112-117.

92. Finkler MS, Van Orman JB, Sotherland PR (1998) Experimental manipulation of egg quality in chickens: influence of albumen and yolk on the size and body composition of near-term embryos in a precocial bird. J Comp Physiol [B] 168: 17-24.

93. Flecknell PA, Wootton R, John M (1983) Cerebral blood flow and cerebral metabolism in normal and intrauterine growth retarded neonatal piglets. Clin Sci (Lond) 64: 161-165.

94. Forbes KP, Pipe JG, Bird R (2000) Neonatal hypoxic-ischemic encephalopathy: detection with diffusion-weighted MR imaging. AJNR Am J Neuroradiol 21: 1490-1496.

95. Foster NM, Leudke AJ (1968) Direct assay for bluetongue virus by intravascular inoculation of embryonating chicken eggs. Am J Vet Res 29: 749-753.

96. Fouron JC, Gosselin J, Amiel-Tison C, Infante-Rivard C, Fouron C, Skoll A, Veilleux A (2001) Correlation between prenatal velocity waveforms in the aortic isthmus and neurodevelopmental outcome between the ages of 2 and 4 years. Am J Obstet Gynecol 184: 630-636.

97. Froen JF, Munkeby BH, Stray-Pedersen B, Saugstad OD (2002) Interleukin-10 reverses acute detrimental effects of endotoxin-induced inflammation on perinatal cerebral hypoxia-ischemia. Brain Research 942: 87-94.

98. Gaffney G, Squier MV, Johnson A, Flavell V, Sellers S (1994) Clinical associations of prenatal ischaemic white matter injury. Arch Dis Child Fetal Neonatal Ed 70: F101-F106.

99. Gardosi J (1998) The application of individualised fetal growth curves. J Perinat Med 26: 137-142.

100. Gerretsen G, Huisjes HJ, Elema JD (1981) Morphological changes of the spiral arteries in the placental bed in relation to pre-eclampsia and fetal growth retardation. Br J Obstet Gynaecol 88: 876-881.

101. Gilbert RD, Pearce WJ, Ashwal S, Longo LD (1990) Effects of hypoxia on contractility of isolated fetal lamb cerebral arteries. J Dev Physiol 13: 199-203.

102. Govindaraju V, Young K, Maudsley AA (2000) Proton NMR chemical shifts and coupling constants for brain metabolites. NMR Biomed 13: 129-153.

103. Gray PH, Jones P, O'Callaghan MJ (2001) Maternal antecedents for cerebral palsy in extremely preterm babies: a case-control study. Dev Med Child Neurol 43: 580-585.

104. Grether JK, Nelson KB (1997) Maternal infection and cerebral palsy in infants of normal birth weight. JAMA 278: 207-211.

105. Griffin JL, Rae C, Dixon RM, Radda GK, Matthews PM (1998) Excitatory amino acid synthesis in hypoxic brain slices: does alanine act as a substrate for glutamate production in hypoxia? J Neurochem 71: 2477-2486.

106. Groenendaal F, Veenhoven RH, van der GJ, Jansen GH, Witkamp TD, de Vries LS (1994) Cerebral lactate and N-acetyl-aspartate/choline ratios in asphyxiated full-term neonates demonstrated in vivo using proton magnetic resonance spectroscopy. Pediatr Res 35: 148-151.

107. Grubb B, Colacino JM, Schmidt-Nielsen K (1978) Cerebral blood flow in birds: effect of hypoxia. Am J Physiol 234: H230-H234.

108. Gruss M, Bredenkotter M, Braun K (1999) N-methyl-D-aspartate receptor-mediated modulation of monoaminergic metabolites and amino acids in the chick forebrain: an in vivo microdialysis and electrophysiology study. J Neurobiol 40: 116-135.

109. Guissani DA, Spencer JA, Hanson MA (1994) Fetal cardiovascular reflex responses to hypoxeamia. Fetal and Maternal Medicine Review 16: 17-37.

110. Gunn AJ, Parer JT, Mallard EC, Williams CE, Gluckman PD (1992) Cerebral histologic and electrocorticographic changes after asphyxia in fetal sheep. Pediatr Res 31: 486-491.

111. Guyer B, Martin JA, MacDorman MF, Anderson RN, Strobino DM (1997) Annual summary of vital statistics--1996. Pediatrics 100: 905-918.

112. Hackett GA, Campbell S, Gamsu H, Cohen-Overbeek T, Pearce JM (1987) Doppler studies in the growth retarded fetus and prediction of neonatal necrotising enterocolitis, haemorrhage, and neonatal morbidity. Br Med J (Clin Res Ed) 294: 13-16.

113. Hagberg B (1993) The origins of cerebral palsy. In: Recent advances in paediatrics (David TJ, ed), London: Churchill.

114. Hagberg B, Kyllerman M (1983) Epidemiology of mental retardation--a Swedish survey. Brain Dev 5: 441-449.

115. Hagberg H, Peebles D, Mallard C (2002) Models of white matter injury: comparison of infectious, hypoxic-ischemic, and excitotoxic insults. [Review] [80 refs]. Mental Retardation & Developmental Disabilities Research Reviews 8: 30-38.

116. Hamilton PA, Hope PL, Cady EB, Delpy DT, Wyatt JS, Reynolds EO (1986) Impaired energy metabolism in brains of newborn infants with increased cerebral echodensities. Lancet 1: 1242-1246.

117. Hanson MA (1988) The importance of baro- and chemoreflexes in the control of the fetal cardiovascular system. J Dev Physiol 10: 491-511.

118. Harding JE, Evans PC (1991) beta-Hydroxybutyrate is an alternative substrate for the fetal sheep brain. J Dev Physiol 16: 293-299.

119. Hattori H, Morin AM, Schwartz PH, Fujikawa DG, Wasterlain CG (1989) Posthypoxic treatment with MK-801 reduces hypoxic-ischemic damage in the neonatal rat. Neurology 39: 713-718.

120. Hay PE, Lamont RF, Taylor-Robinson D, Morgan DJ, Ison C, Pearson J (1994) Abnormal bacterial colonisation of the genital tract and subsequent preterm delivery and late miscarriage. BMJ 308: 295-298.

121. Hecher K, Snijders R, Campbell S, Nicolaides K (1995) Fetal venous, intracardiac, and arterial blood flow measurements in intrauterine growth retardation: relationship with fetal blood gases. Am J Obstet Gynecol 173: 10-15.

122. Hedtjarn M, Leverin AL, Eriksson K, Blomgren K, Mallard C, Hagberg H (2002) Interleukin-18 involvement in hypoxic-ischemic brain injury. J Neurosci 22: 5910-5919.

123. Heilmann L, von Tempelhoff GF, Pollow K (2003) Antiphospholipid syndrome in obstetrics. Clin Appl Thromb Hemost 9: 143-150.

124. Heinrichs WL, Fong P, Flannery M, Heinrichs SC, Crooks LE, Spindle A, Pedersen RA (1988) Midgestational exposure of pregnant BALB/c mice to magnetic resonance imaging conditions. Magn Reson Imaging 6: 305-313.

125. Herrington J, Park YB, Babcock DF, Hille B (1996) Dominant role of mitochondria in clearance of large Ca2+ loads from rat adrenal chromaffin cells. Neuron 16: 219-228.

126. Higuchi T, Graham SH, Fernandez EJ, Rooney WD, Gaspary HL, Weiner MW, Maudsley AA (1997) Effects of severe global ischemia on N-acetylaspartate and other metabolites in the rat brain. Magn Reson Med 37: 851-857.

127. Hill RM, Verniaud WM, Deter RL, Tennyson LM, Rettig GM, Zion TE, Vorderman AL, Helms PG, McCulley LB, Hill LL (1984) The effect of intrauterine malnutrition on the term infant. A 14-year progressive study. Acta Paediatr Scand 73: 482-487.

128. Hoehn-Berlage M, Norris DG, Kohno K, Mies G, Leibfritz D, Hossmann KA (1995) Evolution of regional changes in apparent diffusion coefficient during focal ischemia of rat brain: the relationship of quantitative diffusion NMR imaging to reduction in cerebral blood flow and metabolic disturbances. J Cereb Blood Flow Metab 15: 1002-1011.

129. Holst K, Andersen E, Philip J, Henningsen I (1989) Antenatal and perinatal conditions correlated to handicap among 4-year-old children. American Journal of Perinatology 6: 258-267.

130. Hooper SB (1995) Fetal metabolic responses to hypoxia. [Review] [75 refs]. Reproduction, Fertility, & Development 7: 527-538.

131. Hooper SB, Coulter CL, Deayton JM, Harding R, Thorburn GD (1990) Fetal endocrine responses to prolonged hypoxemia in sheep. Am J Physiol 259: R703-R708.

132. Hope PL, Costello AM, Cady EB, Delpy DT, Tofts PS, Chu A, Hamilton PA, Reynolds EO, Wilkie DR (1984) Cerebral energy metabolism studied with phosphorus NMR spectroscopy in normal and birth-asphyxiated infants. Lancet 2: 366-370.

133. Hope PL, Reynolds EO (1985) Investigation of cerebral energy metabolism in newborn infants by phosphorus nuclear magnetic resonance spectroscopy. Clinics in Perinatology 12: 261-275.

134. Hsu SD, Cardell RR, Jr., Drake RL (1993) Maternal malnutrition does not affect fetal hepatic glycogen synthase ontogeny. Dig Dis Sci 38: 1500-1504.

135. Hudome S, Palmer C, Roberts RL, Mauger D, Housman C, Towfighi J (1997) The role of neutrophils in the production of hypoxic-ischemic brain injury in the neonatal rat. Pediatric Research 41: 607-616.

136. Hull J, Dodd KL (1992) Falling incidence of hypoxic-ischaemic encephalopathy in term infants. Br J Obstet Gynaecol 99: 386-391.

137. Huppi PS, Posse S, Lazeyras F, Burri R, Bossi E, Herschkowitz N (1991) Magnetic resonance in preterm and term newborns: 1H-spectroscopy in developing human brain. Pediatr Res 30: 574-578.

138. Ivacko J, Szaflarski J, Malinak C, Flory C, Warren JS, Silverstein FS (1997) Hypoxic-ischemic injury induces monocyte chemoattractant protein-1 expression in neonatal rat brain. J Cereb Blood Flow Metab 17: 759-770.

139. Jansen AH, Belik J, Ioffe S, Chernick V (1989) Control of organ blood flow in fetal sheep during normoxia and hypoxia. Am J Physiol 257: H1132-H1139.

140. Jansson T, Persson E (1990) Placental transfer of glucose and amino acids in intrauterine growth retardation: studies with substrate analogs in the awake guinea pig. Pediatr Res 28: 203-208.

141. Jensen A, Kunzel W, Kastendieck E (1985) Dynamics of fetal blood flow redistribution and catecholamine release during acute asphyxia. In: The Physiological Development of the Fetus and Newborn (Jones C.T., Natthanielsz P.W., eds), pp 405-410. London: Academic Press.

142. Jones CA, Edens FW, Denbow DM (1983) Influence of age on the temperature response of chickens to Escherichia coli and Salmonella typhimurium endotoxins. Poult Sci 62: 1553-1558.

143. Jones CT, Rolph TP (1985) Metabolism during fetal life: a functional assessment of metabolic development. Physiol Rev 65: 357-430.

144. Jones MD, Jr., Sheldon RE, Peeters LL, Makowski EL, Meschia G (1978) Regulation of cerebral blood flow in the ovine fetus. Am J Physiol 235: H162-H166.

145. Juorio AV, Vogt M (1967) Monoamines and their metabolites in the avian brain. J Physiol 189: 489-518.

146. Kaiser P, Rothwell L, Galyov EE, Barrow PA, Burnside J, Wigley P (2000) Differential cytokine expression in avian cells in response to invasion by Salmonella typhimurium, Salmonella enteritidis and Salmonella gallinarum. Microbiology 146 Pt 12: 3217-3226.

147. Kamitomo M, Alonso JG, Okai T, Longo LD, Gilbert RD (1993) Effects of long-term, high-altitude hypoxemia on ovine fetal cardiac output and blood flow distribution. Am J Obstet Gynecol 169: 701-707.

148. Kane E, Peterson RA (1976) Effects on body temperature produced by micro-injection of Salmonella typhimurium lipopolysaccharide into the third cerebral ventricle of the chicken. Poult Sci 55: 1580-1582.

149. Kato T, Nishina M, Matsushita K, Hori E, Mito T, Takashima S (1997) Neuronal maturation and N-acetyl-L-aspartic acid development in human fetal and child brains. Brain Dev 19: 131-133.

150. Ke Y, Cohen BM, Hirashima F, Nassar L, Renshaw P (2001) Phosphocreatine has shorter T2* then Creatine in vivo. Proc Intl Soc Mag Reson Med 9: 213.

151. Keith RD, Greene KR (1994) Development, evaluation and validation of an intelligent system for the management of labour. Baillieres Clin Obstet Gynaecol 8: 583-605.

152. Kilby MD, Gittoes N, McCabe C, Verhaeg J, Franklyn JA (2000) Expression of thyroid receptor isoforms in the human fetal central nervous system and the effects of intrauterine growth restriction. Clin Endocrinol (Oxf) 53: 469-477.

153. Kilby MD, Verhaeg J, Gittoes N, Somerset DA, Clark PM, Franklyn JA (1998) Circulating thyroid hormone concentrations and placental thyroid hormone receptor expression in normal human pregnancy and pregnancy complicated by intrauterine growth restriction (IUGR). J Clin Endocrinol Metab 83: 2964-2971.

154. King P, Parkin H, Macdonald IA, Barber C, Tattersall RB (1997) The effect of intravenous lactate on cerebral function during hypoglycaemia. Diabet Med 14: 19-28.

155. Kiserud T., Eik-Nes S.H., Blaas H.G., Hellevik L.R., Simensen B. (1994) Ductus venosus blood velocity and the umbilical circulation in the seriously growth-retarded fetus. Ultrasound Obstet Gynecol 4: 109-114.

156. Klasing KC, Peng RK (1987) Influence of cell sources, stimulating agents, and incubation conditions on release of interleukin-1 from chicken macrophages. Dev Comp Immunol 11: 385-394.

157. Kliegman RM (1986) Cerebral metabolic intermediate response following severe canine intrauterine growth retardation. Pediatric Research 20: 662-667.

158. Koh TS, Peng RK, Klasing KC (1996) Dietary copper level affects copper metabolism during lipopolysaccharide-induced immunological stress in chicks. Poult Sci 75: 867-872.

159. Kok JH, den Ouden AL, Verloove-Vanhorick SP, Brand R (1998) Outcome of very preterm small for gestational age infants: the first nine years of life. Br J Obstet Gynaecol 105: 162-168.

160. Kok RD, van den Berg PP, van den Bergh AJ, Nijland R, Heerschap A (2002) Maturation of the human fetal brain as observed by 1H MR spectroscopy. Magn Reson Med 48: 611-616.

161. Kok RD, van den Bergh AJ, Heerschap A, Nijland R, van den Berg PP (2001) Metabolic information from the human fetal brain obtained with proton magnetic resonance spectroscopy. Am J Obstet Gynecol 185: 1011-1015.

162. Koops BL, Morgan LJ, Battaglia FC (1982) Neonatal mortality risk in relation to birth weight and gestational age: update. J Pediatr 101: 969-977.

163. Kreis R (1997) Quantitative localized 1H MR spectroscopy for clinical use. Prog Nucl Magn Reson Spectrosp 31: 155-195.

164. Kruger K, Hallberg B, Blennow M, Kublickas M, Westgren M (1999) Predictive value of fetal scalp blood lactate concentration and pH as markers of neurologic disability. Am J Obstet Gynecol 181: 1072-1078.

165. Kuenzel WJ, Masson M (1998) A Stereotaxic Atlas of the Brain of the Chick (Gallus domesticus). Baltimore and London: The John Hopkins University Press.

166. Lagerstrom M, Bremme K, Eneroth P, Janson CG (1991) School marks and IQ-test scores for low birth weight children at the age of 13. Eur J Obstet Gynecol Reprod Biol 40: 129-136.

167. Lampe LG, Vojcek L, Princzkel E, Csomor S (1988) Blood flow redistribution during isocapnic hypoxia in foetal lamb. Acta Physiol Hung 71: 529-534.

168. Lapidot A, Haber S (2000) Effect of acute insulin-induced hypoglycemia on fetal versus adult brain fuel utilization, assessed by (13)C MRS isotopomer analysis of [U-(13)C]glucose metabolites. Dev Neurosci 22: 444-455.

169. Le Bihan D, Breton E, Lallemand D, Grenier P, Cabanis E, Laval-Jeantet M (1986) MR imaging of intravoxel incoherent motions: application to diffusion and perfusion in neurologic disorders. Radiology 161: 401-407.

170. Lee C, Kim DW, Jeon GS, Roh EJ, Seo JH, Wang KC, Cho SS (2001) Cerebellar alterations induced by chronic hypoxia: an immunohistochemical study using a chick embryonic model. Brain Res 901: 271-276.

171. Leitner Y, Fattal-Valevski A, Geva R, Bassan H, Posner E, Kutai M, Many A, Jaffa AJ, Harel S (2000) Six-year follow-up of children with intrauterine growth retardation: long-term, prospective study. J Child Neurol 15: 781-786.

172. Levene ML, Kornberg J, Williams TH (1985) The incidence and severity of post-asphyxial encephalopathy in full-term infants. Early Hum Dev 11: 21-26.

173. Li F, Liu KF, Silva MD, Meng X, Gerriets T, Helmer KG, Fenstermacher JD, Sotak CH, Fisher M (2002) Acute postischemic renormalization of the apparent diffusion coefficient of water is not associated with reversal of astrocytic swelling and neuronal shrinkage in rats. AJNR Am J Neuroradiol 23: 180-188.

174. Lieberman E, Eichenwald E, Mathur G, Richardson D, Heffner L, Cohen A (2000) Intrapartum fever and unexplained seizures in term infants. Pediatrics 106: 983-988.

175. Lin CC, Moawad AH, Rosenow PJ, River P (1980) Acid-base characteristics of fetuses with intrauterine growth retardation during labor and delivery. Am J Obstet Gynecol 137: 553-559.

176. Lin CH, Gelardi NL, Cha CJ, Oh W (1998) Cerebral metabolic response to hypoglycemia in severe intrauterine growth-retarded rat pups. Early Human Development 52: 1-11.

177. Liszka-Hackzell JJ (2001) Categorization of fetal heart rate patterns using neural networks. J Med Syst 25: 269-276.

178. Llanos AJ, Riquelme RA, Sanhueza EM, Herrera E, Cabello G, Giussani DA, Parer JT (2002) Regional brain blood flow and cerebral hemispheric oxygen consumption during acute hypoxaemia in the llama fetus. J Physiol 538: 975-983.

179. Lorek A, Takei Y, Cady EB, Wyatt JS, Penrice J, Edwards AD, Peebles D, Wylezinska M, Owen-Reece H, Kirkbride V, . (1994) Delayed ("secondary") cerebral energy failure after acute hypoxia-ischemia in the newborn piglet: continuous 48-hour studies by phosphorus magnetic resonance spectroscopy. Pediatr Res 36: 699-706.

180. Low JA, Handley-Derry MH, Burke SO, Peters RD, Pater EA, Killen HL, Derrick EJ (1992) Association of intrauterine fetal growth retardation and learning deficits at age 9 to 11 years. Am J Obstet Gynecol 167: 1499-1505.

181. Low JA, Panagiotopoulos C, Derrick EJ (1995) Newborn complications after intrapartum asphyxia with metabolic acidosis in the preterm fetus. Am J Obstet Gynecol 172: 805-810.

182. Lucas W, Kirschbaum T, Assali NS (1966) Cephalic circulation and oxygen consumption before and after birth. Am J Physiol 210: 287-292.

183. Macari M, Furlan RL, Gregorut FP, Secato ER, Guerreiro JR (1993) Effects of endotoxin, interleukin-1 beta and prostaglandin injections on fever response in broilers. Br Poult Sci 34: 1035-1042.

184. Macphail EM (1996) Cognitive function in mammals: the evolutionary perspective. Brain Res Cogn Brain Res 3: 279-290.

185. Maeda Y, Matsumoto M, Hori O, Kuwabara K, Ogawa S, Yan SD, Ohtsuki T, Kinoshita T, Kamada T, Stern DM (1994) Hypoxia/reoxygenation-mediated induction of astrocyte interleukin 6: a paracrine mechanism potentially enhancing neuron survival. J Exp Med 180: 2297-2308.

186. Magistretti PJ, Pellerin L (1999) Cellular mechanisms of brain energy metabolism and their relevance to functional brain imaging. Philos Trans R Soc Lond B Biol Sci 354: 1155-1163.

187. Mallard EC, Rees S, Stringer M, Cock ML, Harding R (1998) Effects of chronic placental insufficiency on brain development in fetal sheep. Pediatr Res 43: 262-270.

188. Mallard EC, Williams CE, Johnston BM, Gluckman PD (1994) Increased vulnerability to neuronal damage after umbilical cord occlusion in fetal sheep with advancing gestation. American Journal of Obstetrics & Gynecology 170: 206-214.

189. Mamelle N, Cochet V, Claris O (2001) Definition of fetal growth restriction according to constitutional growth potential. Biol Neonate 80: 277-285.

190. Mancini L, Bertossi M, Roncali L (1985) [Differentiation of cerebellar Purkinje neurons of the normal and chronically hypoxic chick embryo]. Boll Soc Ital Biol Sper 61: 79-85.

191. Manning FA (1999) Fetal biophysical profile. Obstet Gynecol Clin North Am 26: 557-77, v.

192. Marconi AM, Cetin I, Ferrazzi E, Ferrari MM, Pardi G, Battaglia FC (1990) Lactate metabolism in normal and growth-retarded human fetuses. Pediatr Res 28: 652-656.

193. Mari G, Uerpairojkit B, Abuhamad AZ, Copel JA (1996) Adrenal artery velocity waveforms in the appropriate and small-for-gestational-age fetus. Ultrasound Obstet Gynecol 8: 82-86.

194. Marteniuk JV, Herdt TH (1988) Pregnancy toxemia and ketosis of ewes and does. Veterinary Clinics of North America - Food Animal Practice 4: 307-315.

195. Martinez E, Figueroa R, Garry D, Visintainer P, Patel K, Verma U, Sehgal PB, Tejani N (1998) Elevated Amniotic Fluid Interleukin-6 as a Predictor of Neonatal Periventricular Leukomalacia and Intraventricular Hemorrhage. JOURNAL OF MATERNAL-FETAL INVESTIGATION 8: 101-107.

196. Matijevic R, Johnston T (1999) In vivo assessment of failed trophoblastic invasion of the spiral arteries in pre-eclampsia. Br J Obstet Gynaecol 106: 78-82.

197. Mays J, Verma U, Klein S, Tejani N (1995) Acute appendicitis in pregnancy and the occurrence of major intraventricular hemorrhage and periventricular leukomalacia. Obstetrics & Gynecology 86: 650-652.

198. Merboldt KD, Hanicke W, Frahm J (1991) Diffusion imaging using stimulated echoes. Magn Reson Med 19: 233-239.

199. Miller AL (1986) Regional glucose and beta-hydroxybutyrate use by developing rat brain. Metab Brain Dis 1: 53-61.

200. Miller L, Qureshi MA (1992) Heat-shock protein synthesis in chicken macrophages: influence of in vivo and in vitro heat shock, lead acetate, and lipopolysaccharide. Poult Sci 71: 988-998.

201. Miller SL, Green LR, Peebles DM, Hanson MA, Blanco CE (2002) Effects of chronic hypoxia and protein malnutrition on growth in the developing chick. Am J Obstet Gynecol 186: 261-267.

202. Minematsu K, Li L, Sotak CH, Davis MA, Fisher M (1992) Reversible focal ischemic injury demonstrated by diffusion-weighted magnetic resonance imaging in rats. Stroke 23: 1304-1310.

203. Mishra OP, Delivoria-Papadopoulos M (1992) NMDA receptor modification in the fetal guinea pig brain during hypoxia. Neurochem Res 17: 1211-1216.

204. Moorcraft J, Bolas NM, Ives NK, Ouwerkerk R, Smyth J, Rajagopalan B, Hope PL, Radda GK (1991a) Global and depth resolved phosphorus magnetic resonance spectroscopy to predict outcome after birth asphyxia. Arch Dis Child 66: 1119-1123.

205. Moorcraft J, Bolas NM, Ives NK, Sutton P, Blackledge MJ, Rajagopalan B, Hope PL, Radda GK (1991b) Spatially localized magnetic resonance spectroscopy of the brains of normal and asphyxiated newborns. Pediatrics 87: 273-282.

206. Mulder AL, van Golde JC, Prinzen FW, Blanco CE (1998) Cardiac output distribution in response to hypoxia in the chick embryo in the second half of the incubation time. J Physiol 508 (Pt 1): 281-287.

207. Murphy DJ, Sellers S, MacKenzie IZ, Yudkin PL, Johnson AM (1995) Case-control study of antenatal and intrapartum risk factors for cerebral palsy in very preterm singleton babies. Lancet 346: 1449-1454.

208. Myers SA, Ferguson R (1989) A population study of the relationship between fetal death and altered fetal growth. Obstet Gynecol 74: 325-331.

209. Naeye RL, Peters EC, Bartholomew M, Landis JR (1989) Origins of cerebral palsy. Am J Dis Child 143: 1154-1161.

210. Naicker T, Khedun SM, Moodley J, Pijnenborg R (2003) Quantitative analysis of trophoblast invasion in preeclampsia. Acta Obstet Gynecol Scand 82: 722-729.

211. Naressi A, Couturier C, Castang I, de Beer R, Graveron-Demilly D (2001a) Java-based graphical user interface for MRUI, a software package for quantitation of in vivo/medical magnetic resonance spectroscopy signals. Comput Biol Med 31: 269-286.

212. Naressi A, Couturier C, Devos JM, Janssen M, Mangeat C, de Beer R, Graveron-Demilly D (2001b) Java-based graphical user interface for the MRUI quantitation package. MAGMA 12: 141-152.

213. Neil JJ, Shiran SI, McKinstry RC, Schefft GL, Snyder AZ, Almli CR, Akbudak E, Aronovitz JA, Miller JP, Lee BC, Conturo TE (1998) Normal brain in human newborns: apparent diffusion coefficient and diffusion anisotropy measured by using diffusion tensor MR imaging. Radiology 209: 57-66.

214. Nelson KB (2002) The epidemiology of cerebral palsy in term infants. Ment Retard Dev Disabil Res Rev 8: 146-150.

215. Nelson KB, Dambrosia JM, Grether JK, Phillips TM (1998) Neonatal cytokines and coagulation factors in children with cerebral palsy. Ann Neurol 44: 665-675.

216. Nelson KB, Dambrosia JM, Ting TY, Grether JK (1996) Uncertain value of electronic fetal monitoring in predicting cerebral palsy. N Engl J Med 334: 613-618.

217. Nelson KB, Ellenberg JH (1985) Antecedents of cerebral palsy. I. Univariate analysis of risks. Am J Dis Child 139: 1031-1038.

218. Nelson KB, Ellenberg JH (1986) Antecedents of cerebral palsy. Multivariate analysis of risk. N Engl J Med 315: 81-86.

219. Nelson KB, Grether JK (1998) Potentially asphyxiating conditions and spastic cerebral palsy in infants of normal birth weight. Am J Obstet Gynecol 179: 507-513.

220. Nelson KB, Leviton A (1991) How much of neonatal encephalopathy is due to birth asphyxia? Am J Dis Child 145: 1325-1331.

221. Newman JP, Peebles DM, Hanson MA (2001) Adenosine produces changes in cerebral hemodynamics and metabolism as assessed by near-infrared spectroscopy in late-gestation fetal sheep in utero. Pediatric Research 50: 217-221.

222. Nicolaides KH, Economides DL, Soothill PW (1989) Blood gases, pH, and lactate in appropriate- and small-for-gestational-age fetuses. Am J Obstet Gynecol 161: 996-1001.

223. Nitsos I, Rees S (1990) The effects of intrauterine growth retardation on the development of neuroglia in fetal guinea pigs. An immunohistochemical and an ultrastructural study. Int J Dev Neurosci 8: 233-244.

224. O'Shaughnessy CT, Lythgoe DJ, Butcher SP, Kendall L, Wood B, Steward MC (1991) Effects of hypoxia on fetal rat brain metabolism studied in utero by 31P-NMR spectroscopy. Brain Res 551: 334-337.

225. O'Shea TM (2002) Cerebral palsy in very preterm infants: new epidemiological insights. [Review] [118 refs]. Mental Retardation & Developmental Disabilities Research Reviews 8: 135-145.

226. Ogata ES, Bussey ME, Finley S (1986) Altered gas exchange, limited glucose and branched chain amino acids, and hypoinsulinism retard fetal growth in the rat. Metabolism 35: 970-977.

227. Ogata ES, Bussey ME, LaBarbera A, Finley S (1985) Altered growth, hypoglycemia, hypoalaninemia, and ketonemia in the young rat: postnatal consequences of intrauterine growth retardation. Pediatr Res 19: 32-37.

228. Olah L, Wecker S, Hoehn M (2001) Relation of apparent diffusion coefficient changes and metabolic disturbances after 1 hour of focal cerebral ischemia and at different reperfusion phases in rats. J Cereb Blood Flow Metab 21: 430-439.

229. Olszowka AJ, Tazawa H, Rahn H (1988) A blood-gas nomogram of the chick fetus: blood flow distribution between the chorioallantois and fetus. Respir Physiol 71: 315-330.

230. Owen OE, Morgan AP, Kemp HG, Sullivan JM, Herrera MG, Cahill GF, Jr. (1967) Brain metabolism during fasting. J Clin Invest 46: 1589-1595.

231. Owens JA, Falconer J, Robinson JS (1987) Effect of restriction of placental growth on fetal and utero-placental metabolism. J Dev Physiol 9: 225-238.

232. Palmer C, Menzies SL, Roberts RL, Pavlick G, Connor JR (1999) Changes in iron histochemistry after hypoxic-ischemic brain injury in the neonatal rat. [erratum appears in J Neurosci Res 1999 Oct 15;58(2):349-55.]. Journal of Neuroscience Research 56: 60-71.

233. Palmer C, Roberts RL, Bero C (1994) Deferoxamine posttreatment reduces ischemic brain injury in neonatal rats. Stroke 25: 1039-1045.

234. Pattison N, McCowan L (2000) Cardiotocography for antepartum fetal assessment. Cochrane Database Syst Rev CD001068.

235. Paz I, Laor A, Gale R, Harlap S, Stevenson DK, Seidman DS (2001) Term infants with fetal growth restriction are not at increased risk for low intelligence scores at age 17 years. J Pediatr 138: 87-91.

236. Pearson R (1972) The Avian Brain. London & New York: Academic Press.

237. Peebles DM, Dixon JC, Thornton JS, Cady EB, Priest A, Miller SL, Blanco CE, Mulder TL, Ordidge RJ, Rodeck CH (2003) Magnetic resonance proton spectroscopy and diffusion weighted imaging of chick embryo brain in ovo. Brain Res Dev Brain Res 141: 101-107.

238. Peebles DM, Wyatt JS (2002) Synergy between antenatal exposure to infection and intrapartum events in causation of perinatal brain injury at term. BJOG: an International Journal of Obstetrics & Gynaecology 109: 737-739.

239. Pegorier JP, Ferre P, Leturque A, Girard J (1978) The metabolic effects of sodium dichloroacetate in the suckling newborn rat. Diabetologia 15: 459-463.

240. Pellerin L, Pellegri G, Martin JL, Magistretti PJ (1998) Expression of monocarboxylate transporter mRNAs in mouse brain: support for a distinct role of lactate as an energy substrate for the neonatal vs. adult brain. Proc Natl Acad Sci U S A 95: 3990-3995.

241. Penrice J, Cady EB, Lorek A, Wylezinska M, Amess PN, Aldridge RF, Stewart A, Wyatt JS, Reynolds EO (1996) Proton magnetic resonance spectroscopy of the brain in normal preterm and term infants, and early changes after perinatal hypoxia-ischemia. Pediatr Res 40: 6-14.

242. Penrice J, Lorek A, Cady EB, Amess PN, Wylezinska M, Cooper CE, D'Souza P, Brown GC, Kirkbride V, Edwards AD, Wyatt JS, Reynolds EO (1997) Proton magnetic resonance spectroscopy of the brain during acute hypoxia-ischemia and delayed cerebral energy failure in the newborn piglet. Pediatr Res 41: 795-802.

243. Perkins RP (1987) Perspectives on perinatal brain damage. Obstet Gynecol 69: 807-819.

244. Petroff OA, Prichard JW, Behar KL, Alger JR, den Hollander JA, Shulman RG (1985) Cerebral intracellular pH by 31P nuclear magnetic resonance spectroscopy. Neurology 35: 781-788.

245. Pharoah PO, Cooke RW (1997) A hypothesis for the aetiology of spastic cerebral palsy--the vanishing twin. Dev Med Child Neurol 39: 292-296.

246. Pouwels PJ, Frahm J (1998) Regional metabolite concentrations in human brain as determined by quantitative localized proton MRS. Magn Reson Med 39: 53-60.

247. Provencher SW (1993) Estimation of metabolite concentrations from localized in vivo proton NMR spectra. Magn Reson Med 30: 672-679.

248. Qiao M, Malisza KL, Del Bigio MR, Tuor UI (2002) Transient hypoxia-ischemia in rats: changes in diffusion-sensitive MR imaging findings, extracellular space, and Na+-K+ -adenosine triphosphatase and cytochrome oxidase activity. Radiology 223: 65-75.

249. Rahn H, Paganelli CV (1985) Transport by gas-phase diffusion: lessons learned from the hen's egg. Clin Physiol 5 Suppl 3: 1-7.

250. Reed KL, Appleton CP, Anderson CF, Shenker L, Sahn DJ (1990) Doppler studies of vena cava flows in human fetuses. Insights into normal and abnormal cardiac physiology. Circulation 81: 498-505.

251. Rees S, Clark M, Snowden M, Harding R (1990) The effects of intrauterine growth retardation on the structural development of cranial nerves (optic, trochlear) in fetal sheep. Int J Dev Neurosci 8: 133-141.

252. Rees S, Mallard C, Breen S, Stringer M, Cock M, Harding R (1998) Fetal brain injury following prolonged hypoxemia and placental insufficiency: a review. Comp Biochem Physiol A Mol Integr Physiol 119: 653-660.

253. Reith J, Jorgensen HS, Pedersen PM, Nakayama H, Raaschou HO, Jeppesen LL, Olsen TS (1996) Body temperature in acute stroke: relation to stroke severity, infarct size, mortality, and outcome. Lancet 347: 422-425.

254. Reuss ML, Parer JT, Harris JL, Krueger TR (1982) Hemodynamic effects of alpha-adrenergic blockade during hypoxia in fetal sheep. Am J Obstet Gynecol 142: 410-415.

255. Rezaie P, Dean A (2002) Periventricular leukomalacia, inflammation and white matter lesions within the developing nervous system. [Review] [282 refs]. Neuropathology 22: 106-132.

256. Rice JE, III, Vannucci RC, Brierley JB (1981) The influence of immaturity on hypoxic-ischemic brain damage in the rat. Ann Neurol 9: 131-141.

257. Richardson BS, Bocking AD (1998) Metabolic and circulatory adaptations to chronic hypoxia in the fetus. Comp Biochem Physiol A Mol Integr Physiol 119: 717-723.

258. Richardson BS, Carmichael L, Homan J, Gagnon R (1989) Cerebral oxidative metabolism in lambs during perinatal period: relationship to electrocortical state. Am J Physiol 257: R1251-R1257.

259. Richardson BS, Carmichael L, Homan J, Johnston L, Gagnon R (1996) Fetal cerebral, circulatory, and metabolic responses during heart rate decelerations with umbilical cord compression. Am J Obstet Gynecol 175: 929-936.

260. Rizzo G, Arduini D (1991) Fetal cardiac function in intrauterine growth retardation. Am J Obstet Gynecol 165: 876-882.

261. Robinson JN, Norwitz ER, Mulkern R, Brown SA, Rybicki F, Tempany CM (2001) Prenatal diagnosis of pyruvate dehydrogenase deficiency using magnetic resonance imaging. Prenat Diagn 21: 1053-1056.

262. Robinson JS, Jones CT, Kingston EJ (1983) Studies on experimental growth retardation in sheep. The effects of maternal hypoxaemia. J Dev Physiol 5: 89-100.

263. Roeder DJ, Lei MG, Morrison DC (1989) Endotoxic-lipopolysaccharide-specific binding proteins on lymphoid cells of various animal species: association with endotoxin susceptibility. Infect Immun 57: 1054-1058.

264. Roelants-van Rijn AM, Nikkels PG, Groenendaal F, van der GJ, Barth PG, Snoeck I, Beek FJ, de Vries LS (2001) Neonatal diffusion-weighted MR imaging: relation with histopathology or follow-up MR examination. Neuropediatrics 32: 286-294.

265. Rosenberg AA (1988) Response of the cerebral circulation to profound hypocarbia in neonatal lambs. Stroke 19: 1365-1370.

266. Roth SC, Baudin J, Cady E, Johal K, Townsend JP, Wyatt JS, Reynolds EO, Stewart AL (1997) Relation of deranged neonatal cerebral oxidative metabolism with neurodevelopmental outcome and head circumference at 4 years. Dev Med Child Neurol 39: 718-725.

267. Rudolph AM (1984) The fetal circulation and its response to stress. J Dev Physiol 6: 11-19.

268. Rumpel H, Nedelcu J, Aguzzi A, Martin E (1997) Late glial swelling after acute cerebral hypoxia-ischemia in the neonatal rat: a combined magnetic resonance and histochemical study. Pediatr Res 42: 54-59.

269. Rurak DW, Richardson BS, Patrick JE, Carmichael L, Homan J (1990) Blood flow and oxygen delivery to fetal organs and tissues during sustained hypoxemia. Am J Physiol 258: R1116-R1122.

270. Saliba E, Henrot A (2001) Inflammatory mediators and neonatal brain damage. Biol Neonate 79: 224-227.

271. Saliba E, Marret S (2001) Cerebral white matter damage in the preterm infant: pathophysiology and risk factors. [Review] [105 refs]. Seminars in Neonatology 6: 121-133.

272. Sarnat HB, Sarnat MS (1976) Neonatal encephalopathy following fetal distress. A clinical and electroencephalographic study. Arch Neurol 33: 696-705.

273. Schendel DE, Schuchat A, Thorsen P (2002) Public health issues related to infection in pregnancy and cerebral palsy. Ment Retard Dev Disabil Res Rev 8: 39-45.

274. Scherjon S, Briet J, Oosting H, Kok J (2000) The discrepancy between maturation of visual-evoked potentials and cognitive outcome at five years in very preterm infants with and without hemodynamic signs of fetal brain-sparing. Pediatrics 105: 385-391.

275. Scherjon SA, Oosting H, de Visser BW, de Wilde T, Zondervan HA, Kok JH (1996) Fetal brain sparing is associated with accelerated shortening of visual evoked potential latencies during early infancy. Am J Obstet Gynecol 175: 1569-1575.

276. Schifrin B.S., Clement D. (1991) Routine antenatal fetal heart rate. In: Fetal Monitoring: Physiology and Techniques of Antenatal and Intrapartum Assessment (Spencer JAD, ed), pp 98-103. Oxford: Oxford University Press.

277. Scott DL FAU, White SP FAU, Otwinowski ZF, Yuan WF, Gelb MH FAU, Sigler PB (1990) - Interfacial catalysis: the mechanism of phospholipase A2. - Science 1990 Dec 14;250(4987):1541-6 1541-1546.

278. Sell KM, Crowe SF, Kent S (2001) Lipopolysaccharide induces memory-processing deficits in day-old chicks. Pharmacol Biochem Behav 68: 497-502.

279. Seufert R, Woernle F, Casper F (2000) [Computer-assisted cardiotocogram analysis--from descriptive to perinatal expert system]. Zentralbl Gynakol 122: 328-333.

280. Shalak LF, Laptook AR, Jafri HS, Ramilo O, Perlman JM (2002) Clinical chorioamnionitis, elevated cytokines, and brain injury in term infants.[comment]. Pediatrics 110: 673-680.

281. Shalak LF, Perlman JM (2002) Infection markers and early signs of neonatal encephalopathy in the term infant. Ment Retard Dev Disabil Res Rev 8: 14-19.

282. Shambaugh GE, III (1985) Ketone body metabolism in the mother and fetus. Fed Proc 44: 2347-2351.

283. Shambaugh GE, III, Angulo MC, Koehler RR (1984) Fetal fuels. VII. Ketone bodies inhibit synthesis of purines in fetal rat brain. Am J Physiol 247: E111-E117.

284. Sijben JW, Klasing KC, Schrama JW, Parmentier HK, van der Poel JJ, Savelkoul HF, Kaiser P (2003) Early in vivo cytokine genes expression in chickens after challenge with Salmonella typhimurium lipopolysaccharide and modulation by dietary n-3 polyunsaturated fatty acids. Dev Comp Immunol 27: 611-619.

285. Silverstein FS, Barks JD, Hagan P, Liu XH, Ivacko J, Szaflarski J (1997) Cytokines and perinatal brain injury. Neurochem Int 30: 375-383.

286. Simmons ML, Frondoza CG, Coyle JT (1991) Immunocytochemical localization of N-acetyl-aspartate with monoclonal antibodies. Neuroscience 45: 37-45.

287. Smart SC, Fox GB, Allen KL, Swanson AG, Newman MJ, Swayne GT, Clark JB, Sales KD, Williams SC (1994) Identification of ethanolamine in rat and gerbil brain tissue extracts by NMR spectroscopy. NMR Biomed 7: 356-365.

288. Smith-Bindman R, Chu PW, Ecker J, Feldstein VA, Filly RA, Bacchetti P (2003) Adverse birth outcomes in relation to prenatal sonographic measurements of fetal size. J Ultrasound Med 22: 347-356.

289. Sommerfelt K, Andersson HW, Sonnander K, Ahlsten G, Ellertsen B, Markestad T, Jacobsen G, Hoffman HJ, Bakketeig L (2000) Cognitive development of term small for gestational age children at five years of age. Arch Dis Child 83: 25-30.

290. Soothill PW, Ajayi RA, Campbell S, Ross E.M., Candy D.C.A., Snijders RM, Nicolaides KH (1992) Relationship between fetal acidemia at cordocentesis and subsequent neurodevelopment. Ultrasound Obstet Gynecol 2: 80-83.

291. Soothill PW, Nicolaides KH, Bilardo K, Hackett GA, Campbell S (1986) Utero-placental blood velocity resistance index and umbilical venous pO2, pCO2, pH, lactate and erythroblast count in growth-retarded fetuses. Fetal Ther 1: 176-179.

292. Soothill PW, Nicolaides KH, Campbell S (1987) Prenatal asphyxia, hyperlacticaemia, hypoglycaemia, and erythroblastosis in growth retarded fetuses. Br Med J (Clin Res Ed) 294: 1051-1053.

293. Spencer JA, Badawi N, Burton P, Keogh J, Pemberton P, Stanley F (1997) The intrapartum CTG prior to neonatal encephalopathy at term: a case-control study. Br J Obstet Gynaecol 104: 25-28.

294. Strauss RS, Dietz WH (1998) Growth and development of term children born with low birth weight: effects of genetic and environmental factors. J Pediatr 133: 67-72.

295. Sun PM, Wilburn W, Raynor BD, Jamieson D (2001) Sickle cell disease in pregnancy: twenty years of experience at Grady Memorial Hospital, Atlanta, Georgia. Am J Obstet Gynecol 184: 1127-1130.

296. Sunwoo HH, Nakano T, Dixon WT, Sim JS (1996) Immune responses in chickens against lipopolysaccharide of Escherichia coli and Salmonella typhimurium. Poult Sci 75: 342-345.

297. Sutterlin MW, Seelbach-Gobel B, Oehler MK, Heupel M, Dietl J (1999) Doppler ultrasonographic evidence of intrapartum brain-sparing effect in fetuses with low oxygen saturation according to pulse oximetry. Am J Obstet Gynecol 181: 216-220.

298. Suzuki S, Murata T, Jiang L, Power GG (2000) Hyperthermia prevents metabolic and cerebral flow responses to hypoxia in the fetal sheep. Journal of the Society for Gynecologic Investigation 7: 45-50.

299. Takeoka M, Soman TB, Yoshii A, Caviness VS, Jr., Gonzalez RG, Grant PE, Krishnamoorthy KS (2002) Diffusion-weighted images in neonatal cerebral hypoxic-ischemic injury. Pediatr Neurol 26: 274-281.

300. Tan J, Bluml S, Hoang T, Dubowitz D, Mevenkamp G, Ross B (1998) Lack of effect of oral choline supplement on the concentrations of choline metabolites in human brain. Magn Reson Med 39: 1005-1010.

301. Tanner SF, Ramenghi LA, Ridgway JP, Berry E, Saysell MA, Martinez D, Arthur RJ, Smith MA, Levene MI (2000) Quantitative comparison of intrabrain diffusion in adults and preterm and term neonates and infants. AJR Am J Roentgenol 174: 1643-1649.

302. Taylor DJ, Howie PW (1989) Fetal growth achievement and neurodevelopmental disability. Br J Obstet Gynaecol 96: 789-794.

303. Thacker SB (2004) Continuous electronic heart rate monitoring for fetal assessment during labor. Cochrane Database of Systematic Reviews 1, 2004..

304. Thordstein M, Andine P, Lehmann A, Hagberg H (1992) Cerebral amino acids and energy metabolites in the growth retarded rat fetus under normoxia and hypoxia. J Dev Physiol 18: 59-65.

305. Thornberg E, Thiringer K, Odeback A, Milsom I (1995) Birth asphyxia: incidence, clinical course and outcome in a Swedish population. Acta Paediatr 84: 927-932.

306. Thornton JS, Ordidge RJ, Penrice J, Cady EB, Amess PN, Punwani S, Clemence M, Wyatt JS (1998) Temporal and anatomical variations of brain water apparent diffusion coefficient in perinatal cerebral hypoxic-ischemic injury: relationships to cerebral energy metabolism. Magn Reson Med 39: 920-927.

307. Thurston JH, Hauhart RE, Schiro JA (1983) Lactate reverses insulin-induced hypoglycemic stupor in suckling-weanling mice: biochemical correlates in blood, liver, and brain. J Cereb Blood Flow Metab 3: 498-506.

308. Toft PB, Leth H, Ring PB, Peitersen B, Lou HC, Henriksen O (1995) Volumetric analysis of the normal infant brain and in intrauterine growth retardation. Early Hum Dev 43: 15-29.

309. Topp M, Langhoff-Roos J, Uldall P, Kristensen J (1996) Intrauterine growth and gestational age in preterm infants with cerebral palsy. Early Hum Dev 44: 27-36.

310. Trudinger BJ, Stevens D, Connelly A, Hales JR, Alexander G, Bradley L, Fawcett A, Thompson RS (1987) Umbilical artery flow velocity waveforms and placental resistance: the effects of embolization of the umbilical circulation. Am J Obstet Gynecol 157: 1443-1448.

311. Tuor UI, Kozlowski P, Del Bigio MR, Ramjiawan B, Su S, Malisza K, Saunders JK (1998) Diffusion- and T2-weighted increases in magnetic resonance images of immature brain during hypoxia-ischemia: transient reversal posthypoxia. Exp Neurol 150: 321-328.

312. Tuorto F, Alifragis P, Failla V, Parnavelas JG, Gulisano M (2003) Tangential migration of cells from the basal to the dorsal telencephalic regions in the chick. Eur J Neurosci 18: 3388-3393.

313. Tweed WA, Cote J, Pash M, Lou H (1983) Arterial oxygenation determines autoregulation of cerebral blood flow in the fetal lamb. Pediatr Res 17: 246-249.

314. Tyndall DA, Sulik KK (1991) Effects of magnetic resonance imaging on eye development in the C57BL/6J mouse. Teratology 43: 263-275.

315. Ulbricht C, Dorffner G, Lee A (1998) Neural networks for recognizing patterns in cardiotocograms. Artif Intell Med 12: 271-284.

316. Uvebrant P, Hagberg G (1992) Intrauterine growth in children with cerebral palsy. Acta Paediatr 81: 407-412.

317. Vacotto M, Rodriguez Gil DJ, Mitridate dN, Fiszer dP (2003) Differential and irreversible CNS ontogenic reduction in maximal MK-801 binding site number in the NMDA receptor after acute hypoxic hypoxia. Brain Res 976: 202-208.

318. van Cappellen van Walsum AM, Heerschap A, Nijhuis JG, Oeseburg B, Jongsma HW (1998) Proton magnetic resonance spectroscopy of fetal lamb brain during hypoxia. Am J Obstet Gynecol 179: 756-757.

319. van Cappellen van Walsum AM, Jongsma HW, Wevers RA, Nijhuis JG, Crevels J, Engelke UF, Moolenaar SH, Oeseburg B, Nijland R (2001) Hypoxia in fetal lambs: a study with (1)H-MNR spectroscopy of cerebrospinal fluid. Pediatr Res 49: 698-704.

320. van den Wijngaard JA, Groenenberg IA, Wladimiroff JW, Hop WC (1989) Cerebral Doppler ultrasound of the human fetus. Br J Obstet Gynaecol 96: 845-849.

321. van Gelderen P, de Vleeschouwer MH, DesPres D, Pekar J, van Zijl PC, Moonen CT (1994) Water diffusion and acute stroke. Magn Reson Med 31: 154-163.

322. van Golde J (1999) Chick embryo as a model in fetal physiology. Maastricht, The Netherlands.

323. van Golde J, Mulder T, Blanco CE (1997) Changes in mean chorioallantoic artery blood flow and heart rate produced by hypoxia in the developing chick embryo. Pediatr Res 42: 293-298.

324. Vanhamme L, Sundin T, Hecke PV, Huffel SV (2001) MR spectroscopy quantitation: a review of time-domain methods. NMR Biomed 14: 233-246.

325. Vanhamme L, van den BA, Van Huffel S (1997) Improved method for accurate and efficient quantification of MRS data with use of prior knowledge. J Magn Reson 129: 35-43.

326. Vannucci SJ, Seaman LB, Brucklacher RM, Vannucci RC (1994) Glucose transport in developing rat brain: glucose transporter proteins, rate constants and cerebral glucose utilization. Mol Cell Biochem 140: 177-184.

327. Vicario C, Arizmendi C, Malloch G, Clark JB, Medina JM (1991) Lactate utilization by isolated cells from early neonatal rat brain. J Neurochem 57: 1700-1707.

328. Vigneswaran R (2000) Infection and preterm birth: evidence of a common causal relationship with bronchopulmonary dysplasia and cerebral palsy. Journal of Paediatrics & Child Health 36: 293-296.

329. Volpe J.J (1995) Metabolic encephalopathies. In: Neurology of the newborn pp 467-582. Philadelphia: Saunders.

330. Walker V, Bennet L, Mills GA, Green LR, Gnanakumaran K, Hanson MA (1996) Effects of hypoxia on urinary organic acid and hypoxanthine excretion in fetal sheep. Pediatr Res 40: 309-318.

331. Wang Y, Li SJ (1998) Differentiation of metabolic concentrations between gray matter and white matter of human brain by in vivo 1H magnetic resonance spectroscopy. Magn Reson Med 39: 28-33.

332. Whittow G (2000) Sturkie's Avian Physiology. San Diego and London: Academic Press.

333. Williams MC, O'Brien WF (1997) A comparison of birth weight and weight/length ratio for gestation as correlates of perinatal morbidity. J Perinatol 17: 346-350.

334. Wladimiroff JW, Tonge HM, Stewart PA (1986) Doppler ultrasound assessment of cerebral blood flow in the human fetus. Br J Obstet Gynaecol 93: 471-475.

335. Wolf RL, Zimmerman RA, Clancy R, Haselgrove JH (2001) Quantitative apparent diffusion coefficient measurements in term neonates for early detection of hypoxic-ischemic brain injury: initial experience. Radiology 218: 825-833.

336. Wu YW, Colford JM, Jr. (2000) Chorioamnionitis as a risk factor for cerebral palsy: A meta-analysis. JAMA 284: 1417-1424.

337. Wyatt JS (1996) Fetal and Maternal Medicine Review 8: 95-108.

338. Xie H, Rath NC, Huff GR, Huff WE, Balog JM (2000) Effects of Salmonella typhimurium lipopolysaccharide on broiler chickens. Poult Sci 79: 33-40.

339. Yanowitz TD, Jordan JA, Gilmour CH, Towbin R, Bowen A, Roberts JM, Brozanski BS (2002) Hemodynamic disturbances in premature infants born after chorioamnionitis: association with cord blood cytokine concentrations. Pediatric Research 51: 310-316.

340. Yip YP, Capriotti C, Yip JW (1995) Effects of MR exposure on axonal outgrowth in the sympathetic nervous system of the chick. J Magn Reson Imaging 5: 457-462.

341. Yoon BH, Romero R, Yang SH, Jun JK, Kim IO, Choi JH, Syn HC (1996) Interleukin-6 concentrations in umbilical cord plasma are elevated in neonates with white matter lesions associated with periventricular leukomalacia. American Journal of Obstetrics & Gynecology 174: 1433-1440.

342. Young GB (1995) Neurologic complications of systemic critical illness. Neurol Clin 13: 645-658.

343. Young RS, Yagel SK, Towfighi J (1983) Systemic and neuropathologic effects of E. coli endotoxin in neonatal dogs. Pediatr Res 17: 349-353.

344. Zeitlin J, Ancel PY, Saurel-Cubizolles MJ, Papiernik E (2000) The relationship between intrauterine growth restriction and preterm delivery: an empirical approach using data from a European case-control study. BJOG 107: 750-758.